Development of Computer Aided Heat Treatment Planning System for Quenching & Tempering (CHT – *q/t*) and Industrial Application of CHT-*bf* & CHT-*cf*

A

Thesis

Submitted to the faculty

of the

WORCESTER POLYTECHNIC INSTITUTE

In partial fulfillment of the requirements for the

Degree of Master of Science

In

Mechanical Engineering

By

Amarjit Kumar Singh

Prof. Yiming (Kevin) Rong, (Major Advisor)	Prof. Diran Apelian, Thesis Committee
Prof. R. D. Sisson. Jr, Thesis Committee	Prof. M. A. Demetriou, Graduate Committee Representative

ABSTRACT

Heat treatment can be defined as a combination of heating and cooling operations applied to a metal or alloy in solid state. It is an important manufacturing process, which controls the mechanical properties of metals, therefore contributes to the product quality. Computerized Heat Treatment Planning System for Quenching and Tempering (CHT-*q/t*), a windows based stand alone software, is developed to assist the heat treatment process design. The goal of CHT-*q/t* is to predict the temperature profile of load in batch as well as continuous furnace during heating, quenching and tempering of steel, then to predict the mechanical properties as Quenched & Tempered, and finally to optimize the heat treatment process design.

The thesis reviews existing heat treating simulation software and identifies the industrial need of a software tool which integrates part load and furnace model with heat treating process. The thesis discusses cooling curve of specimen and Time Temperature Transformation (TTT) diagram to determine the microstructure evolution and subsequently the mechanical properties of steel after quenching. An extensive database has been developed to support the various function modules. The thesis focuses mainly in the TTT and quenchant database development, property prediction after quenching and tempering and the implementation of software. The properties determined in the thesis are hardness, ultimate tensile strength, yield strength, toughness and percentage elongation. Hardness has been predicted by the use of some well known analytical equations and the TTT database, finally regression analysis has been used to give the value as a function of carbon percentage and volume fraction of martensite. The other mechanical properties are calculated based on a relation of hardness and volume fraction of martensite.

Various case studies were performed to show the application of CHT-*bf* and CHT-*cf* at Bodycote Thermal Processing, Worcester & Waterbury. The objective behind the case studies was to study the effect of change in load arrangement, production rate and cycle time on the heat treated parts and finally to give recommendations in order to save energy and improve productivity and quality.

ACKNOWLEDGEMENT

It gives me great pleasure to thank all the people who helped me during my thesis and research work at Worcester Polytechnic Institute.

I would like to express my gratitude to Prof. Kevin Rong, my advisor, for helping, guiding and encouraging me to complete this thesis. Without his numerous suggestions and immense knowledge, the thesis would never have been completed. I also like to thank Prof. Diran Apelian and Prof. Richard Sisson for their enthusiastic service on the thesis committee.

I would like to thank CHTE, MPI for providing me assistantship position in the CHTE group. I would like to thank Mr. Ed Jamieson, Director, Technology and Quality of Bodycote Thermal Processing for giving me an opportunity to work in their company and necessary help whenever required. I would like thank my research group member Dr. Jinwu Kang, Dr. Lei Zhang and Radha Purshothamn for providing technical knowledge and valuable advice whenever I needed during my research work. I would like to thank my entire group members in the Computer Aided Manufacturing Lab for their help during my research work. I would also like to thank the program secretary, Ms. Barbara Edilberti, for helping me out during my stay at WPI

I would like to thank my family for supporting me throughout, during my study in WPI. I would also like to thank my friends for helping me out during my study in WPI.

TABLE OF CONTENTS

LIST OF FIGURES

LIST OF TABLES

CHAPTER 1. INTRODUCTION

Heat Treatment may be defined as heating and cooling operations applied to metals and alloys in solid state so as to obtain the desired properties. Heat treatment is sometimes done inadvertently due to manufacturing processes that either heat or cool the metal such as welding or forming. In this research we will mostly consider the heat treatment of steel. Steels can be categorized as low, medium or high carbon steels.

Steels – Carbon in steel may be present up to 2.03 percent. Steels with carbon content from 0.025 percent to 0.8 percent are called hypoeutectoid steel. Steel with a carbon content of 0.8 percent is known as eutectoid steel. Steels with carbon content greater then 0.8 percent are called hypereutectoid steel. There are three major categories of steel which are as follows:

- Low carbon steels (carbon upto 0.3 percent)
- Medium carbon steels (carbon from 0.3 to 0.6 percent)
- High carbon steel (carbon more than 0.6 percent)

Heat treatment is often associated with increasing the strength of material, but it can also be used to refine the grain size, relieve internal stress, to improve machinability and formability and to restore ductility after a cold working process. Some of the objectives of heat treatment are summarized as follows:

- Improvement in ductility
- Relieving internal stresses
- Refinement of grain size
- Increasing hardness or tensile strength
- Improvement in machinability
- Alteration in magnetic properties
- Modification of electrical conductivity
- Improvement in toughness

1.1 Heat Treatment Processes

Heat treatment is an important $15 billion industry. A heated workpiece in a heat-treating furnace will undergo a given thermal schedule, typically, a heating — soaking — cooling cycle. In this research the cooling process is studied.

The main types of heat treatment applied in practice are

1) Annealing
2) Normalization
3) Hardening and
4) Tempering

The heat treating processes are further classified as follows

Austempering:

This is a special Heat Treatment process in which austenite is transformed into bainite at constant temperature. Austempering consists of heating steel to above the austenitizing temperature. It is then quenched in a bath maintained at a constant temperature above M_s point and within the bainitic range (200 to 400^0C, in general). The steel is quenched and maintained at a constant temperature in the bath itself till all the austenite is transformed into bainite. After complete transformation steel is taken out of the bath and is cooled in air or at any desired rate to room temperature. The preferred temperature of the quenching bath is generally on the lower side of the bainitic range resulting in the formation of lower bainite which has better mechanical properties than tempered martensite, and hence austempered components rarely needs tempering.

This process as compared to conventional hardening and tempering treatment, results in better ductility at high hardness levels, improved impact and fatigue strength and freedom from distortion.

Martempering:

Similar to austempering, martempering involves heating the steel to the austenitizing temperature, followed by quenching in a constant temperature bath maintained above M_s point (180-250^{0}C). Steel is held in the bath till temperature throughout the section becomes uniform and is equal to the bath temperature. As soon as this temperature is attained, steel is withdrawn and cooled in air. The cooling rate is sufficiently high and holding time considerably short to prevent transformation of austenite to pearlite or to bainite. Martensite is formed in the second stage, namely during cooling in air. Martempering results in minimum internal stress reduced tendency towards distortion and cracking and improved mechanical properties as compared to conventional quenching and tempering treatment. The resultant microstructure of martempred steel is martensite. In order to improve properties, martempered steels are generally tempered.

Patenting:

The special heat treatment given to medium carbon, high carbon and low alloy steels wire rod is called patenting. The process consists of heating the material well above the austenitizing temperature to ensure formation of homogeneous austenite. After soaking for sufficient time at this temperature, the steel is quenched in a bath maintained at a constant temperature (450-550^{0}C) for a given steel, the quenching bath temperature is kept in the vicinity of the nose of TTT curve. This results in transformation of austenite to fine pearlite. Once the transformation is complete, the steel is cooled either in air or by spraying water. In some cases, a small amount of upper bainite has been observed. Lead bath or salt baths are commonly used for quenching the steel.

Tempering:

Tempering can be defined as a process, which consists of heating hardened steel below the lower critical temperature, followed by cooling in air or at any desired rate. The higher the tempering temperature, the more is the restored ductility and tougher the steel.

The objectives during the Tempering process are;

- Relieving of internal stress.
- Restoration of ductility and toughness
- Transformation of retained austenite.
- Tempering treatment also lowers hardness, strength and wear resistance of the hardened steel marginally.

Structural changes during tempering: A number of structural changes take place during tempering treatment, which are as follows:

- Isothermal transformation of retained austenite.
- Ejection of carbon from body centered tetragonal lattice of martensite.
- Growth and spherodiziation of carbide particles.
- Formation of ferrite-carbide mixture.

Effect of alloying elements on tempering:

Alloying elements can be classified into two classes, namely carbide forming elements and non-carbide forming elements.

- Carbide forming elements: Such as Chromium, Molybdenum, Tungsten, Vanadium, Tantalum and Titanium. These resist softening considerably due to the formation of respective alloy carbides.
- Non-carbide forming elements: Such as Nickel, Aluminum, Silicon and Manganese. These enter into ferrite and/or austenite and have very little impact on the tempered hardness of steel.

1.2 Problem Formulations

Heat treatment is performed to improve the mechanical properties of steel. To ensure the desired properties one has to look into many factors such as heating history, temperature distribution of furnace and workpiece, prior workpiece temperature for quenching, quenching rate. If these factors are not achieved, heat treatment will result in loss of mechanical properties and distortion. To achieve the desired properties part load design and temperature control during heating and cooling is of the utmost importance. The

product quality and productivity are greatly affected by heating control. To solve this problem the key point is the prediction of heating history and temperature distributions in furnace and in part [1]. Unfortunately there is no comprehensive technique to simulate the whole heat treatment process. The earlier developed software CHT-*bf* and CHT-*cf* is only good for heating.

The basic three categories of problems that need to be considered and addressed by CHT-*q/t* can be described as follows:

- Productivity: The parameters that effect the productivity in heat treating industries are energy consumption, time involved in heat treating process and optimization of the part load. Generally the part load design and furnace control in heat treating industry is based on the experience. It is very important to predict the temperature distribution inside the workpiece to carry any optimization of the part load

- Quality control: In the current practice there is no direct method to measure the inside-workpiece temperature during cooling. The temperature of workpiece varies with time and location, from surface to interior. The three dimensional enmeshment of the workpiece gives the temperature distribution inside the arbitrary geometrical shapes.

- Property Prediction: As already stated the final outcome of the heat treating process is to achieve the desired properties. At present there is hardly any software tool or analytical method to measure the properties after heat treatment. The determination of properties after heat treating is based on experience and experimental method.

1.3 Research Objective:

The research group of Professor Kevin Rong has been developing software based on the industrial need and current industrial practices. They have already developed CHT-*bf* and CHT-*cf*. These were insufficient for the requirements of heat treating process industry as

it was unable to optimize the whole heat treating process. To incorporate the Quenching and Tempering operations and thus to complete the whole heat treating cycle we proposed to develop "Computerized Heat Treating and Planning System for Quenching and Tempering, CHT-*q/t* ". The research objectives were set as follows.

- To develop physical-mathematical models based on the heat transfer theory for the various models of heat transfer including heating and cooling, taking place between the furnace and the workpiece and among the workpiece itself.

- Three dimensional enmeshment of workpiece based on their biot numbers.

- To study and analyze the various model parameters and their effects and develop a database containing the above model parameters that are properties of materials. Much of the database are taken from CHT-*bf* and CHT-*cf,* but Quenchant , material database with TTT diagram and tempering database has been developed entirely for CHT-*q/t*

- A database approach for the calculation of h, in different load pattern for gas as well as liquid quenching.

- Microstructure evolution in steel during Quenching based on the TTT diagram and the governing equations.

- Determination of as quenched hardness. Determination of other mechanical properties, i.e Ultimate tensile strength, yield strength, percentage elongation and toughness by mapping it to hardness.

- To develop a user interface so as to obtain all the necessary data inputs or parameters for the models.

- To validate and implement the system in the current industries.

Whereas, the above mentioned, were mostly the research objectives for CHT-*q/t.* The scope of the thesis lies in the work of database development for material and quenchant, development of quenching module including gas and liquid quenching, development of the methodology to predict as quenched mechanical properties of steel and the interface development.

1.4. Current Software Tools

For long, the heat treating community across United States, has been in search for an intelligent and affordable system to help them simulate the heat treatment process.

There are few software for the optimization of heat treating process in batch and continuous furnace, but the scope of these software are very limited. Among them FurnXpert program is developed to optimize furnace design and operation [2]. The program mainly focuses on the heat balance of the furnace. The load pattern is just aligned load pattern with one layer and it cannot deal with the condition of workpieces loaded in the fixtures. While, in this condition the workpieces inside the fixture are heated by adjacent workpieces, not directly by furnace. Figure 1 shows an interface of load pattern specifications in FurnXpert. The result curves are shown in Figure 2.

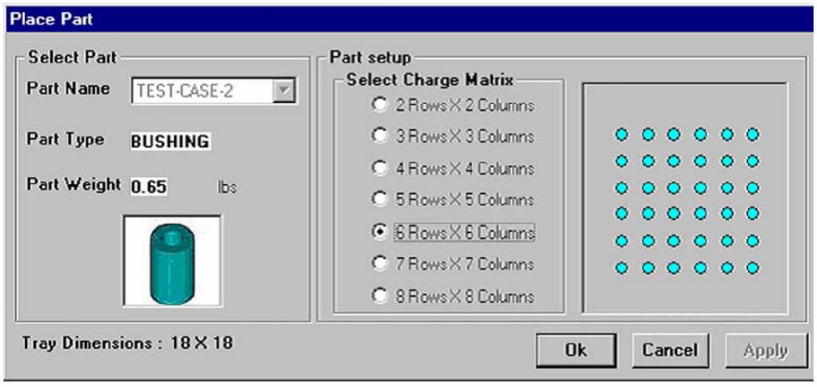

Figure 1. The load pattern for continuous belt in FurnXpert software [2]

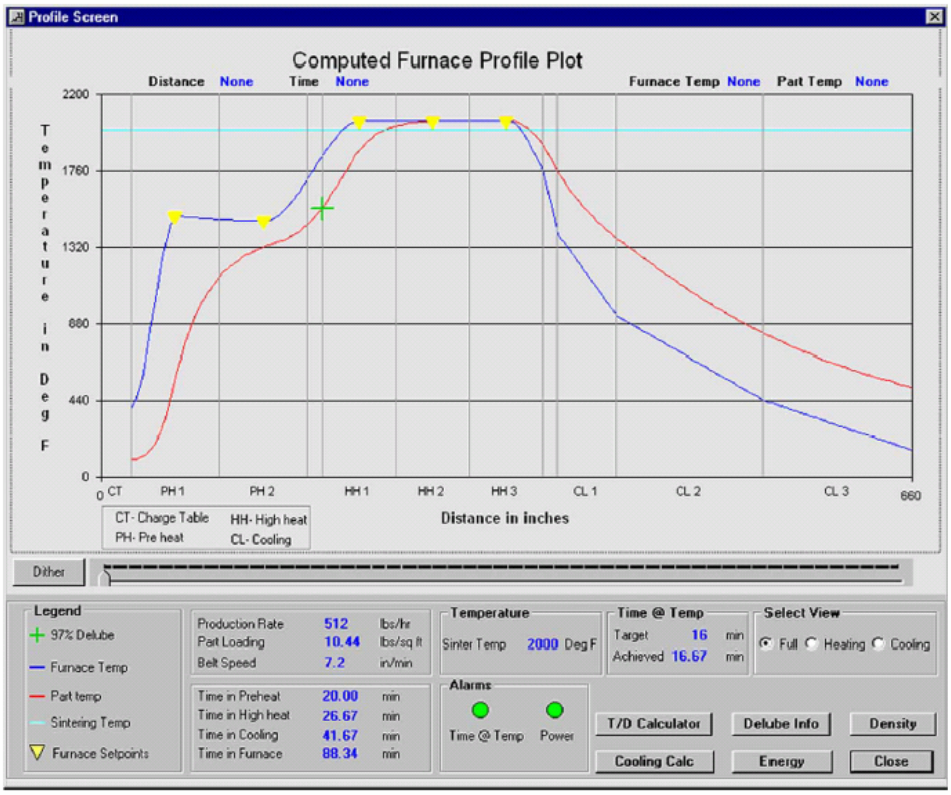

Figure 2. The result illustration of FurnXpert software [2]

The following results can be obtained from FurnXpert:

- Furnace and part profile
- Operating parameters (Production Rate, Time vs Temperature graph)
- Heat Loss Calculations
- Power requirement and consumed energy

On the other hand there are software to simulate a heat treating process, once the boundary conditions and other parameters are assigned. Among them Sysweld is a well known software.

SYSWELD, published by the ESI group is the leading tool for the simulation of heat treatment, welding and welding assembly processes, taking into account all aspects of material behavior, design and process [3]. It can perform FEA on any part geometry that

can be modeled through the modeling component, and can be expanded to include additional process data that has already been obtained through experimentation to generate accurate results.

Heat Treatment Simulation with Sysweld

SYSWELD simulates all usual heat treatment processes like bulk hardening, tempering and hardening, treatment with boron, thermo-chemical treatment like case hardening, carbonitriding, nitriding and nitro-carburising. It can also simulate Surface hardening processes like laser beam hardening, Induction hardening, electron beam hardening, plasma beam hardening, friction hardening and flame hardening. The software computes distortions of parts, residual stresses, plastic strains and the yield strength depending on the mixture of phases of the material in use both during and at the end of the heat treatment process, plus the hardness at the end of the process.

"SYSWELD is a well suited tool for realistic 3D Heat Treatment simulation engineering [3]". Figure 3 shows the capability of Sysweld regarding the prediction of distortion in specimen after quenching.

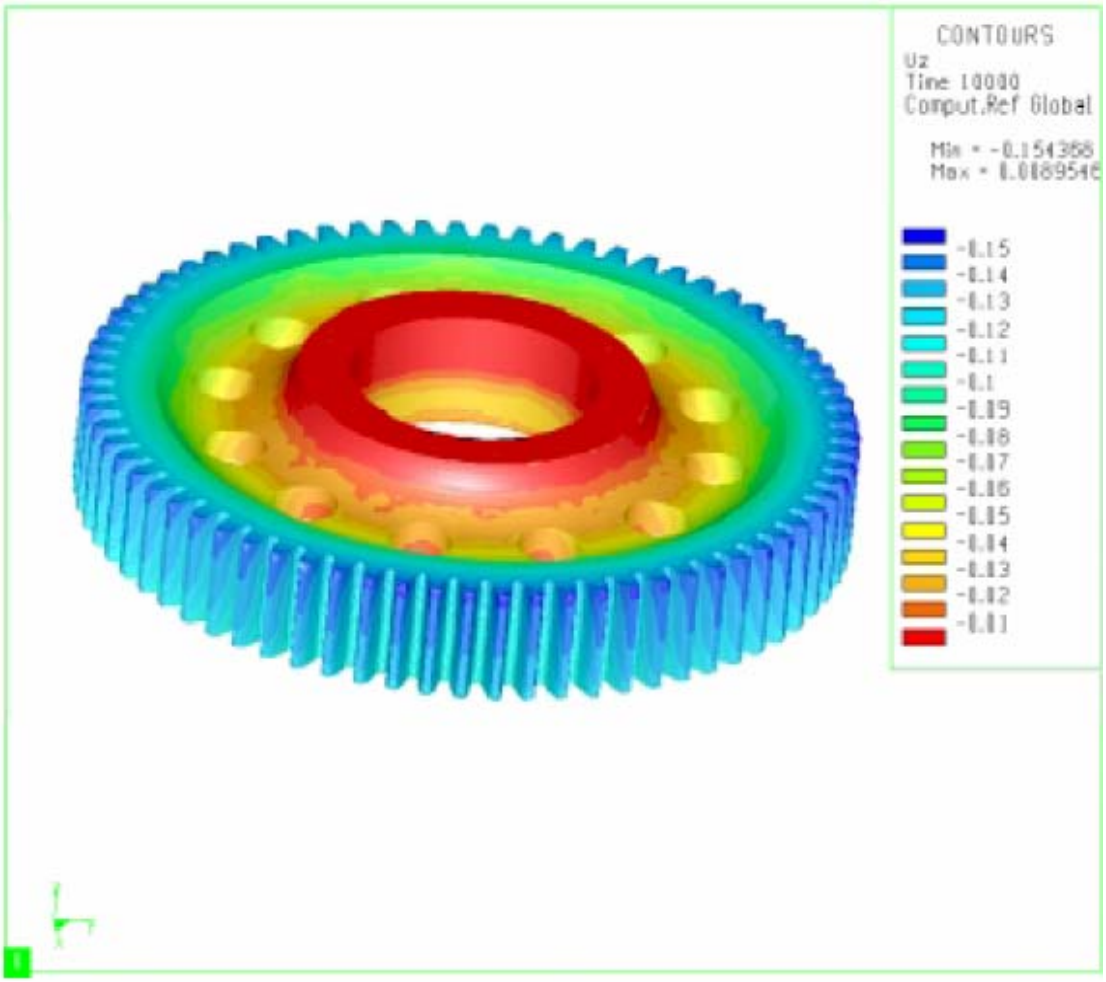

Figure 3. Distortion of large gear after quenching

Where as Sysweld is quite useful for the simulation of heat treatment process, it has the constraint to consider an actual heat treatment furnace.

Other software such as ICON and DCON [4] are developed in the mid 1990's. They were applicable only for very simple workpiece shape and based on DOS, thus they were not proper for the optimization of heat treating process of arbitrary shape workpieces.

1.5 Integrating Furnace Model with Heat Treating Process

We can conclude that although much research was done to simulate various heat treating processes but no actual part load and furnace model was developed to corroborate the

heat treating process with actual industrial demand. CHT-*q/t* aims to integrate the heat treating processes with the part load and furnace model already developed by the research group at CHTE, i.e CHT-*bf* and CHT-*cf.* Much of the heating module, material, workpiece, furnace and atmosphere database has been taken from CHT-*bf* and CHT-*cf*. The main focus of CHT-*q/t* lies in developing the Quenching and tempering model, where the final objective is to give the mechanical properties of steel as quenched and tempered. CHT-*q/t* is applicable for both batch and continuous furnaces, thus it integrates the furnace model of CHT-*bf* and CHT-*cf* other than adding a few furnaces.

The biggest challenge in developing the software is the enrichment of database. As most of the function modules are dependent on the database, it is very important to make the database as complete as possible. Apart from various literatures and ASM handbooks, QuenchPAD developed by Professor Sisson's research group has also been used to populate the database. Analytical equations has been used for the determination of volume fraction of various microstructures evolved and mechainal properties after quenching, with some assumptions, i.e grain size and the incubation time was not considered during the evolution of microstructures.

CHT-*q/t* is an easy to learn and user friendly software. It requires no Finite Element Analysis, which substantially reduces the computation time of the software. It does not require any CAD model of workpiece, either to be drawn or imported from other source. The database already has 13 shapes of the workpiece and has an option for an "Unknown

shape" as well. The features such as "cost effectiveness and easy to use" makes CHT-*q/t* unique to the heat treating community.

CHAPTER 2: BACKGROUND AND LITERATURE REVIEW

This chapter deals with the various heat transfer principles, which are divided into conduction, convection and radiation. In this chapter we will discuss about the quenching method in production, convection heat transfer for gas as well as liquid quenching and comparison of gas and liquid quenching. The chapter also presents a literature review on the quenching and tempering process by various researchers.

2.1 Heat Transfer Models

Heat can be transferred from one body to another in three separate modes, conduction, convection and radiation or a combination of these three modes. Conduction occurs in a stationary medium; convection requires a moving medium and radiation can occur without any medium

2.1.1 Conduction Heat Transfer:

Conduction can be defined as flow of heat in response to a temperature gradient within an object or between objects that are in physical contact. It occurs in a stationary medium. It is most likely to be of concern in solids, although conduction may exist to some extent in gases and liquids.

Conduction is governed by Fourier's law, which states that *'the rate of flow of heat through a simple homogeneous solid is directly proportional to the area of the section at right angles to the direction of heat flow, and to change of temperature with respect to the length of the path of the heat flow.'*

It is represented mathematically by the equation:

$$Q \alpha A \frac{dt}{dx} \tag{1}$$

where Q = heat flow through a body per unit time (watt)

A = surface area of heat flow (perpendicular to direction of heat flow) m^2

dt = temperature difference of the faces of block (homogeneous solid) of thickness "dx" through which heat flows, ^{0}C or K

dx = thickness of body in the direction of flow, m

Thus,

$$Q = -\lambda . A \frac{dt}{dx} \tag{2}$$

where, λ = constant of proportionality and known as thermal conductivity

The negative sign takes care of the decreasing temperature along with the direction of increasing thickness or the direction of flow. The temperature gradient $\frac{dt}{dx}$ is always negative along positive x direction and, therefore the value of Q becomes positive.

2.1.2 Convection Heat Transfer:

Convection can be defined as a method of transferring heat by the actual movement of heated molecules, usually by a freestanding unit such as a furnace. The conduction heat transfer is governed by Newton's law of cooling [5]

$$Q = hA\left(t_s - t_f\right) \tag{3}$$

where Q = rate of convective heat transfer (watt)

A = surface area

t_s = surface temperature

t_f = fluid temperature

h = convective heat transfer coefficient

During quenching, either gas or liquid quenching convection heat transfer is considered as one of the most important boundary conditions. The most important parameter to consider during convection is the calculation of convective heat transfer coefficient (h).

Convection heat transfer model for gas quenching

Here the objective is to develop a theoretical understanding of the process variables in the gas quenching process for the given part load pattern and further to understand the basic principles of convection heat transfer including estimation of heat transfer coefficient.

The heat transfer during quenching process is expressed by:

$$Q = hA(T_{sur} - T_{gas}) \tag{4}$$

where,

Q is the heat flux from the part surface to quenching gas,
h is the heat transfer coefficient,
A the surface area of the part,
*T*sur and *T*gas are the temperatures of the surface and gas, respectively.

Determination of gas temperature (Tgas): Since it is very difficult to determine the gas temperature close to the workpiece, it can be taken as the average temperature of gas in inlet and outlet channel. [6]

As it can be seen from the above equations, the most important factor for the gas quenching is the calculation of h.

The factors affecting “h” is classified as follows.

- velocity and pressure of the quenching gas,
- alignment between gas flow direction and quenched part,
- Geometry of the part

- types of gasses
- furnace to be used,
- The circulation flow of quenching media (i.e. Reynolds number, Prandtl number, Nusselt number etc.)

The factors affecting "h' can be broadly classified as:

1. Fluid mechanics

There are a variety of ways to characterize the flow. We have to consider what is driving the flow and classify it as forced and natural convection.
Dimensionless groups are used extensively in fluid mechanics in the development of theoretical models in order to determine relationships between parameters.

Nusselt Number(Nu): The Nusselt number represents a dimensionless heat transfer from a fluid flow through a specified boundary surface.

It is represented as: $Nu = \frac{hL}{k}$ (5)

where, h: convective heat transfer coefficient

L: Characteristic length, it is chosen as the system length that most affects the fluid flow. For flow over a flat plate, characteristic length is the length, L. The equivalent length can be calculated by [7] as $L = A^{\frac{1}{2}}$, where A is the surface area of part in m^2

K: thermal conductivity of the fluid.

Thus "h" can be written in terms of Nusselt number, L and k as [8]

$$h = \frac{Nu.L}{k} \quad (6)$$

In the calculation of h, the key point is the determination of Nusselt number, Nu. The problem can be classified into two types, natural convection and forced convection.

Each type of convection can be divided into two cases, according to the parts arrangement[9].

Reynolds number- It is the ratio of inertial and viscous effects and is influenced by fluid properties (viscosity and density), flow conditions (velocity) and geometry (relevant length scale).

It can be represented as: $\mathrm{Re} = \frac{\rho VL}{\mu}$,or $\mathrm{Re} = \frac{VL}{\upsilon}$ (7)

where,

ρ : density

V: velocity

L : characteristic length

μ : Dynamic viscosity

υ : Kinematic viscosity

2. Fluid properties

The dimensionless parameter which is used to represent the affect of fluid properties is the Prandtl number.

Prandtl Number: It is a ratio of viscous and thermal effects and is a function only of fluid properties.

$$\mathrm{Pr} = \frac{\nu}{\alpha} \quad \text{or} \quad \mathrm{Pr} = \frac{C_p \mu}{k} \tag{8}$$

where,

Cp : heat capacity

α : Thermal diffusivity

3. Geometry

The influence of geometry may be seen in a couple of ways. First, for those configurations that have two length dimensions, such as cylinder, we have to introduce a dimensionless geometric parameter.

$$X = \frac{D}{L}$$

$$Nu = f(\mathrm{Re}, \mathrm{Pr}, X)$$

Nu is affected by flow conditions (turbulent or laminar, flow speed, gas thermal properties), part geometry, part alignment in furnace and structure of furnace.

For simple situations these may often be written as power law relationships

$$Nu = a\,\mathrm{Re}^{n}\,\mathrm{Pr}^{m} \tag{9}$$

where the constants a, m and n will change for different geometries

Convection heat transfer model for liquid quenching

The cooling curve produced when a component initially at a temperature well above the boiling point of the quenchant is introduced into the liquid, is much more complex than that suggested by Newton's Law of Cooling. Four distinct stages have been recognized and are as follows.

1. Initial liquid contact stage.
2. Vapor blanket stage.
3. nucleate boiling stage(incorporating transition heat transfer stage)
4. Convective stage.

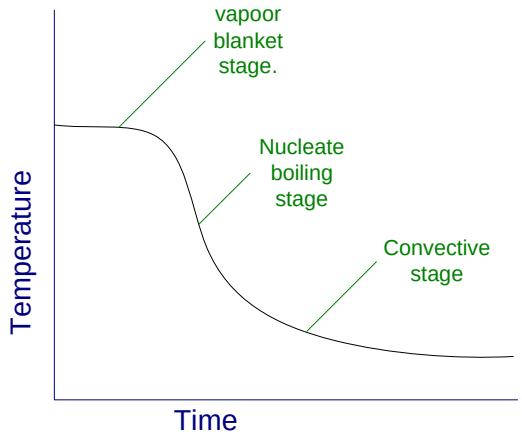

Figure 4. Cooling rate curves for liquid quenching

1. Initial liquid contact stage – This stage lasts for a very short time (about 0.25 sec) and does not register on cooling curves embedded in the specimen. During this time liquid is in contact with a very hot surface, which causes intense boiling of the adjacent loquid. Cooling is extremely rapid, but this process is rapidly terminated as soon as sufficient vapor has been generated to completely surround the surface of the component.

2. Vapor blanket stage - In this stage heat is transferred at a slow rate through the high thermal resistance of the vapor layer. It can be represented by

$$q^{\bullet} = \frac{\lambda}{\Delta x}(\theta_s - \theta_a) \qquad (10)$$

Where Δx is the thickness of the vapor layer and a, refers to ambient temperature.

3. Nucleate boiling stage – In this stage the amount of heat available to vaporize the liquid is insufficient to maintain the blanket, the rate of cooling rises rapidly accompanied by the reappearance of some liquid/solid contact.

4. Convective stage – As the temperature of the component approaches the boiling point of the liquid, the rate of production of vapor falls and the surface heat transfer is reduced

rapidly to the value associated with laminar convective flow. The cooling curve (as shown in the figure) now enters the convective heat flow stage.

2.1.3 Radiation Heat Transfer:

The equation for radiative heat transfer between a surface and its surrounding is given in reference [5]

$$q_{rad} = E\sigma A\left(T_S^4 - T_{Sur}^4\right) \tag{11}$$

where:

q_{rad} = heat flux in watts (W)

E = emissivity, it is a ratio that describes how well a surface emits radiation compared to a perfect emitter.

$\sigma = 5.67 \times 10^{-8}$ W / (m^2 x K^4). It is the Stefan-Boltzmann constant and characterizes radiation from a perfect emitter.

A = surface area in meters squared (m^2).

T_s = Surface temperature in Kelvin (K).

T_{sur} = Surrounding temperature in Kelvin (K)

2.2 Quenching method in production

Several types of quenching processes, i.e oil quenching, gas quenching, salt quenching etc. are used in the industry. In CHT-*q/t* we have broadly described the quenching process as Gas and liquid quenching.

Gas Quenching

Usually two kinds of furnaces are used for gas quenching, hot chamber gas quenching (in the same chamber as of heating), and cold chamber gas quenching (in different chamber as of heating). The advantages of the former are the compact furnace size where as its limitations are the hot chamber (heating elements, insulation, support and accessories) has to be cooled down together with the workload. It is not convenient for continuous production. The advantage of the latter one is faster cooling and it is easier for continuous production. Data from industries indicate that the cooling rate in cold chamber is approximately 30% higher than hot chamber. Its disadvantage is the big furnace size.

The hot chamber furnaces are Quench Pro and HIQ Series [10] by VFS, and Turbo Treater [11] by Abar Ipsen as shown in Figure 5. For cold chamber gas quenching, an external quench chamber is used for quenching. The chamber can be horizontal such as the HEQ series of vacuum furnaces (Horizontal External Quench) vacuum furnace, Turbo Treater by Abar Ipsen and MULTIBAR [12] by Surface Combustion or vertical such as the VEQ series of vacuum furnaces made by VFS, the Metal Master and MulitiMaster by Ispen, as shown in Figure 6. In the vertical chamber, gas quench nozzles are arranged in the hot zone to surround the work load on all four sides for even quench gas distribution. In addition, gas nozzles are mounted on the bottom head panel of the hot zone allowing quench gas to flow up through the work load. Its air flow in the chamber is shown in Figure 7.

(a) The Quench Pro high-pressure quench (QPC) furnace (12 bar)

(b) VFS HIQ Series of vacuum furnaces (Horizontal Internal Quench), single chamber

(c) Turbo Treater by Abar Ipsen

Figure 5. The internal quench

(a) The HEQ Series of vacuum furnaces (Horizontal External Quench), dual chambers

(b) The VEQ Series of vacuum furnaces (Vertical External Quench), single chamber

(c) the Metal Master by Ispen

(d) MultiMaster by Abar Ipsen

(e) MULTIBAR by Surface Combustion

Figure 6. Cold chamber gas quenching

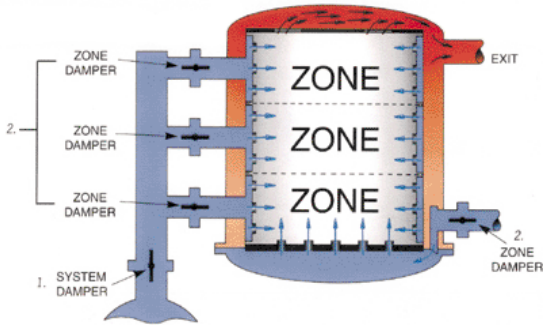

(a) VEQ Series of vacuum furnaces (Vertical External Quench)

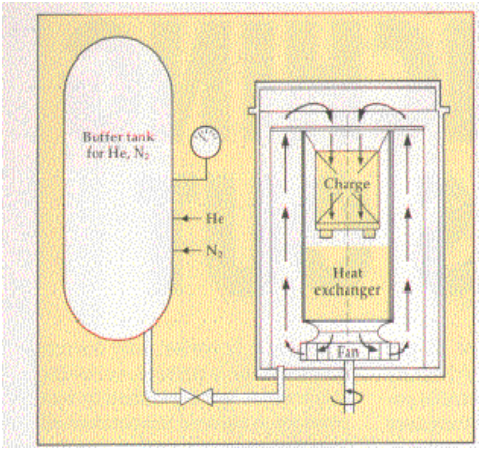

(b) External cold quench chamber

Figure 7. Air flow pattern in external chamber

Work is being done to characterize steel hardenability by a number of researchers including those in Europe. In high-pressure gas quenching applications, the ability to change the quench behavior of gases by varying individual quench parameters (e.g. gas type and composition, pressure; circulation pattern and velocity) play an important role in achieving improved hardenability in high-pressure quench applications. One example is research in the area of development of the gas quench equivalent of the Jominy test[13]

There are a number of probes and other devices designed to measure the heat transfer coefficient within the workload during the gas quenching[14]. The measurement and

recording of the quenching intensity (and heat extraction dynamics) in High Pressure Gas Quenching applications has been solved by using these types of probes.

Another new area is that of controlled heat extraction (CHE) technology [15]. This area explores the possibility of automatically following a predetermined heat extraction (temperature-time) cycle during high-pressure gas quenching. The influence of the heat extraction dynamics on hardness distribution after quenching is being actively studied.

Liquid Quenching

Liquid quenching is classified as:

- **Water quenching:** Water is a good rapid quenching medium, but it is corrosive with steel, and the rapid cooling can sometimes cause distortion or cracking.

- **Salt water quenching:** Salt water is a more rapid quench medium than plain water. However, salt water is even more corrosive than plain water.

- **Oil quenching classification:** Oil is used when a slower cooling rate is desired. Oil quenching results in fumes, spills, and sometimes a fire hazard. Quench tanks are widely used for Oil quenching. In industry several types of quenchant tanks are used. Some common quenchant tanks are:

Figure 8, shows a quench tank which is used for the uniform quenching of hot steels. It may be used with water, light weight polymer, or oil[16].

Figure 8. Quench tank

Figure 9 shows a quench hardening line comprising of salt quench, manufactured by [17]

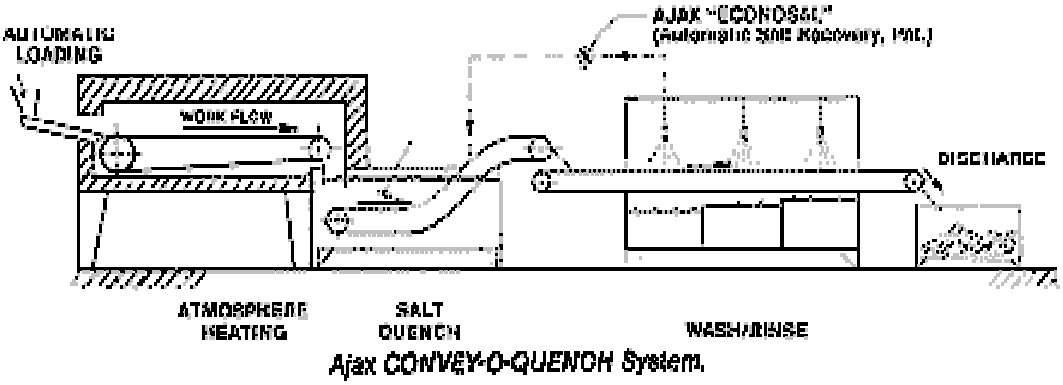

Figure 9. Quench hardening line

- **Polymer quench:** Produces a cooling rate in between water and oil, less corrosive than water and less prone to fire hazard than oil.

The comparison of gas and liquid quenching:

The use of industrial gases for quenching offers significant environmental and performance advantages over oil quenching. For example, handling problems associated with oil such as spillages, or the need for special ventilation systems to take care of vapour exhausts can be eliminated when gas quenching is adopted. Gas quenched parts are clean thus eliminating the need for post-cleaning operations.

In terms of performance, the cooling rate during oil quenching is a function of temperature and can therefore vary dramatically due to the simultaneous presence of three types of cooling; vapour, boiling and convection. This produces large temperature differentials in the parts being quenched. In gas quenching, however, only the convection stage is present thus, cooling rate is less dependent on temperature. Reduced temperature differential and a more uniform cooling rate result in less distortion of parts during quenching. This can further be improved by regulation of parameters affecting the heat transfer coefficient, such as gas velocity, gas pressure and gas mixture. The comparison of the cooling curves of oil quenching and gas quenching is shown in Figure 10.

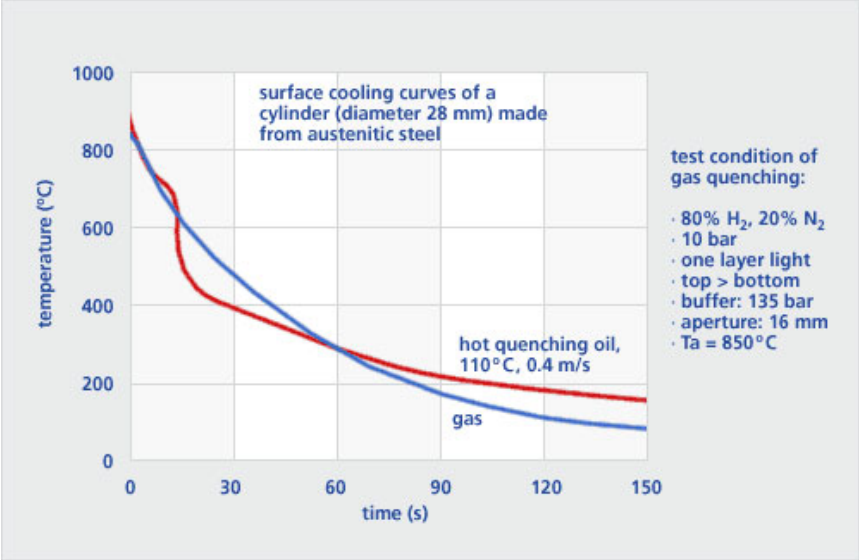

Figure 10. Comparison of gas quenching and oil quenching

High pressure, high velocity gas systems have been developed as alternatives to oil quenching for hardening low alloy steels. These cold quench chambers can use nitrogen to harden thin section parts, while the higher cooling rate properties of helium are needed for thicker sections.

Quenching using hydrogen is also under development due to it's very high heat transfer coefficient, but the stringent safety precautions needed are hindering it's commercialization.

Quench Media	Average -value	Instantaneous -value
Brine or caustic	3500 - 4500	> 15000
Water	3000 - 3900	> 12000
Oil, highly agitated	2000 - 2500	4000 - 6000
Polymmer	1500 - 2000	3000 - 4500
Oil, agitated	1500 - 1750	3000 - 4000
Oil, still	1000 - 1500	
Gas, high pressure	300 - 1000	1000 - 2000
Salt	400- 500	
Air	100 -300	

Figure 11. Comparison of heat transfer coefficient in different quenchants

2.4 Literature Review

As described in the earlier chapters, several softwares are available for the simulation of heat treatment, but there is no complete model which can combine the heat treating process with a part load and furnace model. CHT-*q/t* is an approach to fulfill the industrial need of a ready to use heat treating software. The new developed model in CHT-*q/t* is the quenching and property prediction model, other models such as heating was much taken from CHT-*bf* and CHT-*cf*. This section focuses the research work on determination of convective heat transfer coefficient, microstructure evolution, residual stresses and distortion during quenching and finally the tempering process.

Analytical method for the Calculation of Convective Heat Transfer Coefficient:

Several methods have been proposed by the researchers to analytically determine the convective heat transfer coefficient in the furnace. In CHT-*q/t* database approach for convective heat transfer has been used. One such analytical method has been described below.

Description of the nozzle-field gas-quenching device [18]:

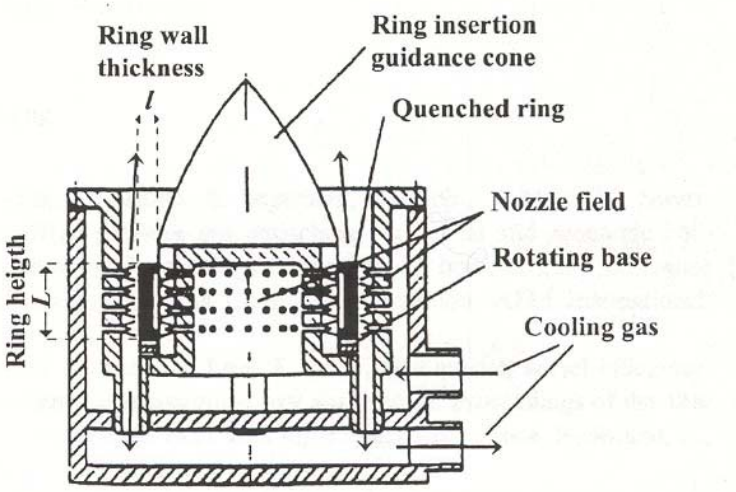

Figure 12. Nozzle-field gas quenching device

The figure shows a commercial nozzle-field gas quenching system. After austenitization, the rings are placed one at a time in the device for quenching. The air (or nitrogen) at approximately atmospheric pressure is blown into the device. The air passes at high speed through the inner and the outer nozzle fields and impinges on the inner and outer faces of the rings. It then exits the device in the upward and downward directions. The ring lies on a rotating base, which makes it spin, improving the uniformity of cooling. The gas jets formed in this way generate high heat transfer rates between the ring and the air.

In the design t = 5 mm, d = 1 mm and H = 5 mm. if we assume an air jet velocity of 100 m/sec and 1 bar at the exit, the jet Reynolds number, *Re*, is about 7000.

They proposed the value of "h" as:

$$h_{av} = \frac{k_g}{d}\left[1+\left(\frac{H/d}{0.6}\sqrt{f}\right)^6\right]^{-0.05} \times \frac{\sqrt{f}\left(1-2.2\sqrt{f}\right)}{1+0.2\left(H/d-6\right)\sqrt{f}}\,\mathrm{Re}^{2/3}\,\mathrm{Pr}^{0.42} \qquad (12)$$

where,

f is the relative nozzle area, given by the ratio of the nozzle exit cross-section to the area of the inline or the hexagon attached to it.

For inline arrays of jets:

$$f = \frac{1}{4}\frac{\pi d^2}{t^2} \tag{13}$$

And for staggered arrays of jets

$$f = \frac{1}{6}\frac{\pi\sqrt{3}d^2}{t^2} \tag{14}$$

d: jet diameter (m)

h: heat transfer coefficient ($W/m^2/K$)

H: jet to plate distance (m)

t: jet pitch, m (or time, s)

k_g: thermal conductivity of gas.

Range of validity is $2000 \le \mathrm{Re} \le 100000$, $0.004 \le f \le 0.04$

Microstructure evolution and determination of volume fraction

Several methods have been proposed by researchers to calculate the volume fraction of microstructures evolved during the quenching process, which when applied to analytical equations, can predict the mechanical properties. The analytical approach and equations can be generalized for all the grade of steels, which is the approach in CHT-*q/t.* Sometimes a particular set of equations can be used for a specific steel. One such approach is described below.

In the case of carbon steel S45C, the volume fraction of pearlite ξ_p is expressed as [19]

$$\xi_p = 1 - \exp\left\{-\int_0^t f_1(T) f_2(C) f_3(\sigma)(t-\tau)^3 d\tau\right\}, \tag{15}$$

$$f_1(T) = a_0\left(\frac{T - a_1}{a_2}\right)^{a_3}\left(\frac{a_4 - T}{a_5}\right)^{a_6}, \quad (16)$$

$$f_2(C) = \exp\{-a_7(C - C_0)\}, \quad (17)$$

$$f_3(\sigma) = \exp\{a_8\sigma_m\}, \quad (18)$$

Where σ_m is mean stress, C and C_0 the current and initial carbon contents, respectively, and a_i (i = 0, 1, 2… 8) are some transformation kinetic parameters.

Diffusionless transformation is controlled by

$$\xi_M = 1 - \exp\{\phi_1 T + \phi_2(C - C_0) + \phi_3(N - N_0) + \phi_4\sigma_m + \phi_5\sigma_e + \phi_6\}, \quad (19)$$

Modified Magee's rule, where ξ_M is the volume fraction of martensite, ϕ_i (i = 1, 2,……..,6) are material parameters. N and N_0 mean the current and initial nitrogen contents (wt. %) in the nodes, respectively.

Relationship between Martensitic start (M_S) temperature and Chemical composition:

$M_s = 512 - 453C - 16.9Ni + 15Cr - 9.5Mo + 217(C)^2 - 71.5(C)(Mn) - 67.6(C)(Cr)$ (20)

Effect of alloying elements on M_S temperature:

Table 1. Alloying elements effect on M_s temperature

Al	Increases M_S temperature
Co	Increases M_S temperature
C	Decreases M_S temperature
Cu	Decreases M_S temperature
Ni	Decreases M_S temperature
Cr	Decreases M_S temperature
Mo	Decreases M_S temperature
Mn	Decreases M_S temperature

Effect of carbon content on Martensitic start (M_s) temperature:

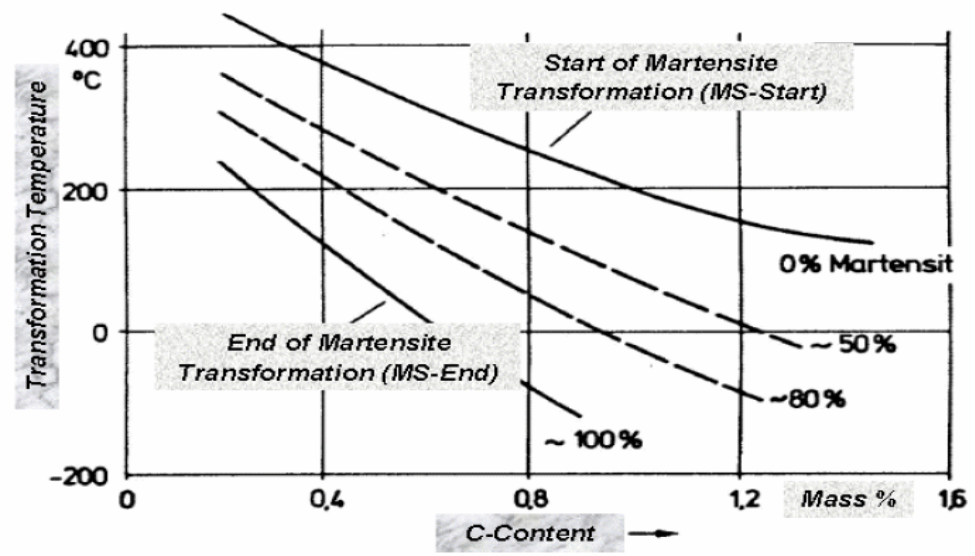

Figure 13. Effect of carbon content on martensitic start (M_s) temperature

Cooling rates has no effect on M_S temperature but M_f temperature is dependent on the cooling rate. Slower cooling rates results in decrease of M_f temperature.

Martensite microstructure of particular steel has a slightly higher specific volume (lower density) than the same steel with ferrite-pearlite microstructure.

Residual stress during quenching:

Residual stresses are three-dimensional and result in visible distortion of a component. The distortion can be useful in estimating the magnitude or direction of the residual stresses. Residual stresses are induced in steel and other high strength alloys during quenching. These residual stresses arise from two different sources [20]:

- The large temperature gradients and the accompanying plastic deformations on a macroscopic scale.
- The solid state phase transformations and the attendant volumetric dilatation as well as the plasticity on a microscopic scale. This is also referred to as transformation plasticity.

The phase transformation is accompanied by two effects:

- A volumetric change.
- Pseudo-plasticity or the so-called transformation plasticity.

Effect of stress and chemical composition on microstructure transformation:

The effect of stress has been found on the bainitic and martensitic transformation during quenching [21]. John-Mehl-Avrami equation is used to depict the transformation kinetics of bainitic transformation, in which effects of stress and chemical composition on transformation kinetics are taken into account [22, 23],

$$\zeta_b = 1 - \exp\left\{- f\left(T, \sigma, C_{eq}\right) t^{n(T)}\right\}, \tag{21}$$

$$f\left(T, \sigma, C_{eq}\right) = 2.3166 \times 10^{-2} \exp\left(-\frac{628.5}{T}\right) C_{eq}^{-16.1506} \times \left[1 + 3.9245 \times 10^{-2} \exp\left(-\frac{568.1}{T}\right) C_{eq}^{-0.124} \sigma_e\right] \tag{22}$$

$$n(T) = 2.5119 - 2.6375 \times 10^{-3} T \tag{23}$$

where, ζ_b is the volume fraction of bainite, T is temperature, and σ_e and C_{eq} mean equivalent stress and carbon equivalent, respectively. Displacive transformation is controlled by Magee equation with the equations

$$\zeta_M = 1 - \exp\left[-1.3474 \times 10^{-2} \left(1 + 3.7348 \times 10^{-3} \sigma_e\right)\left(M_s - T\right)\right] \tag{24}$$

for 26Cr2Ni4MoV [23] and

$$\zeta_M = 1 - \exp\left[-1.7989 \times 10^{-2} \left(1 + 2.0247 \times 10^{-3} \sigma_e\right)\left(M_s - T\right)\right] \tag{25}$$

for 30Cr1Mo1V [23], where ζ_M denotes volume fraction of martensite, and M_s is martensite start temperature.

Distortion during quenching

It is known that, during the cooling part of the quenching process, distortion occurs at high temperature (at the beginning of cooling), while residual stresses essentially develop at low temperature (at the end of cooling) [24]. The numerical simulation to quantify the risk of distortions or cracks during quenching requires a very large amount of data, such as the phase transformation curves, mechanical properties of each constituents, heat exchange coefficients, etc [24]

It is seen that that when austenite begins to transform into martensite it generates a thermal expansion [24].

Quenching distortions of metallic components are mainly due to:

- Plastic deformation, induced by thermal gradients, which are often referred to as "classical plasticity".
- Plastic deformation produced by phase changes, which is often called "transformation plasticity".

Factors leading to dimensional problem after quenching: [25]

- Variation in structure and composition present in the steel blank.
- Movement due to the relief of residual stress.
- Creep of the part at temperature under its own weight.
- Gross differences in section causing differential heating and then during cooling by quenching.
- Volume changes due to phase transformations.
- Differences in heat abstraction within the part during quenching due to variable agitation and part geometry.
- Coefficient of expansion during heating and cooling.

Tempering

Martensite is hard, brittle phase, in fact so brittle that a product of 100% martensite would be impractical. A common approach to reduce this is therefore to reheat carefully to a temperature to form equilibrium phases such as $\alpha - Fe$ and Fe_3C. This process is

called tempering. Tempering is associated with a decrease in hardness and increase in ductility.

A possible problem with conventional quenching and tempering is that the exterior of the workpiece will cool faster than the interior. Therefore, the exterior transform to martensite before the interior. During the period of time in which the exterior and interior have different crystal structures, significant stresses may occur, the result can be distortion and cracks. The problem can be solved using heat treatments known as martempering and austempering, which is discussed in detail in chapter 4 and further can be found in books in material science, Schakerfold[26], or Callister [27].

Time and temperature relationships in tempering

The softening of steels by tempering is considerably affected by the effect of time interval at tempering temperatures. Figure 14 shows the incredible rapid softening during the first few minutes in an 0.82% carbon, quenched steel at 1200^0 F. It is well known that most of the softening action occurs in the first few minutes and that little further reduction of hardness results from increasing the time of tempering from, say, 30 minutes to 2 hours.

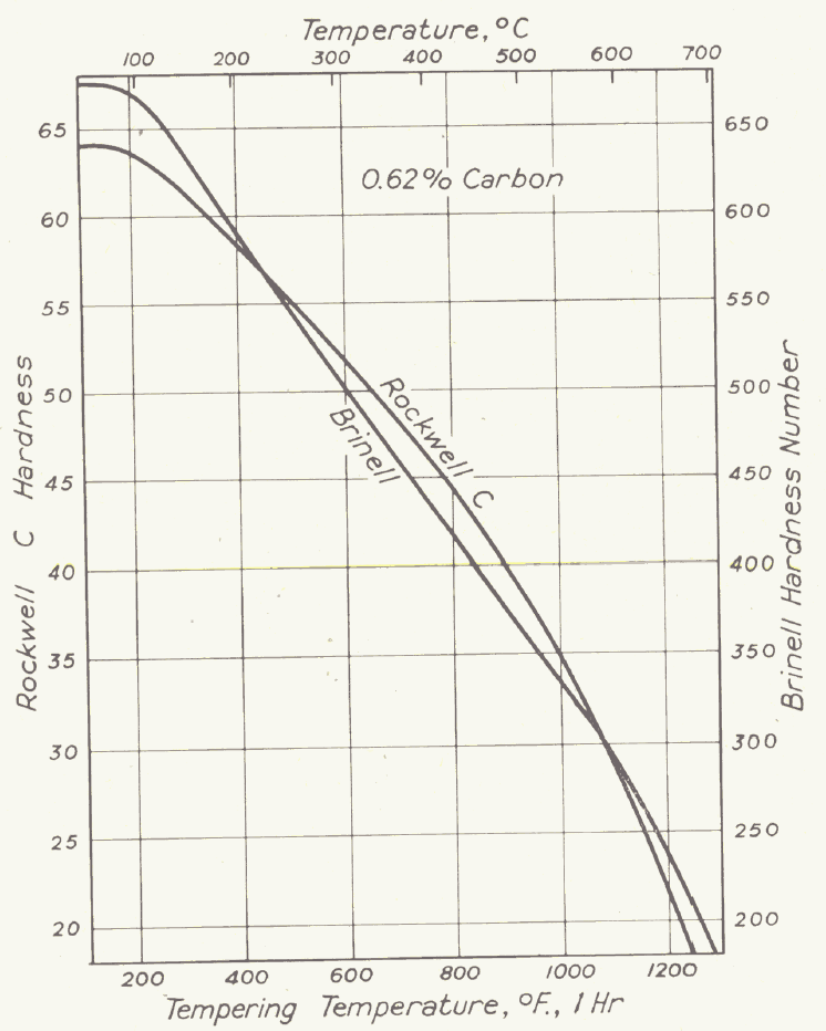

Figure 14. The effect of tempering for 1 hour at various temperatures upon hardness of a 0.62% carbon steel.

Several empirical relationships have been made between the tensile strength and hardness of tempered steels such that the measurement of hardness is commonly used to evaluate the response of steel to tempering. Figure 15 shows the effect of tempering temperature on hardness, tensile and yield strengths, elongation, and reduction in area of a plain carbon steel (AISI 1050) held at temperature for 1 h [28]. It can be seen that both room temperature hardness and strength decrease as the tempering temperature is increased. Ductility at ambient temperatures, measured by either elongation or reduction in area, increases with tempering temperature. The properties summarized are for one heat of

1050 steel that was forged to 38 mm (1.50 in.) in diameter, then water quenched and tempered at various temperatures. Composition of heat: 0.52% C, 0.93% Mn

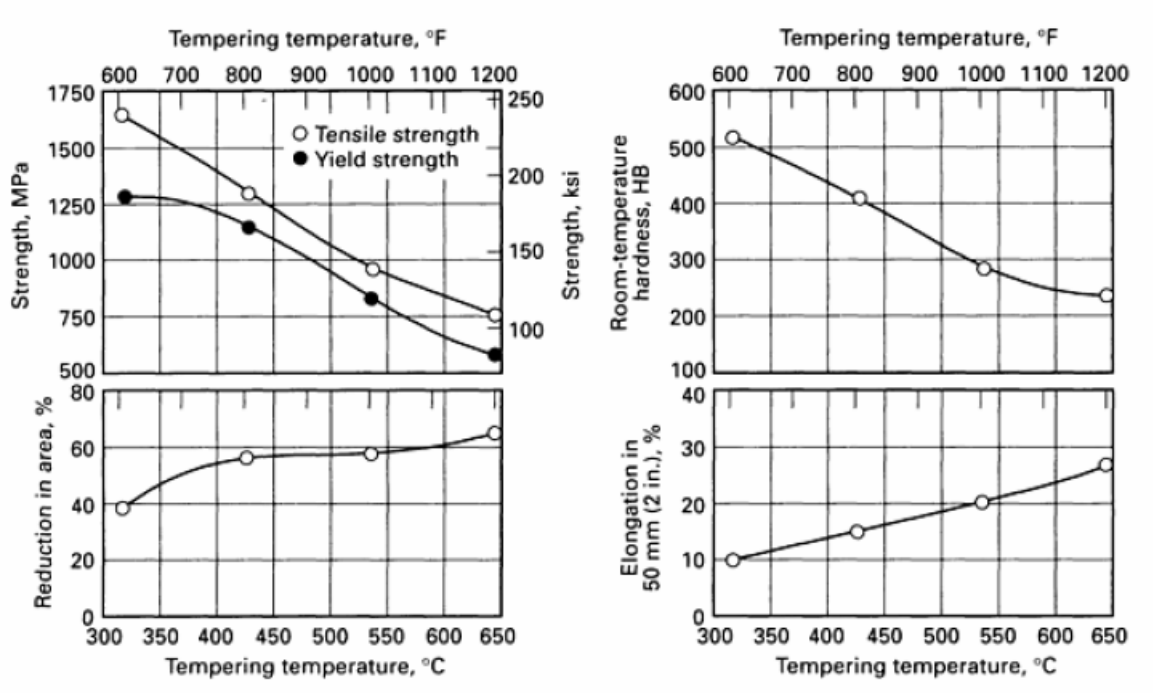

Figure 15. Effect of tempering temperature on room-temperature mechanical properties of 1050 steel

Most medium-alloy steels exhibit a response to tempering similar to that of carbon steels. The change in mechanical properties with tempering temperature for 4340 steel [29] is shown in Figure. 16

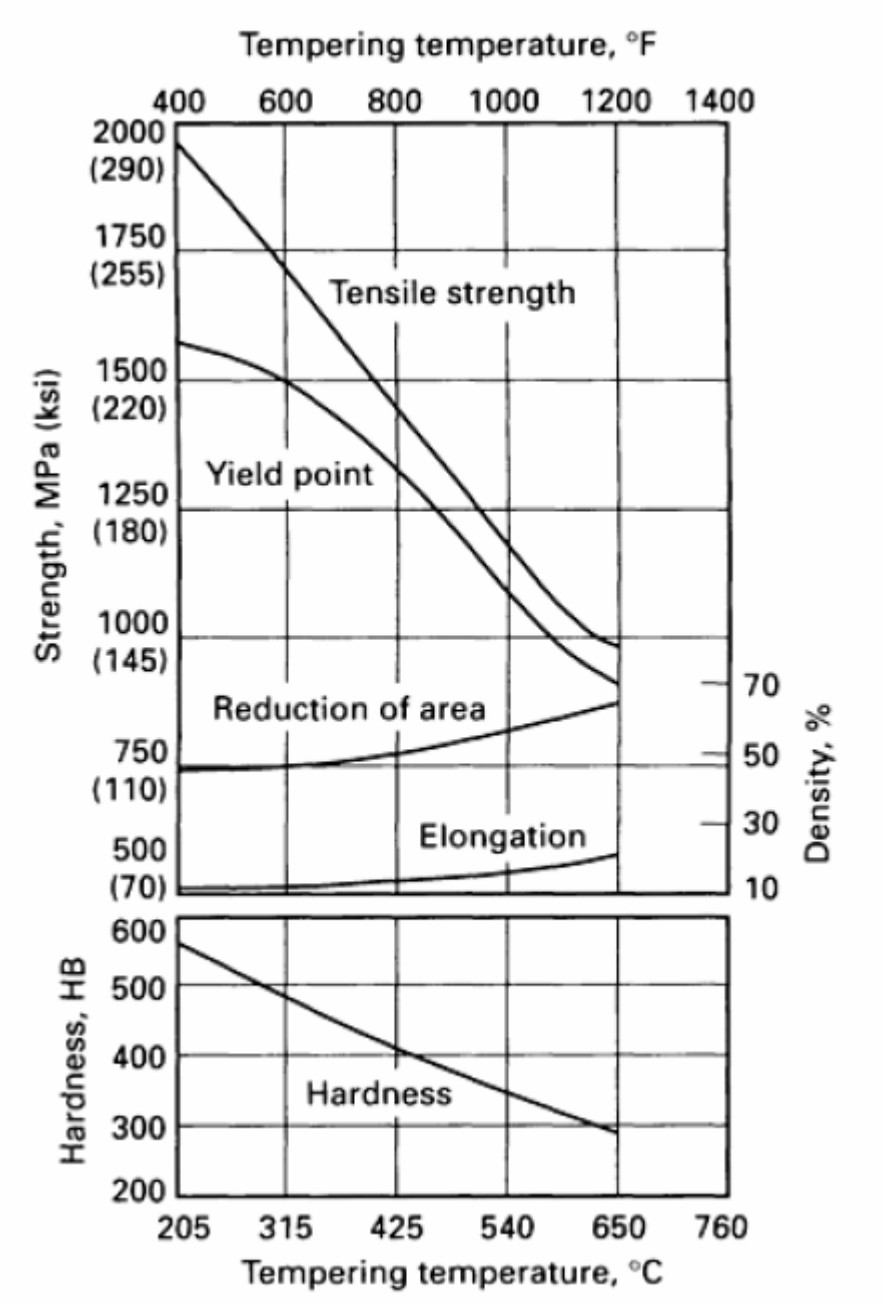

Figure 16. Effect of tempering temperature on the mechanical properties of oil-quenched 4340 steel bar.

Conclusion

The literature review reviews the approach adopted by various researchers to analytically determine the convective heat transfer coefficient, microstructure evolution and stress developed during quenching. While it has been observed the role of residual stress during the microstructure evolution in the quenching processes, it has not been considered in CHT-*q/t,* to generalize it for all the types of steel rather than limiting it for a specific case. CHT-*q/t* deals with some approximation such as, grain size, incubation time before microstructure evolution and the stress developed during quenching has not been considered. A database approach has been adopted for the convective heat transfer coefficient rather than analytical approach, to increase the applicability of the software to various furnaces. This approach can be justified, as the goal of CHT-*q/t* is its wide application in furnace and materials. Thus, CHT-*q/t* has been developed to corroborate the industrial need by using the previous research and some new approach, as discussed in further chapters.

CHAPTER 3. SYSTEM OVERVIEW

CHT-*q/t* is a software tool to predict the temperature profile of load in batch as well as continuous furnace during heating, quenching and tempering of steel, then to predict the mechanical properties as Quenched & Tempered and finally to optimize the heat treatment process design.

3.1 System Function & Flow Chart

A system flow chart, or data flow chart, is used to describe the flow of data through a complete data-processing system. It is a graphic illustration of the physical flow of information through the entire accounting system. A systems flowchart is commonly used in analysis and design. Flowlines represent the sequences of processes. The system flowchart of CHT-*q/t* is shown in Figure 17.

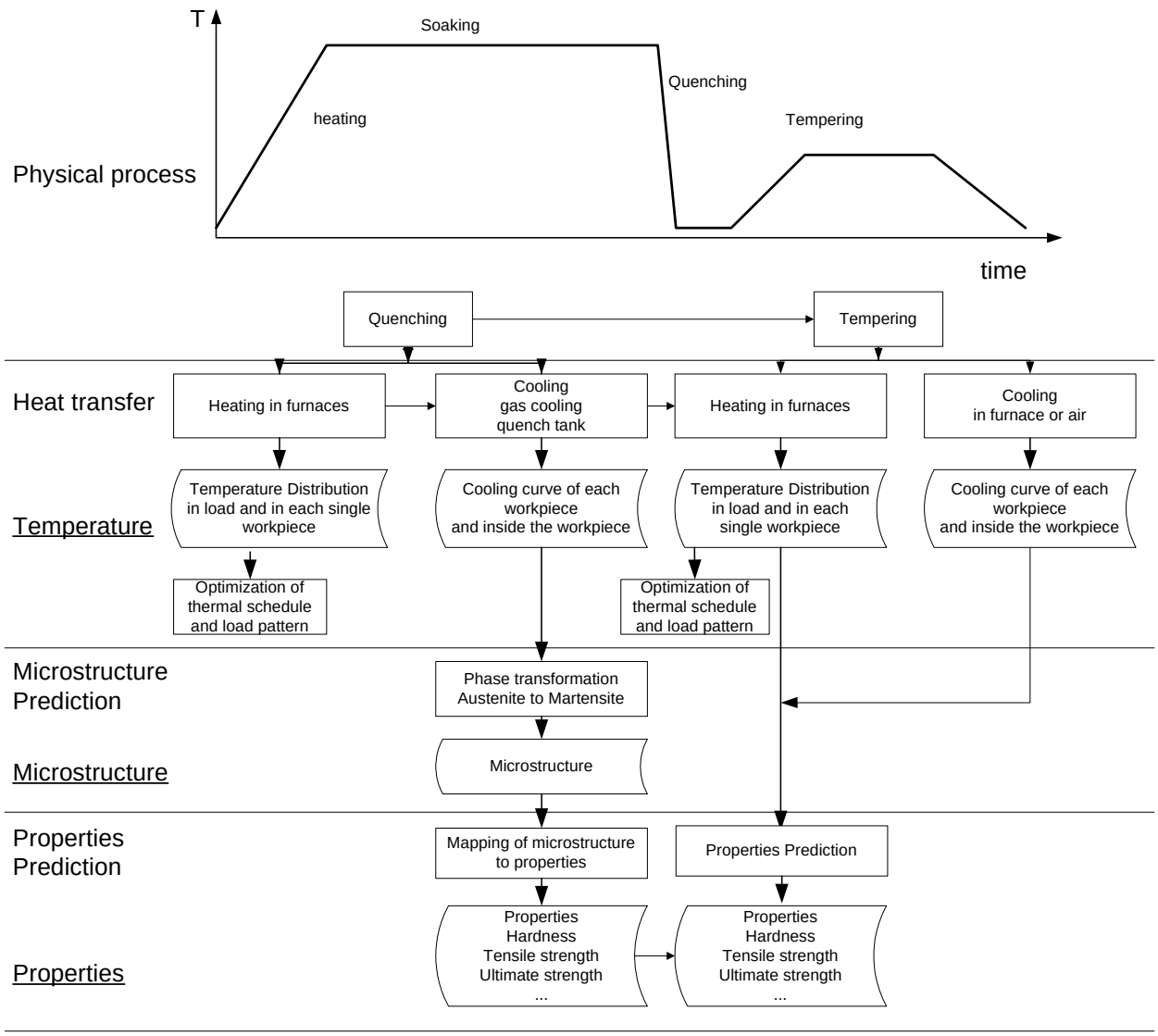

Figure 17. System flowchart

The software consists of mainly five modules: workpiece definition, furnace definition, load pattern, thermal schedule and calculation & report. The file management and database & database management serves the foundation of the software. These five modules have been explained in six function modules. Its structure is shown in Figure 18 and the contents of six function modules is explained in Figure 19.

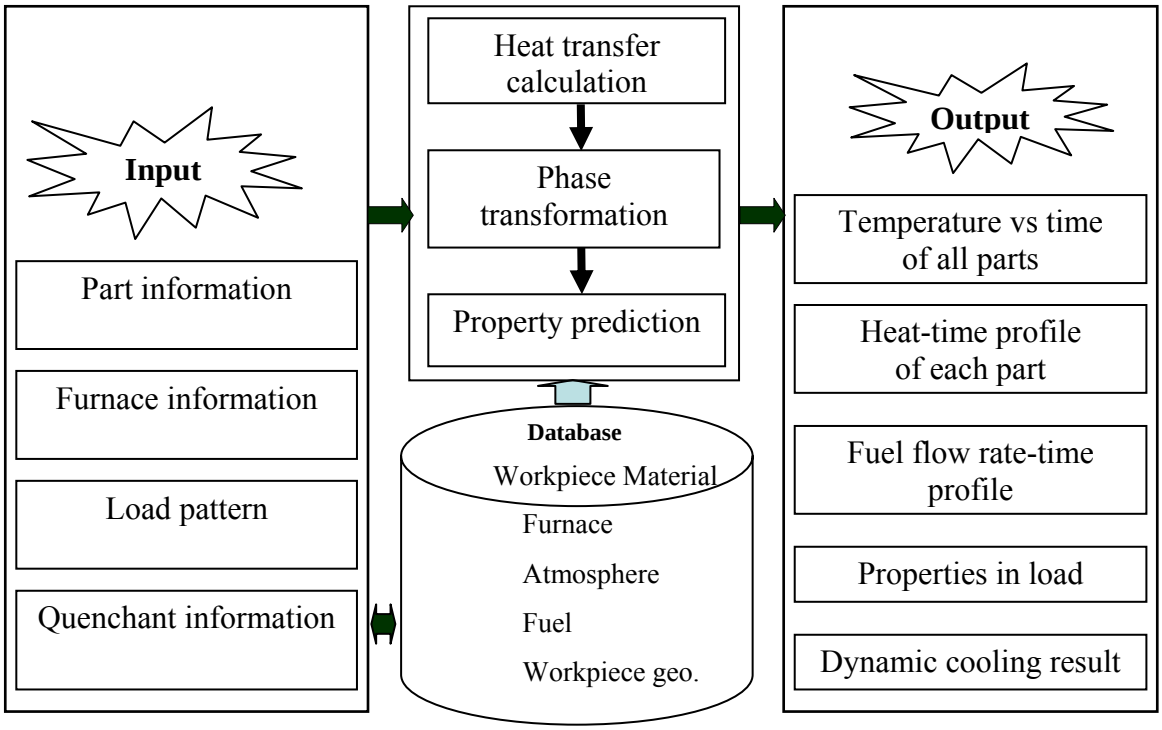

Figure 18. System structure

Function flow chart

The function flow-chart describes the modules, databases and output results of CHT-*q/t*. It depicts the specific database module required for each function modules and their output. The function flow chart describes the flow of the function modules as well.

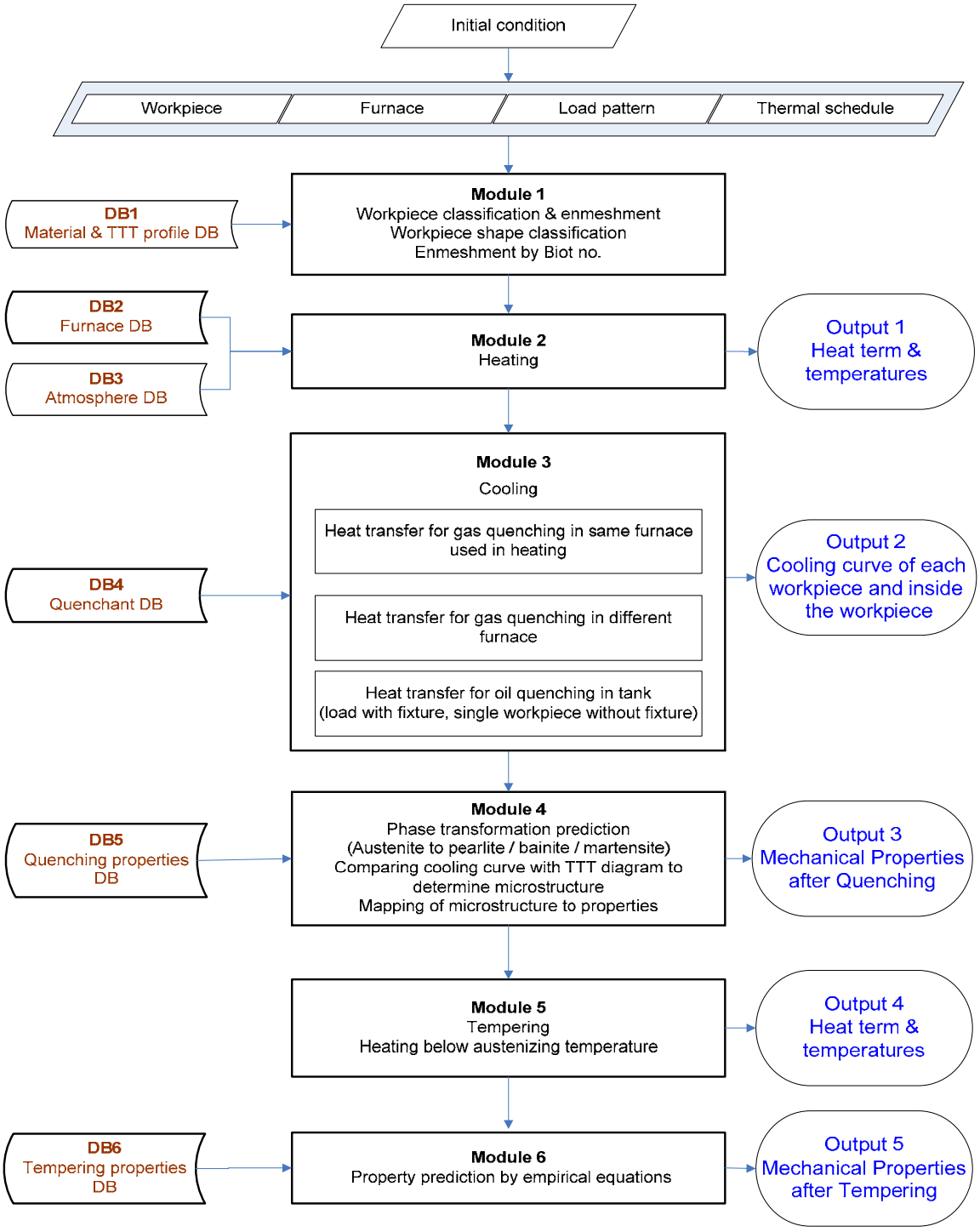

Figure 19. Function flow chart

CHT-*q/t* contains six function modules, which are explained as follows:

Function Module 1 – Workpiece classification & enmeshment: Workpiece enmeshment by Biot number (Bi).

a) Bi < 0.1 (small) – Lumped analysis, no enmeshment of workpiece
b) 0.1 < Bi < C (medium) - 1D enmeshment.
c) Bi > C (large) – 3D enmeshment, Where C is a constant,

For heavy sectioned workpiece with large Biot number, the temperature distribution inside the workpiece should be considered during heating and cooling process (especially in the quenching process to predict microstructure distribution inside the workpiece).

Function Module 2 – Heating: This module will consist of heat transfer equations (conduction, convection & radiation) during heating.

1. Conduction inside the workpiece.
2. Conduction between workpieces.
3. Convection between furnace & workpiece.
4. Radiation between workpieces.
5. Radiation between furnace & workpiece.

Function Module 3 – Cooling & Quenching: This module will consist of heat transfer equations (conduction, convection & radiation) during cooling. Radiation will not be considered during liquid quenching in tanks.

1. Conduction inside the workpiece.
2. Conduction between workpieces (except in case of single workpiece in liquid quenching)
3. Natural & Forced Convection (high pressure, high velocity gas & oil quenching)
4. Radiation between workpieces.
5. Radiation between furnace & workpiece.

Function Module 4 – Phase Transformation: This module will consist of basic equations used to describe the phase transformations (involving diffusional and diffusionless transformation) during quenching. It will also contain the method to determine the mechanical properties from the given microstructure.

Function Module 5 – Tempering Property prediction – Mapping of the properties from the Tempering property database.

3.2 System Interface

While most of the system interface is same as of CHT-*bf* and CHT-*cf*, there are major changes in the furnace definition and calculation & result page which are described in this thesis.

The first screen of the system conveys the name and different modules of the system.

Figure 20. The cover page / welcome screen of CHT-*q/t*

Workpiece definition

The workpiece definition page is similar to earlier versions except a new addition in the database to include TTT diagrams for the property prediction. Based on the material selected the TTT diagram is displayed. Figure 21 shows the change.

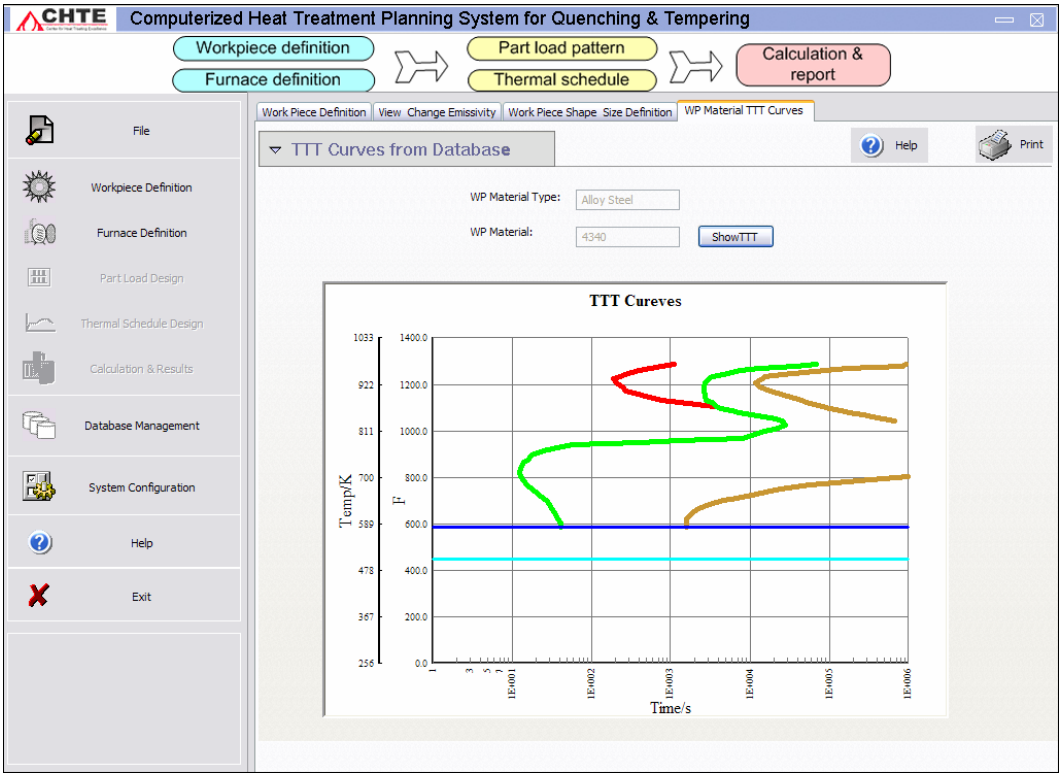

Figure 21. Workpiece definition (new addition TTT curves)

Furnace definition

The furnace definition module in CHT-*q/t* comprises of both batch as well as continuous furnace for heating. For cooling the furnace may be same as that of heating with a separate chamber for cooling or it may be tank for liquid quenching. The furnace definition contains five pages. The new design allows user to select different furnaces for heating and tempering.

Furnace definition includes five pages. Furnace image and the middle three pages are loaded directly from the furnace database. User can check and edit the values according

to users' request. Fuel, atmosphere settings are independent on the furnace database. Fuel type, atmosphere and other material selections are directly lined with respective database.

The figure below shows the first page of furnace definition. In this page, the user has the option to select the furnace for heating, quenching as well as tempering.

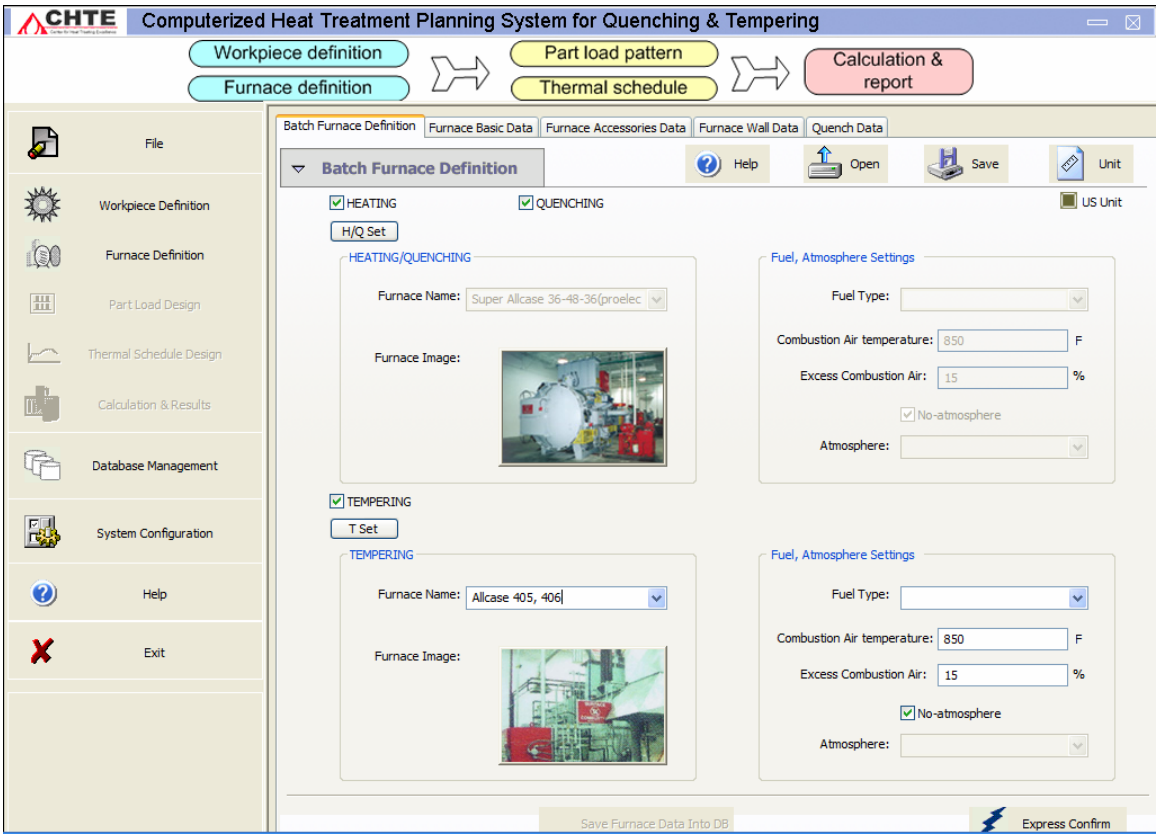

Figure 22. Furnace definition 1

The next three pages of the furnace definition are same as that of CHT-*bf* and CHT-*cf* .

The last page of the furnace definition represents the quench data.

The figure below shows the furnace definition page 5 for quench data.

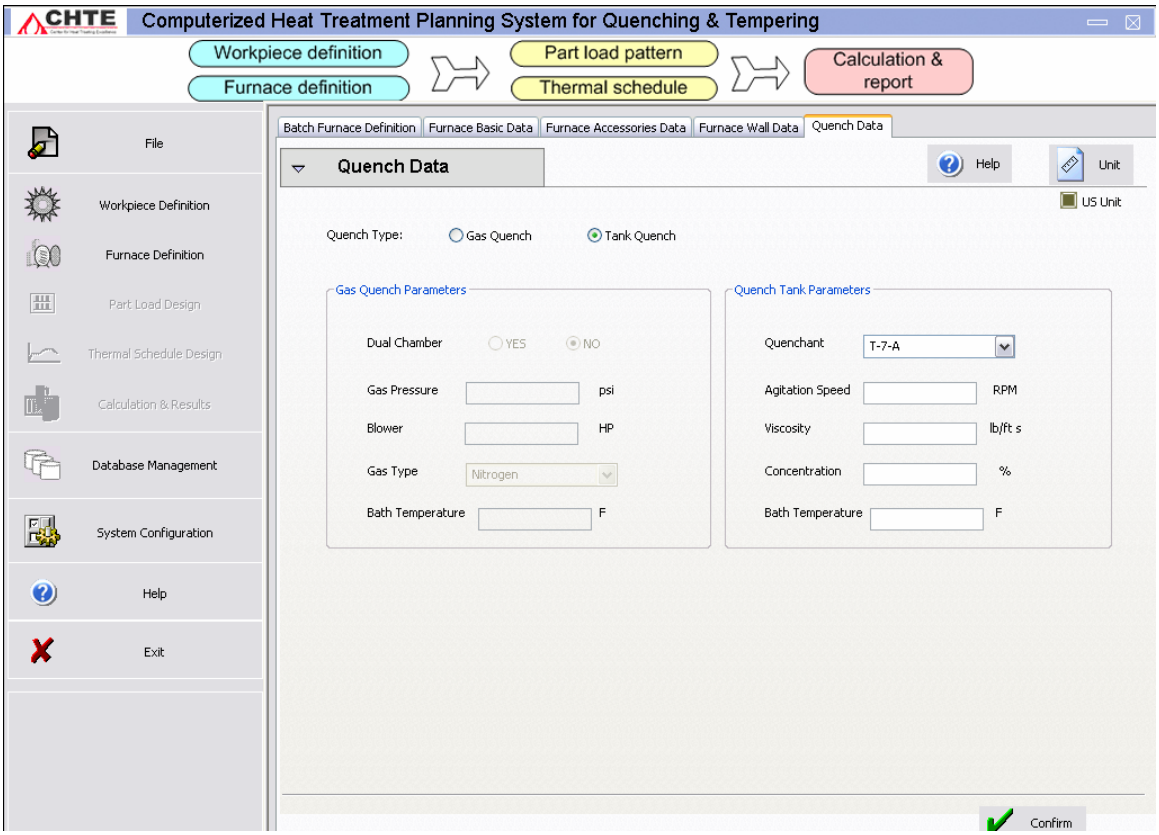

Figure 23. Furnace definition page 5

This page contains information for gas as well as tank quench. Radio buttons are used to activate either gas or tank quench. User has to input the parameter for gas and tank quench. The parameters required for Gas quench are gas pressure, blower horse power, gas type and bath temperature. Parameters used for quench tank are Agitation speed, viscosity, concentration and bath temperature.

Load pattern definition

Load pattern consists of fixture configuration and the part configuration. Fixture configuration consists of fixture shape and type. Part configuration consists of arrangement of workpiece in the fixture. The interface of load pattern definition is same as that of CHT-*bf* and CHT-*cf*.

Thermal schedule definition

The thermal schedule page is where the recipe / thermal schedule for the process is specified. The new input functions to specify the quenching and tempering are added, as shown in Figure 24.

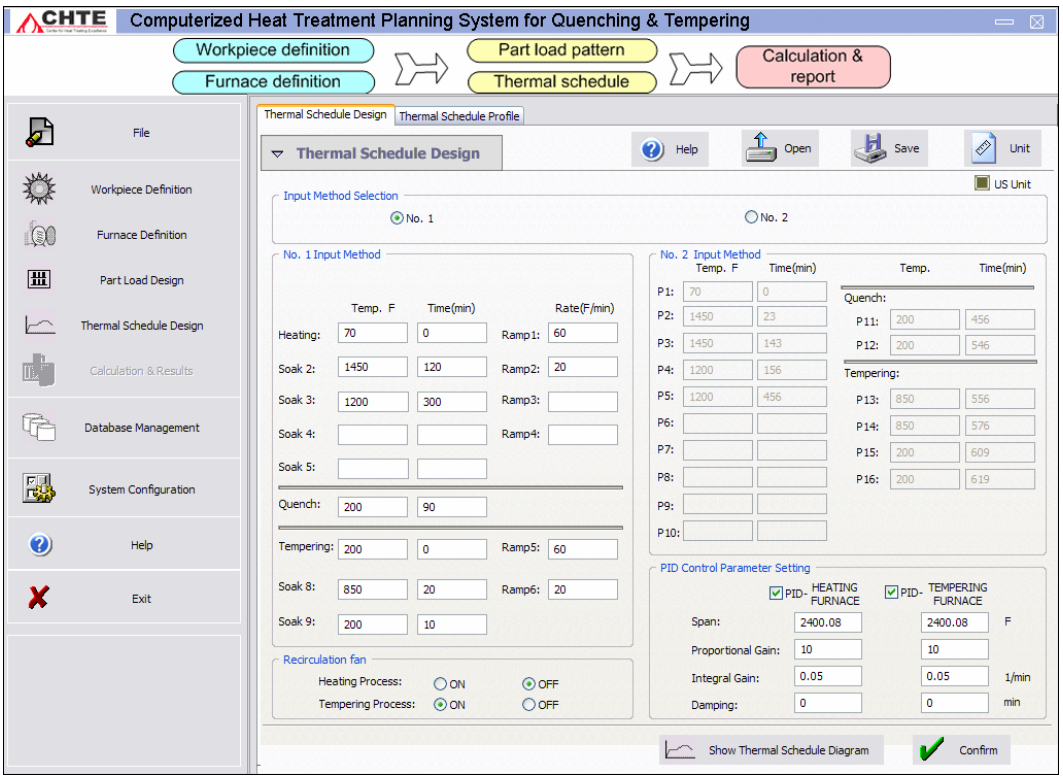

Figure 24. Thermal schedule definition

Calculation & results

It contains seven pages. Temperature profile, heat-time profile and fuel flow rate-time profile are the same as used in CHT-*bf* and CHT-*cf*.

As the objective of CHT-*q/t* is to provide information for the mechanical properties of the part load as quenched, three pages have been included to illustrate that.

The figure below shows the first page of calculation and result. As shown below here user has the option to input initial furnace and load temperature for heating, quenching as well as tempering.

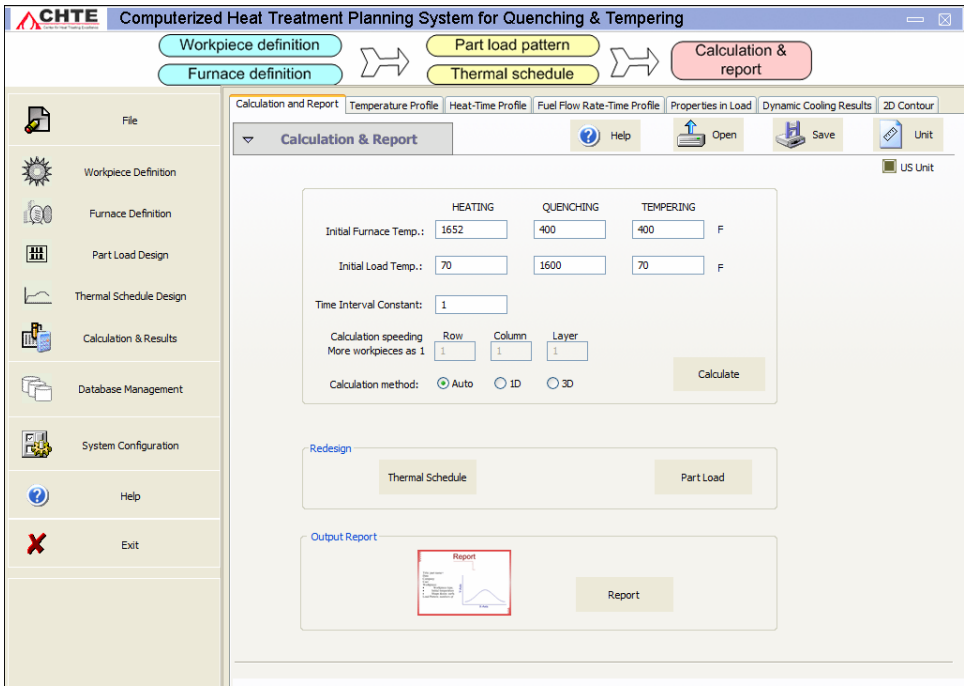

Figure 25. The first page of calculation and results.

The figure below shows the temperature-time profile.

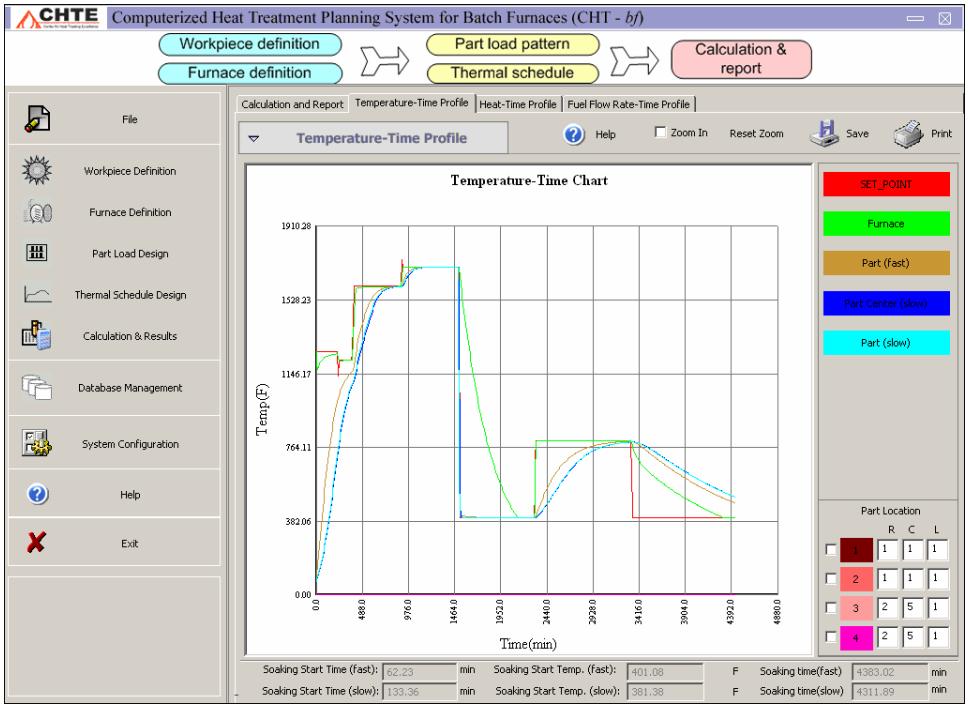

Figure 26. Temperature-Time profile

Properties on load

This page shows the distribution of various mechanical properties on the load.

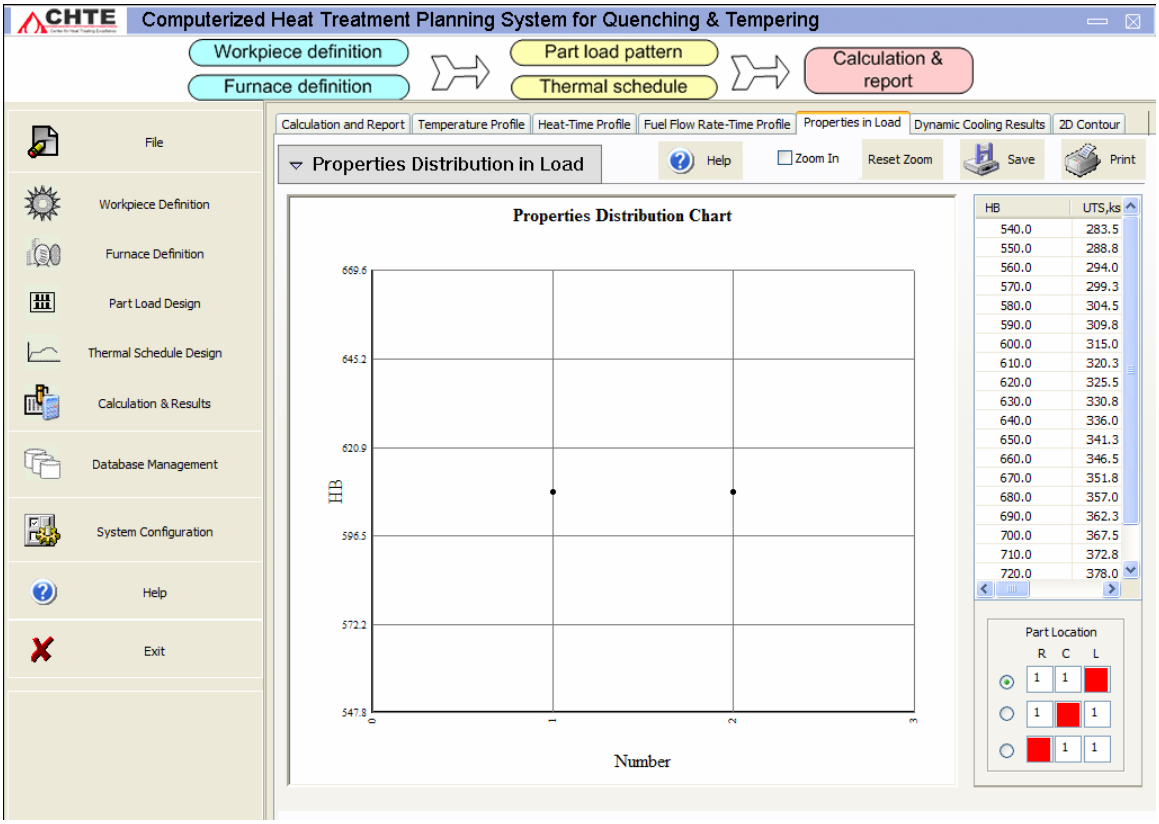

Figure 27. Properties distribution chart

Dynamic cooling results

This page gives a visual image of the cooling curve embedded on the TTT diagram. User can pick any part by select ‘Row’, ‘Column’, ‘Layer’ number, and show its cooling curves together with the material TTT diagrams. Also the properties prediction results are shown beside. In this case, user can directly find out how the temperature of the part changes vs. time, and most important the phase transformation situation depend on the cooling position in the TTT curves. It has option to show or hide the cooling curve.

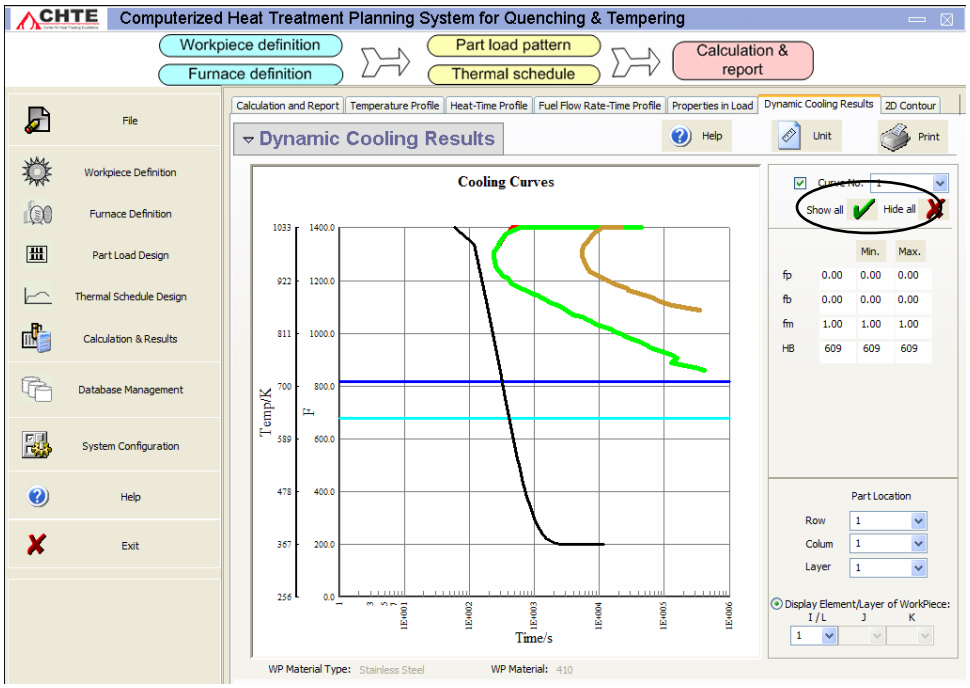

Figure 28. Dynamic cooling results.

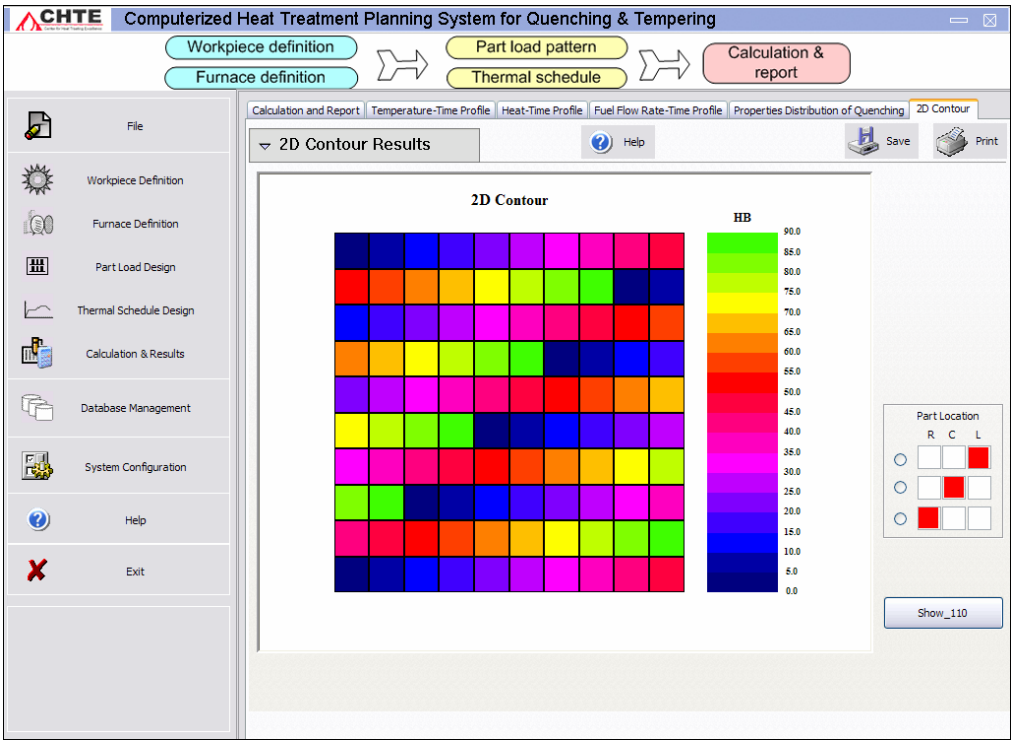

Figure 29. Hardness distribution of workpiece.

After much of research, brainstorming and consultation with the focus group members the above shown interfaces were designed. The basic aim of designing the interfaces were to provide an user friendly and well defined interface which can give maximum possible information whithout going through the laborious process of data entry and report reading. The user has the option to browse through the help file and save each page of the system. The help file is made into html files , when the user presses the help key in each dialog the relative help file appears in web style. The system contains different modules and all the modules are supported by a rich database. Every effort was made to keep the system interface in the same format as that of CHT-*bf* and CHT-*cf,* thus making it simpler for th users having worked with CHT-*bf* and CHT-*cf*.

3.3 Database Design

A database is a collection of information stored in a computer in a systematic way, such that a computer program can consult it to answer questions. The software used to manage and query a database, is known as a database management system (DBMS). Database software, such as Microsoft Access, FileMaker Pro, and MySQL is designed to help organize large amounts of information in a way where the data can be easily searched, sorted, and updated. A database is typically made up of many linked tables of rows and columns.

3.3.1 Database of CHT-*q/t*

CHT-*q/t* works on many data values of material properties, furnace materials, TTT diagram for property prediction, quenchants etc. This data is stored in an easy format for editing and adding using Microsoft Access. The database is developed with the relationships among the various properties. The database management system makes it easy to add new data and edit the existing data.

The contents of the CHT-*q/t* database are described below.

1. Workpiece material and properties

2. Workpiece shape
3. Furnace Data
4. Furnace atmosphere
5. Furnace fuels
6. Quenchants

Database Management is the most important attribute of CHT-*q/t*. The consideration of non-linearity of the material properties i.e thermal conductivity and specific heat makes it technically robust and complete. The data collection was a tedious task, and it had been collected from variety of source including literatures, ASM Handbooks and the data source of Professor Richard Sisson's research work. The technical focus lies in the fact that database captures the whole heat treating procees by Different database managers, e.g the quenchant database considers the variation of conductive heat transfer coefficient with respect to temperature, which is the most important aspect in quenching.

3.3.2 Structure

The data in the database are stored in form of tables. Some of the data values in the database are inter related and inter dependent (i.e quenchant values depend on the temperature), which justifies the tabular form of database. Each table has set entities which are presented in the column. Although care has been taken to include most of the relevant data, but still the user has the option to include data in the database.

3.3.3 Material and Properties Database

The material database consists of all kinds of metals as shown below in Figure 30. The materials database is used for defining the workpiece material, the fixture material, the furnace accessories material and the furnace wall material. Different properties of the materials are required to be input in the system for calculations. The property values are stored in the database and can be viewed and modified as required by the user. The database currently holds data of more then 2000 materials and its properties. Time

Temperature Transformation (TTT) diagram of Carbon steel, Alloy steel, Tool steel and stainless steel is included in the database, thus restricting the workpiece material to these steel only.

	MT_INDEX	MT_TYPE
▶	1	Carbon Steel
	2	Alloy Steel
	3	Tool Steel
	4	Stainless Steel
	6	Cast Aluminum
	7	Wrought Aluminum
	8	Pure/Low Alloy Nickel
	9	Nickel-copper Alloy
	10	NonMetals
	11	Ni-Cr & Ni-Cr-Fe Alloy
	12	Fe-Ni-Cr Alloy
	13	Controlled Exp Alloy(Ni)
	14	Ni-Fe Alloys
	15	Pure Titanium Alloys
	16	Alpha Titanium Alloys
	17	Near Alpha Ti Alloys
	18	Alpha-Beta Ti Alloys
	19	Beta Ti Alloys
	20	Zinc Alloys
	21	Other Alloys
*		

Figure 30. Types of materials included in the database

3.3.4 Time Temperature Transformation (TTT) Data

The TTT diagram is available for the materials used to represent the workpiece. Almost all types of steel have its TTT diagram in the database. The user also has the option to include the TTT data in the database. The TTT diagrams have been taken from “Atlas of Time-Temperature Diagrams for Irons and Steels“, edited by George F. Vander Voort, Carpenter technology corporation, Reading, PA” of ASM International. The TTT data has been scanned thereafter and been converted in Jpg format. Graph digitizer software which is basically a Graph-to-Digital data converter [20] by Nickolay Rodionov (Russia, St. Petersburg) has been used to convert the scanned data to a data in tabular form. The below figure shows the extraction of data in an excel graph. The first two curves are the

start curve, the middle one represents 50% finish curve of microstructure and the last curve represents the finish of a particular microstructure. In the tabular format, it is represented in three columns, two for start value and one for the finish curve.

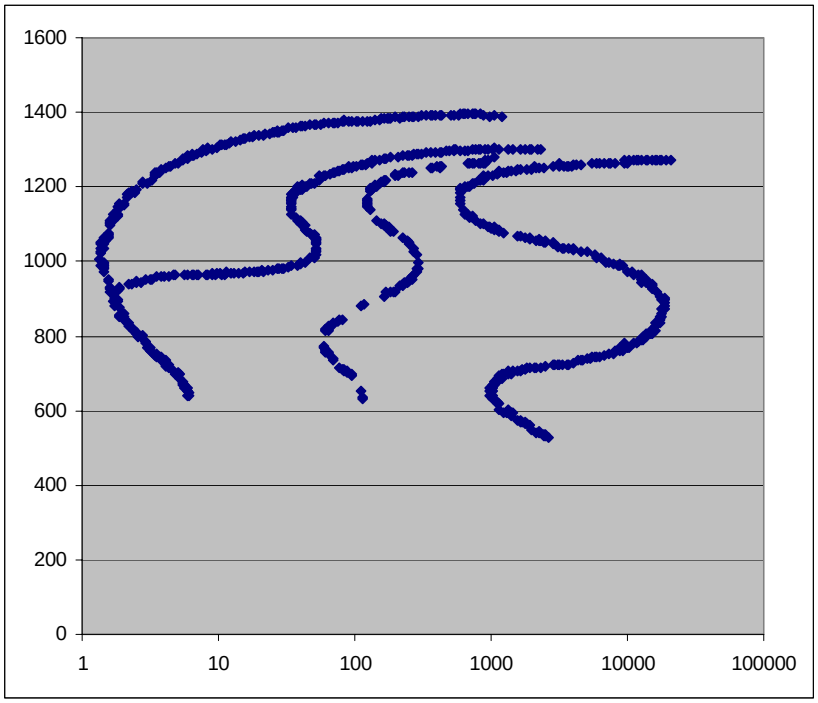

Figure 31. Sample representing TTT in excel

Structure of the TTT database: On 'Material Parameter Database Manager' window, as shown in Figure 32 press "Parameters" after choosing a specific Material Type and Material Name, the window as shown in Figure 33 will popup. This window design inherits the same style used in CHT-*q/t*, so user will not feel confused.

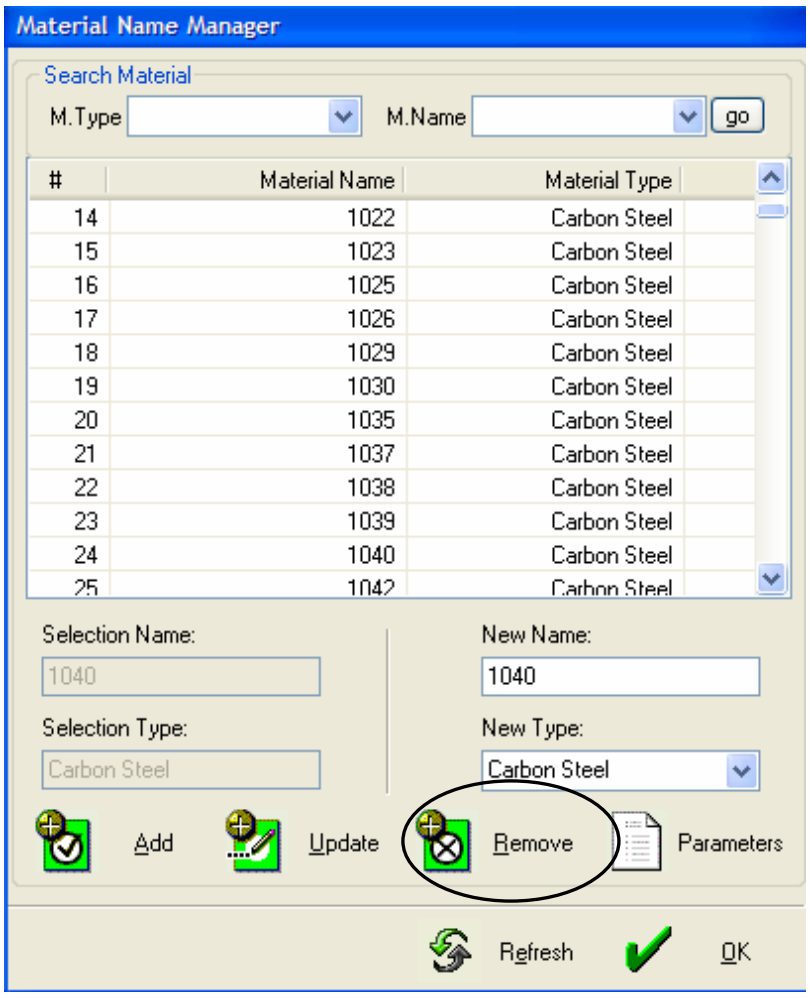

Figure 32. Material properties database manager

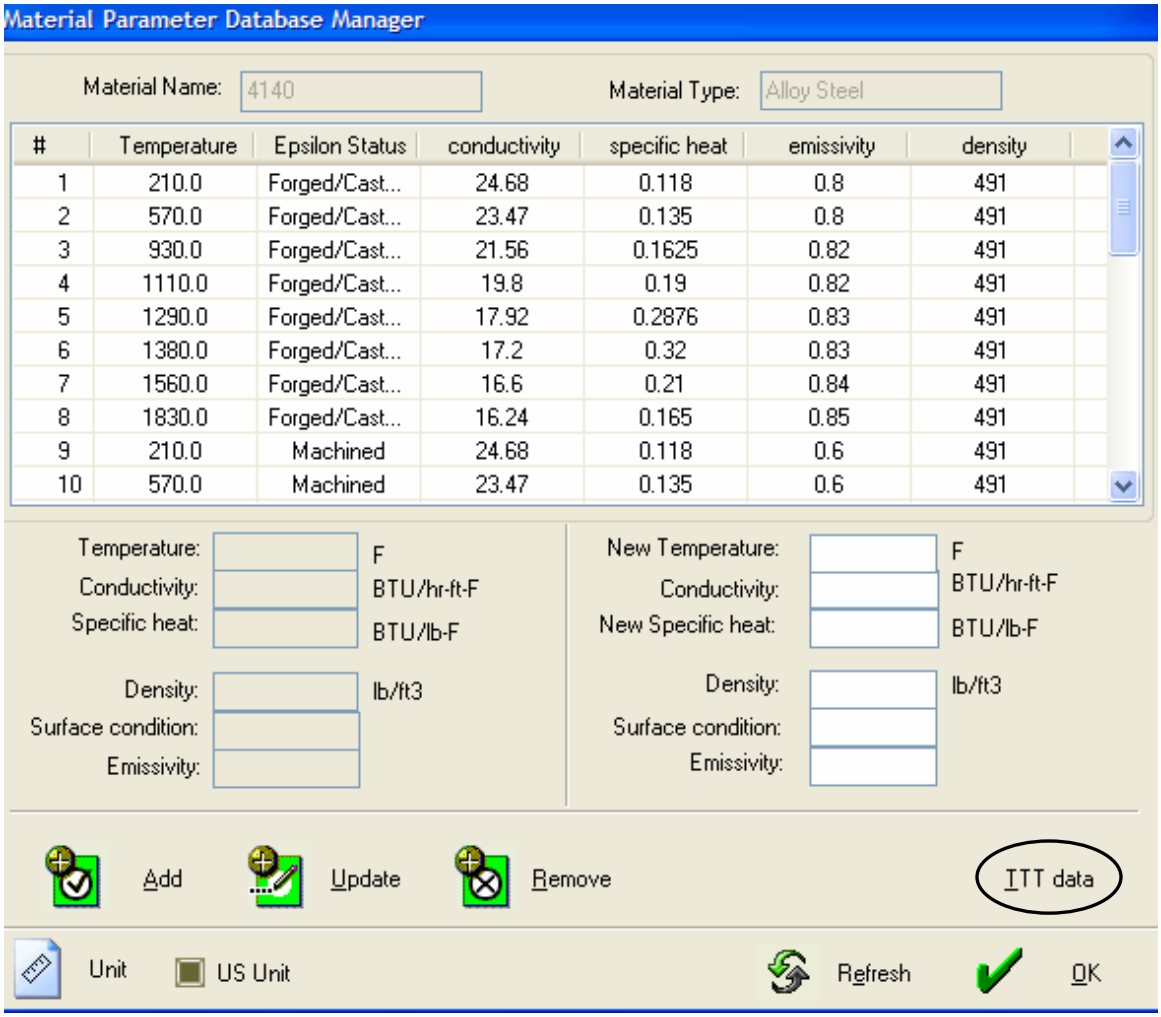

Figure 33. Material database showing parameters

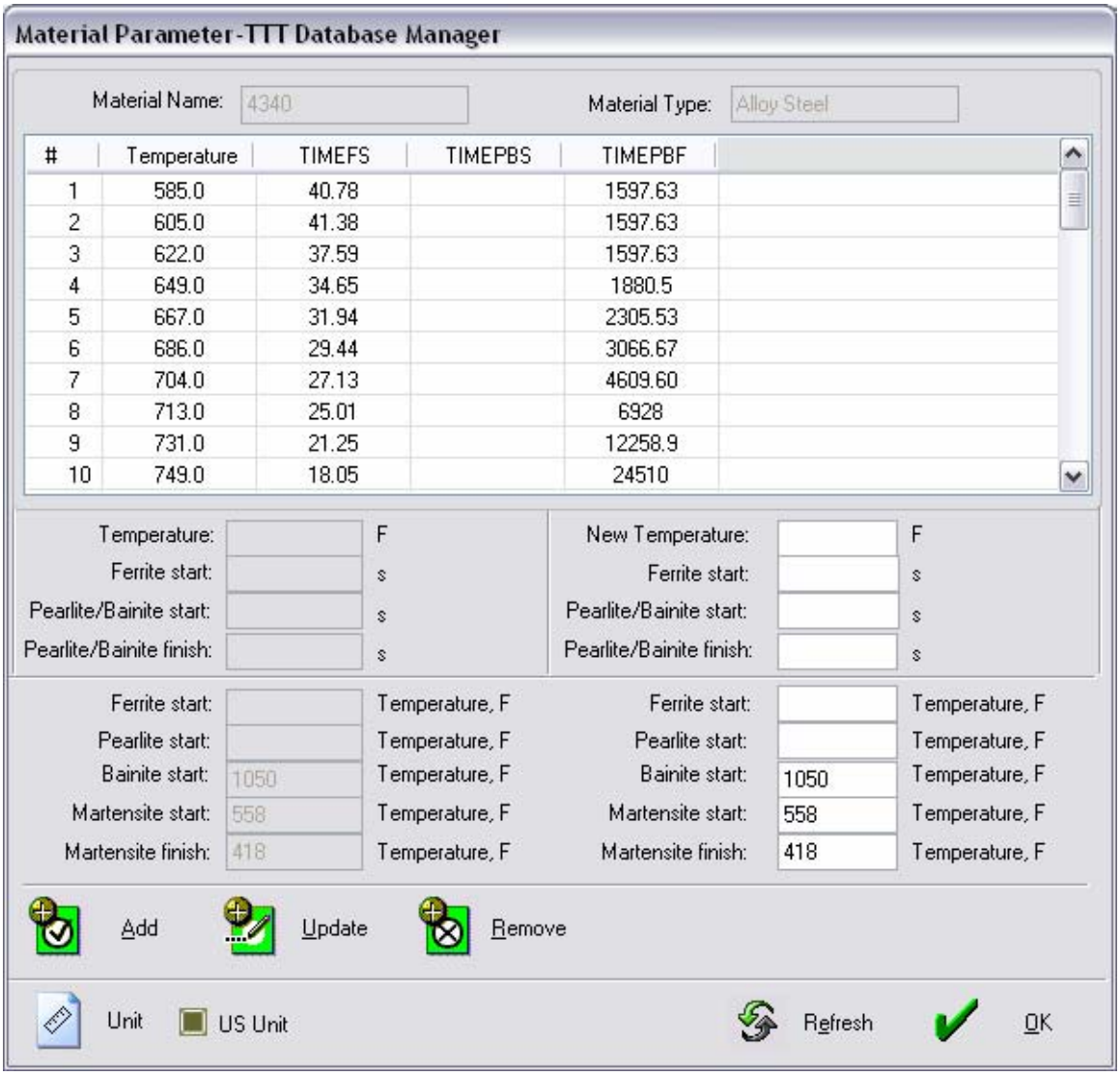

Figure 34. TTT database manager

The TTT database contains four columns. It contains the time taken for the ferrite start, pearlite/bainite start and pearlite/bainite finish at different temperature values. The temperature values ranges from the Austenite start up to martensite start. Theses values are presented in the interval of 20 degree. In addition to these data, it contains the temperature values for Ferrite start, Pearlite start, Bainite start, Martensite start and Martensite finish.

These data are then fed in a series of equations to determine the percentage of the microstructure evolved, which is the further used to determine the property.

The technical focus of the TTT database lies in the fact that, it considers the TTT diagrams for all the grades of steel. As it can be seen in the Figure. 34 there are two columns for the start curve, “Time Ferrite start” and “Time Bainite start”. Right from the Austenitic start temperature (A_s) to the point where, two start curve merges, we have the option to fill both the start columns in the database. Since the program need the final volume fraction of martensite formed, for the hardness and other properties calculation, we can combine the formation of other microstructures. Thus for Hypoectctoid and hypereutectoid steels, the ferrite and cementite start curve has been combined together as pearlite. The volume fraction of pearlite and bainite is needed only when the volume fraction of martensite is less than 50%. The TTT database has been defined in a manner that it can handle all sorts of cases and would be applicable for any grade of steels.

3.3.5 Database Design for Quenching

Various quenchants used in the industry are stored in the database. The properties of the quenchants are also included in the database. The quenchant database has been taken from QuenchPAD developed by Prof. Richard Sisson’s research group at Center for heat treating excellence. Similar to other database manager, the user has the option to add or edit the quenchant data.

The quenchant database contains gas as well as liquid quenchants. The heat transfer coefficient for gas quenchant has a little variation with the quenching temperature as shown in Figure 35. The factors affecting the heat transfer coefficient of the gas quenchants are pressure, blower horse power and velocity.

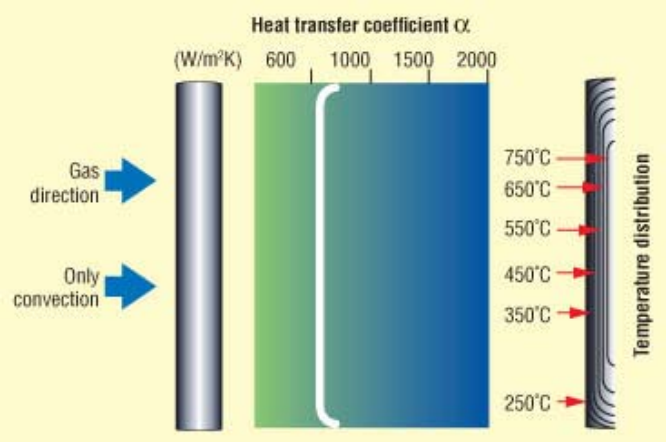

Figure 35. Heat transfer coefficient vs temperature for gas quenching

Based on the industry standards, three most frequently used gas quenchants are added in CHT-*q/t,* which are as follows:

- Helium
- Nitrogen
- Argon

Figure. 36 shows the variation of convective heat transfer coefficient with respect to temperature for liquid quenching. Three stages of cooling exist by using liquid quenchants. These are vapor blanket stage, boiling stage and convection stage and there is a wide variation between the convective heat transfer coefficients within these stages. The database in CHT-*q/t* considers these variations and convective heat transfer coefficient are stored accordingly. The properties of the liquid quenchants included in the database for calculations are bath temperature, viscosity, concentration, agitation, usage of quenchants.

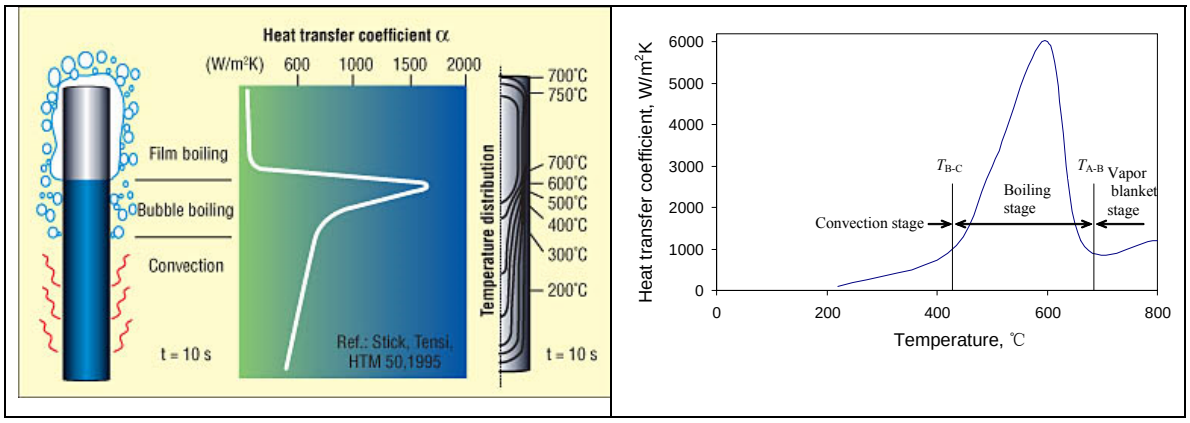

Figure 36. Variation of heat transfer coefficient vs temperature for liquid quenching

The types of liquid quenchant included in CHT-*q/t* are as follows:

- Mineral oil: Durixol HR88A, Durixol W25 , Durixol W72, Durixol V35, Houghton G, Houghton K, T-7-A, Mar-temp 355
- Bio oil: Bio-Quench 700, Synabol 2000
- Water
- Polymer: Aqua-Quench 251, Aqua-Quench 260

Structure of quenchant database

Quenchant property database manager also keeps the same design style used in CHT-*q/t*. Users can reach and control both gas and liquid quenchants parameters on this page. For same quenchant, users can classify them by different conditions, and pick any available value from its combo-list.

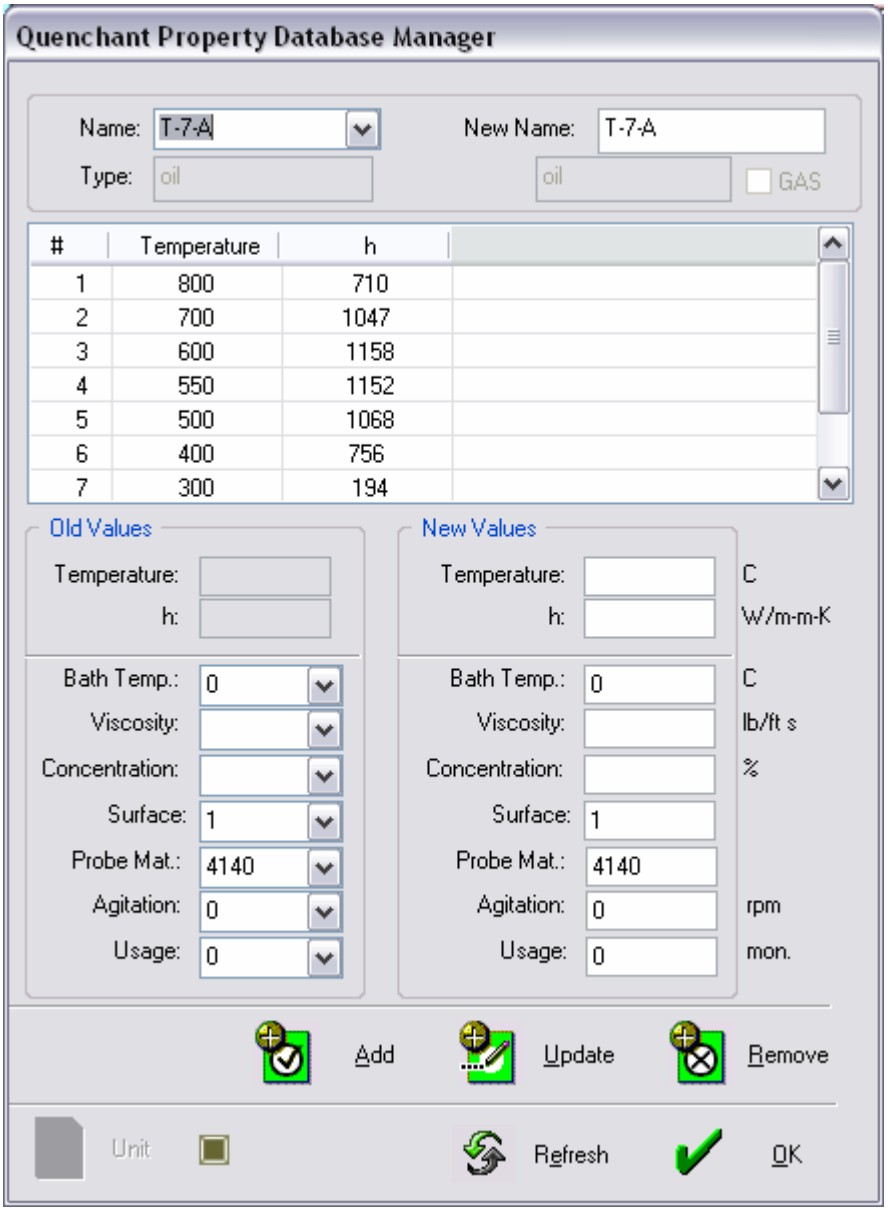

Figure 37. Quenchant properties database manager

The Quenchant DB presents the convective heat transfer (h) data as a function of temperature. The h values are presented in an interval of 100 degree. These “h” values are then used in the program to determine the cooling curve of workpiece.
Figure 38 shows the table of liquid quenchant database.

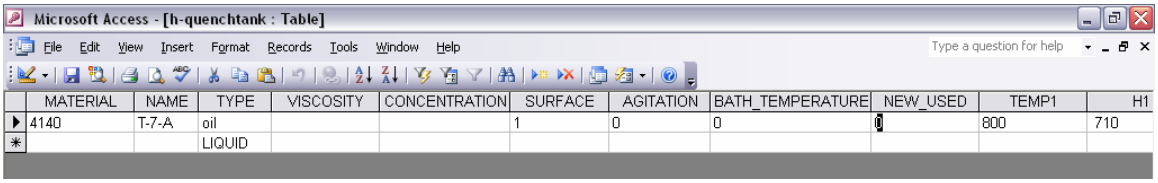

MATERIAL	NAME	TYPE	VISCOSITY	CONCENTRATION	SURFACE	AGITATION	BATH_TEMPERATURE	NEW_USED	TEMP1	H1
4140	T-7-A	oil			1	0	0	0	800	710
		LIQUID								

Figure 38. Liquid quenchant database

3.3.6 Furnace Database

The furnace database is used to store the furnace information of a furnace. As CHT-*q/t* incorporates both heating and cooling operations, separate furnaces may be used for heating and quenching. Some time Dual chamber furnaces are used in which heating and quenching is done in separate zones in the same furnace.

This stored information can be used different times. If furnace being used for the process is same and if the information is stored in the database, the user can directly get the information from the database instead of typing all the information each time for a case.

The furnace data in the database contains all the detailed information of the furnace (the type, shape, wall specifications, size, geometry, workspace, capacity, maximum & minimum temperatures, load capacity, accessories & their weights and etc).

A new function “import a furnace” has been added in the Furnace Database Manger which helps in importing the already saved furnace data from different source. Furnace database manager is as shown in the Figure 39.

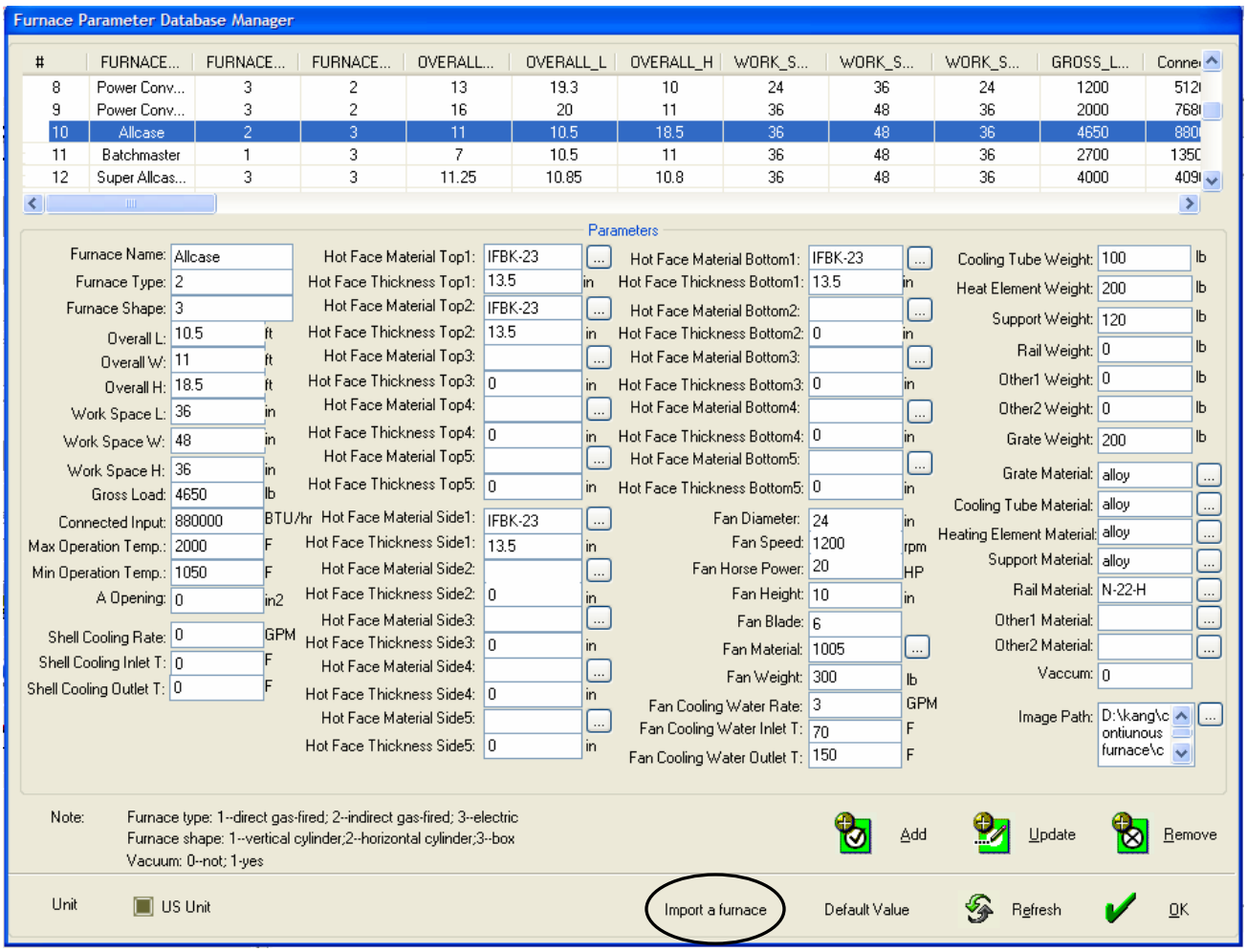

Figure 39. Furnace parameter database manager

3.4 Enmeshment of Workpiece Model

The workpiece can be classified into two categories, lumped capacitance and massive one. For the lumped capacitance the temperature can be assumed to be uniform during heating, while there is significant temperature gradient for the massive workpiece. Therefore the massive workpiece has to be discritized to calculate the temperature distribution. Biot number is used as criteria to classify the workpiece. Three dimensional discretization has been done for workpieces.

3.4. 1 Classification of Workpieces by Biot Number

Biot number: The biot number can be defined as the ratio of thermal internal resistance to the surface film resistance. It is used in heat transfer in general and unsteady state calculations in particular. It is normally defined in the following form:

$$B_i = \frac{h.L_c}{k} \tag{26}$$

where *h* is the heat transfer coefficient of the workpiece surface and environment,

$$h = h_{convection} + h_{radiation} \tag{27}$$

L_c is the characteristic length,

For different shapes the characteristic length is different

For plate, $L_c = \frac{V}{A}$

Cylinder/bar with rectangular section, $L_c = \frac{2V}{A}$

Sphere/cube, $L_c = \frac{3V}{A}$

Where V and A are the workpiece volume and area respectively.

k is conductivity

3.4.2 Enmeshment of Workpiece Belonging to Class I (Box)

In CHT-*q/t* three dimensional enmeshment of workpieces are done, as the aim of CHT-*q/t* is to predict mechanical properties of the workpiece at every nodes, inside the part as well. The enmeshment is done by the finite difference method using the "implicit method" as it is free from any stability criteria.

Consideration of non-linearity: Since thermal conductivity and specific heat are dependent on temperature, these values are stored in the database at different temperature values and these values are called by the program as the time step is increased.

In this section 3-dimensional enmeshment of box is shown.

If $B_i \leq .1$, then the lumped heat capacity model is applicable,

Lumped heat capacity model

Input Conditions: Following are the input conditions needed by the program in order to calculate the temperature of the part. Since no temperature gradient is present inside the part, the temperature of the part is uniform at a specific time.

1. The dimensions of the box (D_1, D_2, & D_3).
2. The initial temperatures of the part.
3. Temperature of the quenchant gas. (It can be taken as the average temperature of gas in inlet and outlet channel)

Following equation can be used to determine the temperature of part at time t.

$$\frac{T - T_a}{T_i - T_a} = \exp\left[- B_i F_0\right] \tag{28}$$

Where F_0 (Fourier number) is $F_0 = \frac{\alpha . t}{L_c^{\,2}}$ (29)

and , $\alpha = \frac{k}{\rho C_p}$ (30)

T_a is the ambient temperature

Thus the final temperature T can be calculated, by using the above equations.

If B_i > .1, exact solution should be used, as described below**:**

Input:

1. The dimensions of the box (D_1, D_2, & D_3).
2. Specify the origin as shown in the figure.
3. Input the values n, l ,m
4. The initial temperatures of the part.
5. The time step Δt
6. Temperature of the quenchant gas. (It can be taken as the average temperature of gas in inlet and outlet channel)

Thus, $\Delta x = \frac{D_1}{n}$, $\Delta y = \frac{D_2}{l}$, $\Delta z = \frac{D_3}{m}$

The different elements of the box may be represented by

i = 0 to n,

j = 0 to l,

k =0 to m

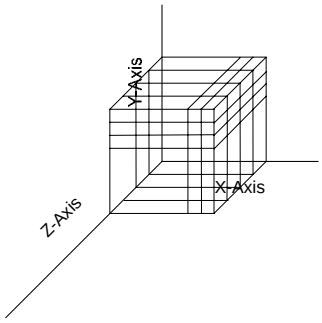

Figure 40. Enmeshment of box

There will be three types of nodes that we have to deal with.

1. Internal node

Matrix representing internal nodes:

i	j	k
1	(1 to L-1)	(1 to m-1)
2	(1 to L-1)	(1 to m-1)
…	…	…
…	…	…
(n-1)	(1 to L-1)	(1 to m-1)

Thus any internal node will be represented by $\mathbf{e_{i,j,k}}$, where i, j, k can take the values from the above matrix.

Only conduction takes place in the internal nodes. Here conduction heat transfer follows the Fourier equation in Cartesian coordinates.

$$\rho c \frac{\partial T}{\partial t} = k\left(\frac{\partial^2 T}{\partial x^2} + \frac{\partial^2 T}{\partial y^2} + \frac{\partial^2 T}{\partial z^2}\right) \tag{31}$$

Here we are considering the material to be isotropic, $k_x = k_y = k_z$ but conductivity and specific heat is dependent on temperature. We are not considering any heat generation.

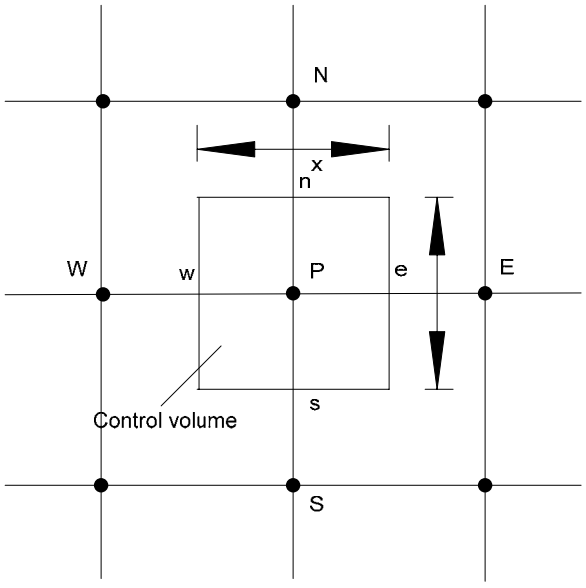

Figure 41. Control volume, as in 2-D

We have to add two more neighbors T and B (top and bottom) for the z direction to complete the three dimensional configuration in the above figure.

The discretization equation can be written as:

$$a_P T_P = a_E T_E + a_W T_W + a_N T_N + a_S T_S + a_T T_T + a_B T_B + b \tag{32}$$

where,

$$a_E = \frac{k_e \Delta y \Delta z}{(\delta x)_e} \tag{33}$$

$$a_W = \frac{k_w \Delta y \Delta z}{(\delta x)_w}, \tag{34}$$

$$a_N = \frac{k_n \Delta z \Delta x}{(\delta y)_n}, \tag{35}$$

$$a_S = \frac{k_s \Delta z \Delta x}{(\delta y)_s}, \tag{36}$$

$$a_T = \frac{k_t \Delta x \Delta y}{(\delta z)_t}, \tag{37}$$

$$a_B = \frac{k_b \Delta x \Delta y}{(\delta z)_b}, \tag{38}$$

$$a_P^0 = \frac{\rho c \Delta x \Delta y \Delta z}{\Delta t}, \tag{39}$$

$$b = a_p^0 T_P^0, \tag{40}$$

$$a_P = a_E + a_W + a_N + a_S + a_T + a_B + a_P^0 \tag{41}$$

2. **Boundary node** (we have to consider 6 faces): Typically three kinds of boundary conditions are encountered:
    - Given boundary temperature
    - Given boundary heat flux

- Boundary heat flux specified via a heat transfer coefficient and the temperature of the surrounding fluid.

We will use the third boundary condition.

Matrix representing the boundary nodes is as follows

i	j	k
0	(1 to L-1)	0, m
1	(0 to L)	0, m
…	…	…
n-1	(0 to L)	0, m
n	(1 to L-1)	0, m

i	j	k
0, n	(1 to L-1)	0
0, n	(0 to L)	1
…	…	…
0,n	(0 to L)	m-1
0, n	(0 to L-1)	m

i	j	k
0	0, L	(1 to m-1)
1	0, L	(0 to m)
…	…	…
n-1	…	(0 to m)
n	0, L	(1 to m-1)

Governing equations representing boundary nodes:

$$\rho c V_{i,j,k} \frac{T_{i,j,k}^{p+1} - T_{i,j,k}^{p}}{\Delta t} = h(T) A_{i,j,k} (T_{quenchant}^{p} - T_{i,j,k}^{p}) \tag{42}$$

Then,

$$T_{i,j,k}^{p+1} = \frac{h(T)\Delta t}{\rho c V_{i,j,k}} A_{i,j,k} (T_{quenchant}^{p} - T_{i,j,k}^{p}) + T_{i,j,k}^{p} \quad (43)$$

Where p is the time step.

3. **Corner nodes** (we will have 8 corner points)

   The corner nodes may be denoted as (0, 0, 0), (n, 0, 0), (0, L, 0), (n, L, 0), (0, 0, m), (n, 0, m), (0, L, m), (n, L, m)

3.4.3 Enmeshment of 2-Stacked Brick

Here the enmeshment is done by using "Finite difference method" to be able to use the nodes for heat transfer calculations.

Input:

1. The dimensions of the box (D_1, D_2, D_3, D_4, D_5, & D_6).
2. Specify the origin as shown in the figure.
3. Input the values n, l ,m

Thus, $\Delta x = \frac{D_1}{n}$, $\Delta y = \frac{D_2}{l}$, $\Delta z = \frac{D_3}{m}$

Constraints or assumptions:

1. The shape is symmetrical if it is cut by a plane parallel to y-z plane and at a distance x = $D_1/2$
2. $\frac{D_1 - D_4}{2.\Delta x}$ is an integer.
3. $\frac{D_4}{\Delta x}$ is an integer.
4. Follow constraints 2 & 3 in y and z direction

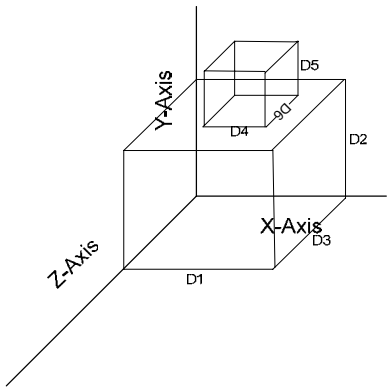

Figure 42. Enmeshment of 2-stacked brick

We have to deal with three types of nodes

1. Internal node

Matrix representing internal nodes:

i	j	k
1	(1 to L-1)	(1 to m-1)
2	(1 to L-1)	(1 to m-1)
…	…	…
…	…	…
(n-1)	(1 to L-1)	(1 to m-1)

For the enmeshment of the small box, we will keep $\Delta x, \Delta y \,\&\, \Delta z$ same, thus we have to calculate the number of elements for the small box. That can be calculated as:

$$n_1 = \frac{D_4}{\Delta x}, \quad L_1 = \frac{D_5}{\Delta y} \;\&\; m_1 = \frac{D_6}{\Delta z}$$

For the enmeshment of the small box, we can shift the origin as shown in the figure below.

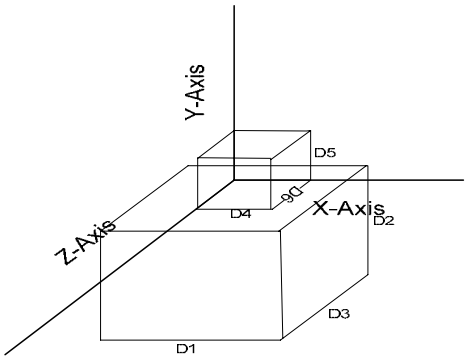

Figure 43. New origin

Matrix representing internal nodes:

i	j	k
1	(1 to L_l-1)	(0 to m_l-1)
2	(1 to L_l-1)	(0 to m_l-1)
…	…	…
…	…	…
(n_l-1)	(1 to L_l-1)	(0 to m_l-1)

2. Boundary node

Matrix representing the boundary nodes (for big box) is as follows

i	j	k
0	(1 to L-1)	0, m
1	(0 to L)	0, m
…	…	…
n-1	(0 to L)	0, m
n	(1 to L-1)	0, m

i	j	k
0, n	(1 to L-1)	0
0, n	(0 to L)	1
…	…	…
0,n	(0 to L)	m-1
0, n	(0 to L-1)	m

i	j	k
0	0	(1 to m-1)
1	0	(0 to m)
…	…	…
n-1	…	(0 to m)
n	0	(1 to m-1)

i	j	k
0	L	(1 to m-1)
1	L	(0 to m)
…	…	…
$\frac{D_1 - D_4}{2.\Delta x}$ -1	L	(1 to m-1)
$\frac{D_1 - D_4}{2.\Delta x}$	L	{1 to ($\frac{D_3 - D_6}{2.\Delta z}$ -1) & ($\frac{D_3 + D_6}{2.\Delta z}$ +1) to (m-1)}
$\frac{D_1 - D_4}{2.\Delta x}$+1	L	{1 to ($\frac{D_3 - D_6}{2.\Delta z}$ -1) & ($\frac{D_3 + D_6}{2.\Delta z}$ +1) to (m-1)}
…	L	{1 to ($\frac{D_3 - D_6}{2.\Delta z}$ -1) & ($\frac{D_3 + D_6}{2.\Delta z}$ +1) to (m-1)}
$\frac{D_1 + D_4}{2.\Delta x}$	L	{1 to ($\frac{D_3 - D_6}{2.\Delta z}$ -1) & ($\frac{D_3 + D_6}{2.\Delta z}$ +1) to (m-1)}
$\frac{D_1 + D_4}{2.\Delta x}$ +1	L	(1 to m-1)
….	L	(1 to m-1)
n	L	(0 to m)

Matrix (after shifting the origin, as described above), representing the boundary nodes (for small box) is as follows:

i	j	k
0	(1 to $\frac{D_5}{\Delta y}$ -1)	0, $\frac{D_6}{\Delta z}$
1	(0 to $\frac{D_5}{\Delta y}$)	0, $\frac{D_6}{\Delta z}$
…	…	…
$\frac{D_4}{\Delta x}$ -1	(0 to $\frac{D_5}{\Delta y}$)	0, $\frac{D_6}{\Delta z}$
$\frac{D_4}{\Delta x}$	(1 to $\frac{D_5}{\Delta y}$ -1)	0, $\frac{D_6}{\Delta z}$

i	j	k
0, $\frac{D_4}{\Delta x}$	(1 to $\frac{D_5}{\Delta y}$ -1)	0
0, $\frac{D_4}{\Delta x}$	(0 to $\frac{D_5}{\Delta y}$)	1
…	…	…
0, $\frac{D_4}{\Delta x}$	(0 to $\frac{D_5}{\Delta y}$)	$\frac{D_6}{\Delta z}$ -1
0, $\frac{D_4}{\Delta x}$	(0 to $\frac{D_5}{\Delta y}$ -1)	$\frac{D_6}{\Delta z}$

i	j	k
0	$\frac{D_5}{\Delta y}$	(1 to $\frac{D_6}{\Delta z}$ -1)
$\frac{D_4}{\Delta x}$	$\frac{D_5}{\Delta y}$	(0 to $\frac{D_6}{\Delta z}$)
…	…	…
$\frac{D_4}{\Delta x}$ -1	…	(0 to $\frac{D_6}{\Delta z}$)
$\frac{D_4}{\Delta x}$	$\frac{D_5}{\Delta y}$	(1 to $\frac{D_6}{\Delta z}$ -1)

3. Corner nodes (for big box): we will have 8 corner points, which are as follows:

The corner nodes may be denoted as (0, 0, 0), (n, 0, 0), (0, L, 0), (n, L, 0), (0, 0, m), (n, 0, m), (0, L, m), (n, L, m)

Corner nodes for small box is as defined: (0, 0, 0), ($\frac{D_4}{\Delta x}$, 0, 0), (0, $\frac{D_5}{\Delta y}$, 0), ($\frac{D_4}{\Delta x}$, $\frac{D_5}{\Delta y}$, 0), (0, 0, $\frac{D_6}{\Delta z}$), ($\frac{D_4}{\Delta x}$, 0, $\frac{D_6}{\Delta z}$), (0, $\frac{D_5}{\Delta y}$, $\frac{D_6}{\Delta z}$), ($\frac{D_4}{\Delta x}$, $\frac{D_5}{\Delta y}$, $\frac{D_6}{\Delta z}$)

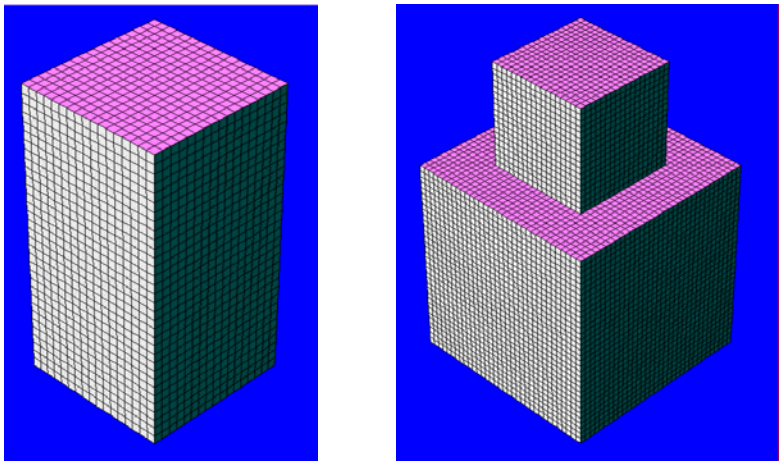

(a) box (b) 2-stacked brick

Figure 44. The enmeshment of class I workpieces [1]

Table 2 Classification of workpiece shapes

Class	Class I	Class II	Class III	Class IV	Class V
Shapes	Box 2-stacked brick	Cylinder Hollow cylinder Base 2-step shaft 3-step shaft	Cone Hollow cone Hollow cone	Sphere	Torus

The pictures of the shapes are depicted below:

Class I

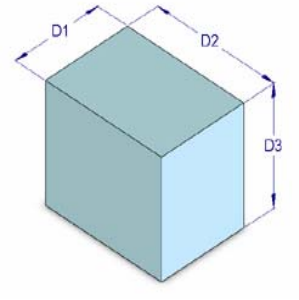

Box

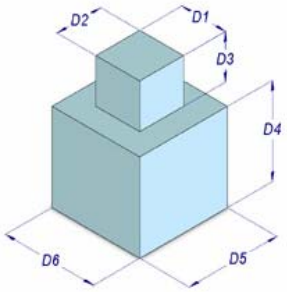

2-stacked brick

Class II

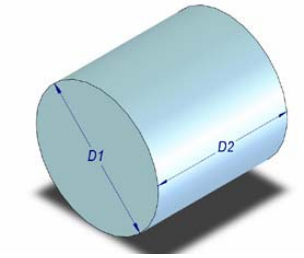

Cylinder

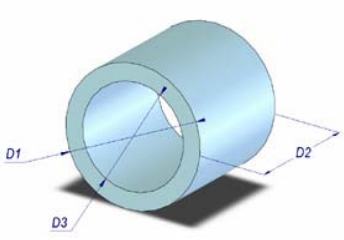

hollow cylinder

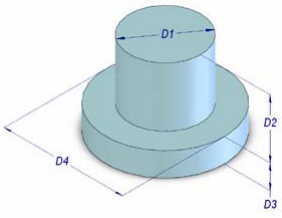

2-step shaft

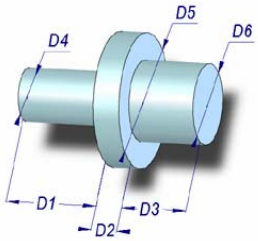

3-step shaft

Class III

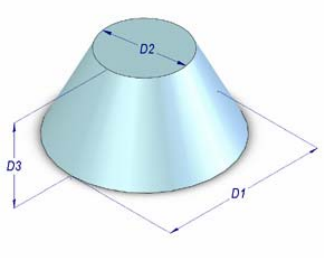

Cone

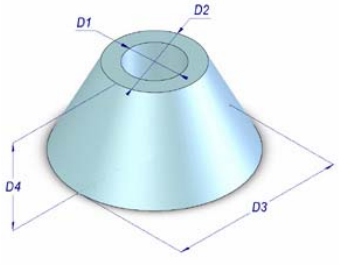

hollow cone shaft

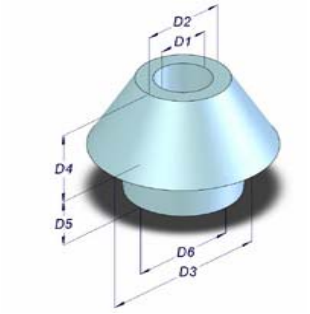

hollow cone shaft

Class IV:

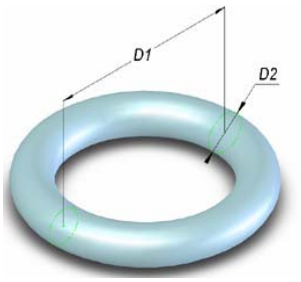

Torus

Class V:

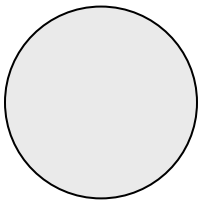

sphere

Figure 45. Workpiece shapes

CHAPTER 4. PROPERTY PREDICTION

Microstructure can be defined as the structure that is observed when a polished and etched specimen of metal is viewed in an optical microscope at magnifications in range of approximately x 25 to x 1500.

The different microstructures of steel can be classified as follows:

Pearlite: Pearlite can be defined as a lamellar mixture of cementite and ferrite formed during the cooling of austenite; a micro constituent of steel and Cast iron.

Bainite: Bainite can be defined as a metastable aggregate of ferrite and cementite resulting from the transformation of austenite at temperatures below the pearlite range but above M_s the martensite start temperature. Bainite formed in the upper part of the bainite transformation range has a feathery appearance and formed in the lower part of the range has an acicular appearance resembling that of tempered martensite.

Martensite: Martensite can be defined as a supersaturated interstitial solid solution of carbon in α iron. It has Body Centered Tetragonal (B.C.T) structure.

Relationship between Martensitic start (M_S) temperature and chemical composition:

$$M_S\ (^0C) = 561 - 474(\%C) - 33(\%Mn) - 17(\%Ni) - 17(\%Cr) - 21(\%Mo) \quad (44)$$

Cooling rates has no effect on M_S temperature but martensitic finish (M_f) temperature is dependent on it. Slower cooling rates results in decrease of M_f temperature. Martensite microstructure of particular steel has a slightly higher specific volume (lower density) than the same steel with ferrite-pearlite microstructure.

Austenite: Austenite can be defined as a solid solution of ferrite carbide or carbon in iron. Austenite cools to form pearlite or martensite.

4.1 Microstructure Evolution

The primary microstructure present at high temperature is austenite. Depending on the cooling rate of the specimen at any particular location, this primary phase transforms to

bainite, pearlite, ferrite and martensite. The TTT (time, temperature and transformation) diagram can be used to determine how this transformation occurs. During the evolution of microstructures latent heat is exchanged. This affects the thermal cycle by introducing/removing latent heat.

The critical temperatures for solid state transformations in steels are:

1) The A_3 temperature: This is the temperature below which austenite starts to decompose to ferrite. Ferrite develops by nucleation at the austenite grain boundaries, and then growth into the austenite grains.
2) The eutectoid temperature A_1: This is the temperature below which austenite starts to transform to pearlite. This reaction occurs in competition with formation of pro-eutectoid ferrite.
3) The temperature of bainite start B_s: When the temperature falls below B_s, the ferrite and pearlite formation reaction stops and austenite transforms to a bainite structure.
4) The temperature of martensite start, M_s: When the temperature is below M_s the remaining austenite which has not yet transformed to the earlier phases transforms to martensite in a diffusionless transformation accompanied by volume change.

The rate of evolution of a phase can be expressed as:

$$\frac{dX_i}{dt} = B(G,T)X_i^m(1-X_i)^p \tag{45}$$

Where T is the temperature, B the effective rate coefficient, G is the austenite grain size, and m and p are semi-empirical coefficients (known for the various phases in steel), and X_i is the fraction of phase i.

This equation can be used to track the evolution of microstructure if one can determine the thermal history of the location of interest. The coefficients m and p are set less than one to assure convergence in a form that is derived from appoint nucleation and impingement growth model. The rate coefficient B includes the effect of grain size on the

density of eligible nucleation sites. It also includes the amount of austenite supercooling and the effect of alloying elements and temperature on diffusion.

In the transformation model the progress of transformation for the diffusional reactions is followed by an *Avrami-Johnson-Mehl* equation, assuming additivity, while the fraction of martensite formed is modeled as a function of holding temperature below the martensite start temperature.

For the diffusional phase transformations of austenite to ferrite and pearlite, the formation of a new phase on cooling is only possible once the temperature is below the equilibrium transformation temperature. This temperature is dependent on the alloy content of the steel.

As the temperature is reduced below the equilibrium transformation temperature for the steel, a finite amount of time is needed before an observable amount of new phase forms. This *incubation time* is dependent on the thermal history of the steel below the equilibrium transformation temperature. This *incubation period* before decomposition of austenite to pearlite or bainite is determined by using Schiel's additivity method [38]. Scheil's principle of additivity of incubation fractions can be calculated as follows[39]

For each time step, denoted as Δt_i, the fraction $\frac{\Delta t_i}{\tau_{iIT}}$ is calculated where τ_{iIT} is the time to the start of the transformation of the temperature prevailing during the time step. The fractions are then summed:

$$\sum \frac{\Delta t_i}{\tau_{iIT}} \tag{46}$$

When this sum attains unity, the incubation period is over.

Section 4.1 describes the hardness prediction methodology adapted in CHT-*q/t.* Section 4.1.1 describes the TTT diagram used for the calculation of hardness. Basically three types of TTT diagrams, each for hypoeutectoid, eutectoid and hypereutectoid steels are used in the database. The database has been scanned from "Atlas of Time-Temperature

Diagrams for Irons and Steels". The scanned TTT data has been converted to isothermal step values, as discussed in detail in the coming section. The data has been taken at the step value of 20 degree from start and finish curve in the TTT diagram. The data at each step value is the input of the program comprising the analytical equations as described below. At each time step, the time value of the cooling curve of the part at the particular temperature is fed in the program in order to calculate the volume fraction of the microstructure evolved. After the calculation of volume fraction, this data is fed in the equations to calculate hardness. Thus, hardness is being calculated at each node. Section 4.1.2 describes the hardness conversion charts, as the hardness equations use the hardness value in micro hardness that is HV, but the final value of hardness is denoted in Rockwell (HRC). Section 4.1.3 describes the Regression Analysis approach to give the final hardness value. Since hardness is a function of % Martensite as well as % carbon content, thus regression analysis is being used to get the hardness at a specific martensitic percentage. The main work performed and the focus of the thesis lies in developing the methodology comprising of TTT diagrams, cooling curves and well defined analytical equations for the prediction of as quenched mechanical properties.

4.2 Hardness Prediction

The kinetics of the growth of ferrite and pearlite are described using the *Avrami-Johnson-Mehl* equation: [32]

$$w = 1 - \exp\left(-b.(t - t_s)^n\right) \tag{47}$$

where,

w : volume fraction of austenite transformed
b,n : coefficient and exponent of the austenite transformation kinetics,
t : time
t_s : start time

The values of b and n are evaluated from the given TTT diagram except for ferrite for which it is assumed that n = 1. More generally it can be stated that:

$$n = \frac{\log\left[\ln(1-w_s)/\ln(1-w_f)\right]}{\log\left[t_s(T)/t_f(T)\right]} \tag{48}$$

$$b = \frac{-\ln(1-w_s)}{t_s(T)} \tag{49}$$

where the subscripts s and f indicate start and finish, respectively. In a TTT diagram, w_s is usually chosen to be 1% and w_f 99%, but other percentages may also be chosen. The volume fraction of martensite is then modeled using an equation proposed by Koistinen and Marburger [32].

Below the martensite start temperature M_s , it is assumed that the remaining austenite is transformed into martensite according to equation as :

$$w_M = (1-w_F-w_P-w_B-w_C)*(1-\exp(-.011.(M_s-T))) \tag{50}$$

W_M : transformed volume fraction of austenite into martensite,
M_s : martensite start temperature
M_f : martensite finish temperature,
T : transformation temperature, $T \leq M_s$

It can be observed from the above equations, to calculate b, n and w we need only t_s and t_f from the TTT diagram, and t from the cooling curve.

A method is proposed here to calculate hardness from the above mentioned equations.

If the transformation of austenite shall be calculated for any time temperature cycle, a continuous cooling curve is divided into constant temperature steps with appropriate times (Figure 46). It is assumed that the horizontal parts of this step function cause a transformation comparable to the transformation occurring at the individual temperatures in the isothermal TTT-diagram. By an iteration of the transformation steps the final microstructure is derived.

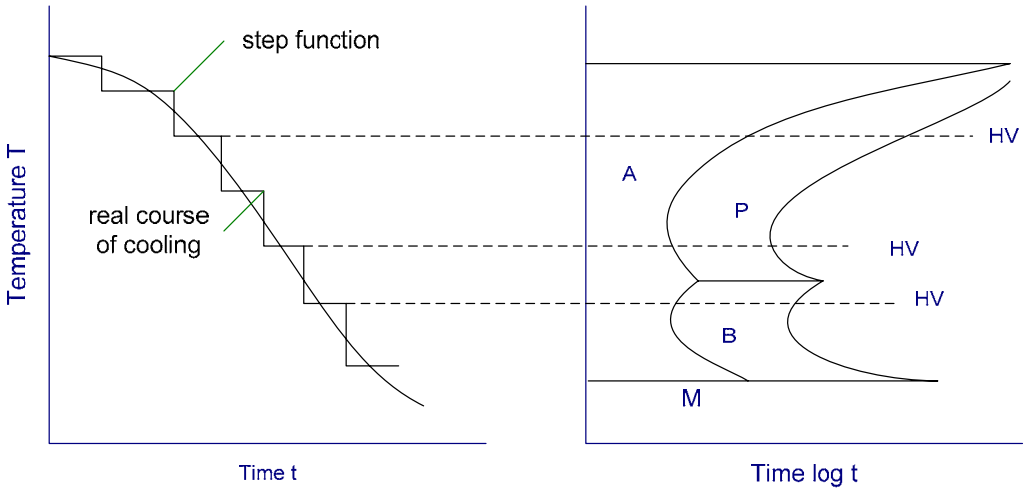

Figure 46. Isothermal representation

The final hardness can then be determined by applying an additivity rule if the hardness values of the different microstructures formed at defined temperatures are known:

$$HV = \sum \left(\sum \left(\Delta w_k \left(T_i \right) \cdot HV_k \left(T_i \right) \right) \right) \tag{51}$$

HV: final hardness at a defined location

$w_{k:}$ volume fraction of microstructure k formed at temperature T_i

HV_k: microhardness of microstructure k formed at temperature T_i

The main advantage of this method is that it uses existing data about the transformation behavior of austenite referring to isothermal TTT-diagrams. But the method also has some serious drawbacks: The isothermal TTT-diagram usually fails to give a sufficiently reliable information of the transformation behavior of austenite due to deviations in the chemical composition, variations in the initial microstructure and different austenitizing conditions. In addition, the question appears whether it is exactly permissible to apply the isothermal transformation kinetics of austenite to a continuous cooling curve which is divided into a step function. Finally, equation 51 is only based on empirical data about the transformation behaviour.

While using the above mentioned equations to predict the hardness, three main types of cases arise.

Cooling conditions in CHT-*q/t*

Three types of cooling conditions of the workpiece, normal fast and slow cooling are considered in CHT-*q/t* as described below.

1. Normal Cooling

The TTT diagram used to describe this case is as mentioned below. All the above mentioned equations are applied to determine the hardness.

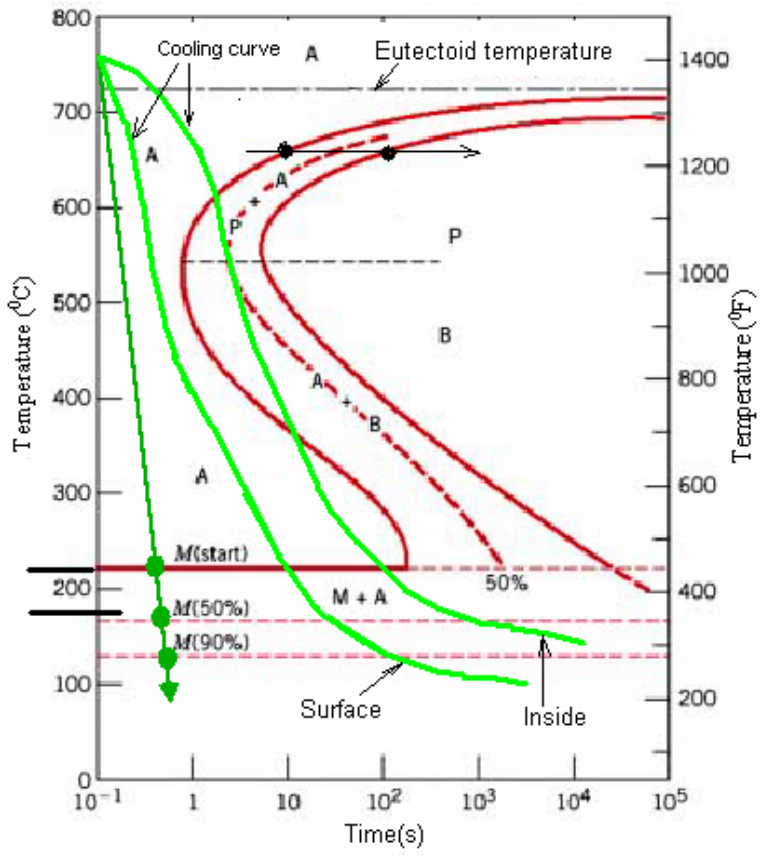

Figure 47. TTT diagram

2. Fast cooling: None of the curves of TTT diagram is being crossed by the cooling curve. In this case the formation of 100% martensite is assumed and accordingly hardness is calculated by the martensitic hardness plot. Regression analysis as described in the below section has been used to determine hardness.

The equation for 99.9% Martensite

$$y = -9.52381\ x^2 + 62x + 32.2438$$

Where x is the carbon percentage.

3. Slow cooling: In this case we will assume 100% (F+C) or 100%(F or P), depending on the TTT diagram and accordingly hardness can be calculated without considering any martensite.

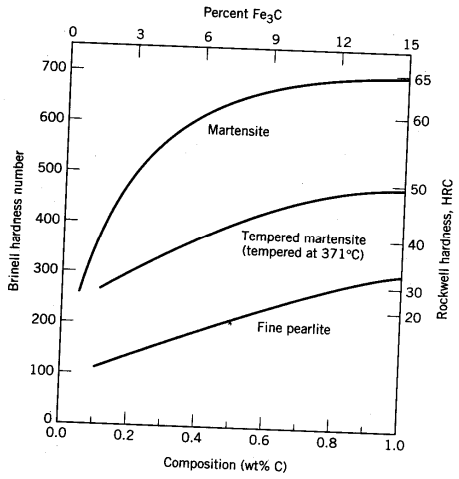

Figure 48. Hardness of martensite and pearlite

Regression analysis will be used to determine hardness.

If martensite%<50%,

$$H=Hp*fP+HB*fB+HM*fM \quad (52)$$

where,

Hardness of pearlite $HP=ax^2+bx+c$, x--C%

Hardness of bainite $HB=ax^2+bx+c$, x--C%

Hardness of martensite $HM=ax^2+bx+c$, x--C%

4.1.1 TTT Diagram: Various types of TTT diagram are included in the Database of CHT-*q/t*. The steel can be categorized in basic three types, hypoeutectoid steel, eutectoid steel and hypereutectoid steel.

1. **Hypoeutectoid steel:** The steel with less than 0.8% Carbon are said to be hypoeutectoid steel. To include the data of this type of TTT diagram, the ferrite and cementite start curve together has been considered as pearlite start curve.

The figure below shows TTT diagram for a hypoeutectoid composition (0.5 wt % C) compared to the Fe-Fe_3C phase diagram.

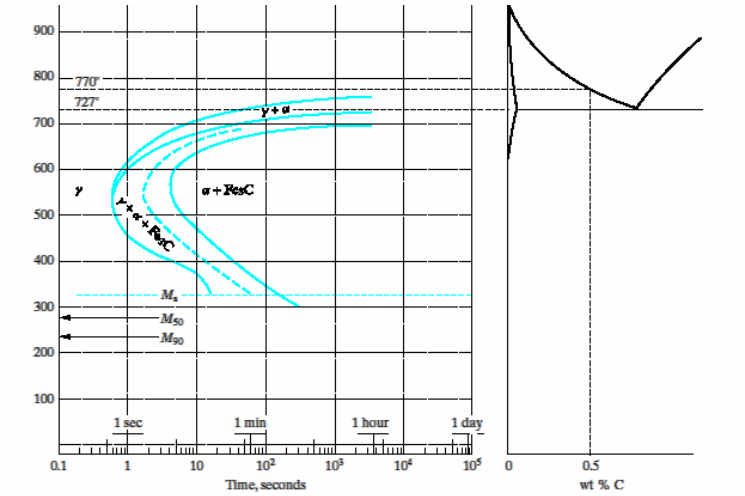

Figure 49. TTT diagram of hypoeutectoid steel

2. **Eutectoid steel:** The steel with 0.8% Carbon are said to be eutectoid steel.

3. **Hypereutectoid steel:** The steel with more than 0.8% Carbon are said to be hypereutectoid steel. To include the data of this type of TTT diagram, the ferrite and cementite curve together has been considered as pearlite start curve.

The figure below shows a TTT diagram for a hypereutectoid composition (1.13 wt% Carbon) compared to the Fe-Fe_3C phase diagram.

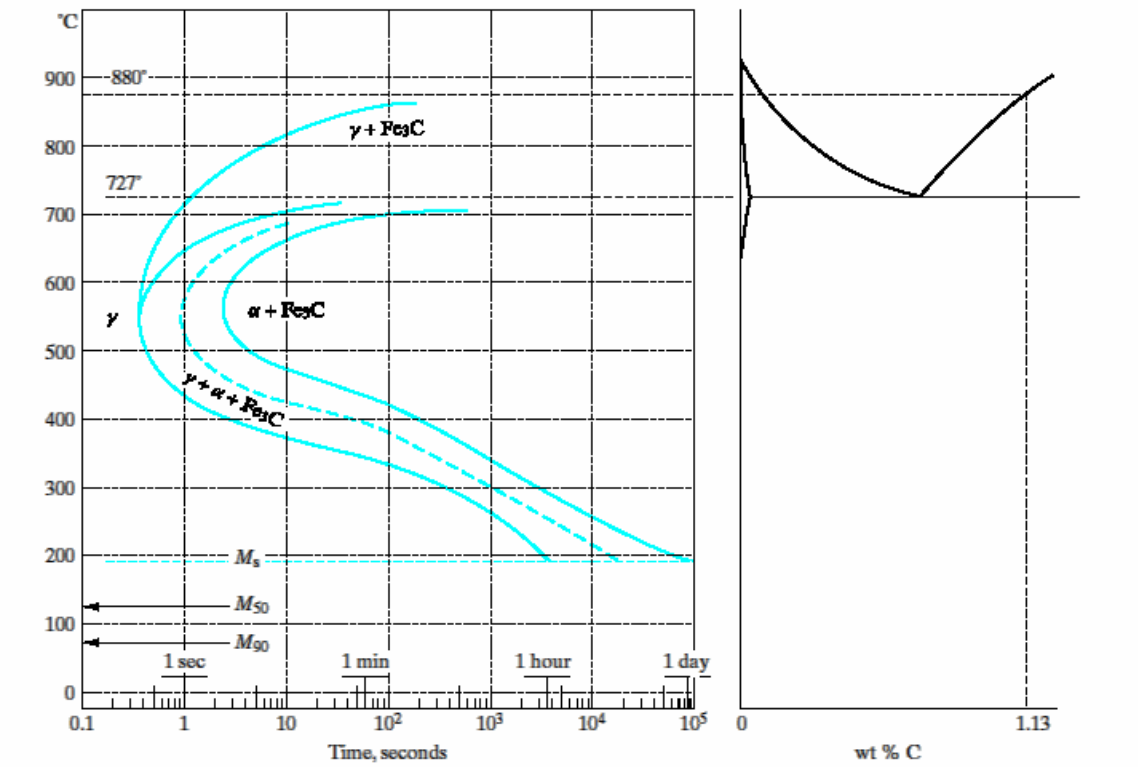

Figure 50. TTT diagram of hypereutectoid steel

Disposal of hypo and hyper-eutectoid steel

As described above the two start curve for the TTT diagram representing hypo and hyper eutectoid curve the start has been considered as a single start curve.

The figure below shows a curve with a combined ferrite and cemitite curve together as pearlite. The figure shows the start and finish curve for 0.1%Carbon, 0.3% carbon and 0.5% carbon.

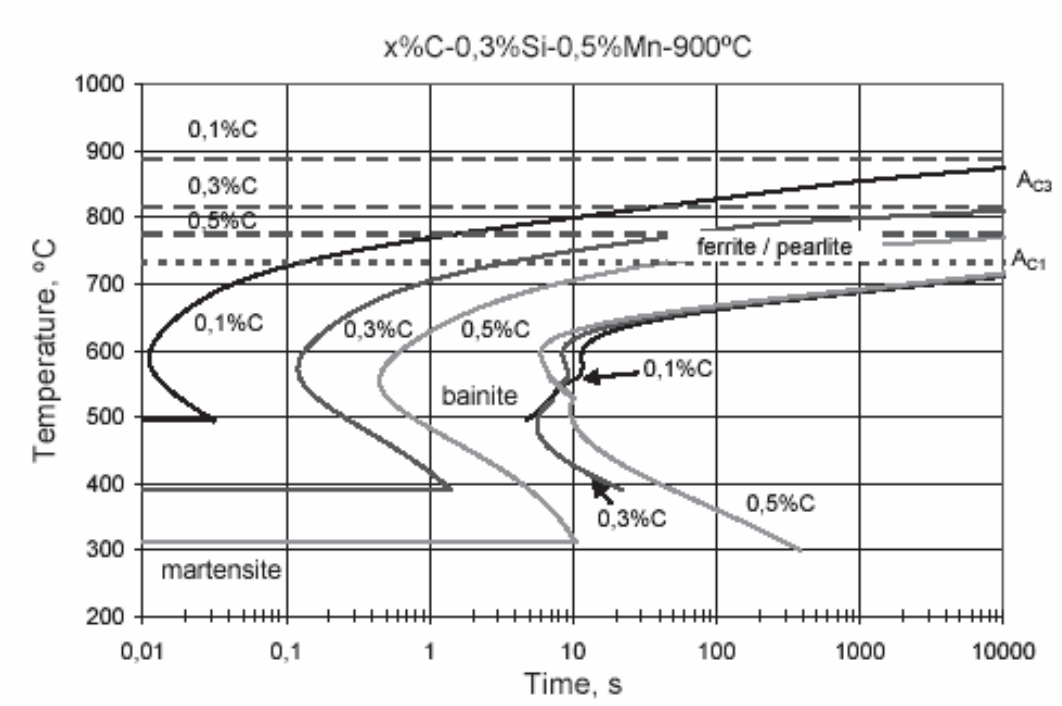

Figure 51. Disposal of hypo and hyper-eutectoid steel

4.1.2 Hardness Conversion:

The final equation used to determine the hardness is $HV = \sum\left(\sum\left(\Delta w_k(T_i)\cdot HV_k(T_i)\right)\right)$

Here microhardness is being used, that is in Vickers. Thus we need to convert Rockwell hardness to Vickers and vice versa.

For conversion, first Rockwell hardness should be converted into Brinell and then Brinell to Vickers.

Following table gives the equation to convert HRC to HB

Table 3. Conversion of HRC to HB

Rockwell Hardness Numbers (HRC)		Equations to convert Rockwell hardness (HRC) Into Brinell Hardness (HB)
from	to	
20	25	HB = 5.329 HRC + 119.6
26	30	HB = 6.984 HRC + 76.1
31	35	HB = 8.379 HRC + 33.7
36	40	HB = 8.872 HRC + 16.0
41	45	HB = 10.025 HRC - 30.8
46	50	HB = 12.473 HRC - 142.6
51	55	HB = 15.962 HRC - 318.7
56	60	HB = 19.038 HRC - 489.4
61	66	HB = 17.602 HRC - 403.8

Following table gives the conversion from HB to HV

Table 4. Conversion of HV to HB

Vickers Hardness Number (HV)		Equations to convert Vickers hardness (HV) into Brinell Hardness (HB)
from	to	
85	149	HB = 0.959 HV - 0.8
150	199	HB = 0.949 HV + 0.9
200	249	HB = 0.954 HV - 0.7
250	299	HB = 0.922 HV + 7.3
300	399	HB = 0.944 HV +1.2
400	499	HB = 0.909 HV + 15.1
500	670	HB = 0.940 HV - 0.2

4.1.3 Regression Analysis:

Regression analysis can be defined as a statistical technique used to find relationships between variables for the purpose of predicting future values. Since hardness is a function

of % martensite as well as % carbon content, thus regression analysis is being used to get the hardness at a specific martensitic percentage.

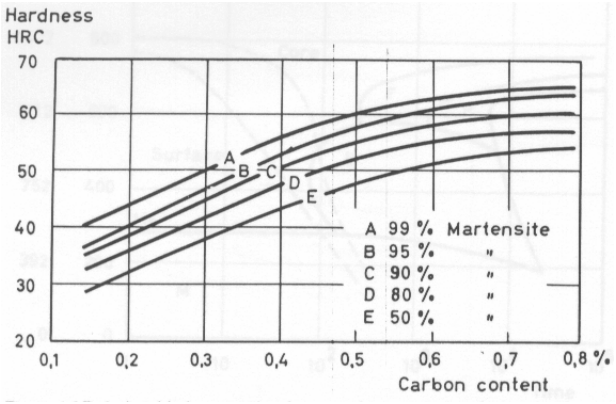

Carbon, %	Rockwell C hardness (HRC) with martensite contents of:				
	50%	80%	90%	95%	99.9%
0.18	31	35	37.5	39	43
0.23	34	37.5	40.5	42	46
0.28	36.5	40.5	43	44.5	49
0.33	39	43.5	46.5	48.5	52
0.38	42	46	49	51	54
0.43	44	48	51	53.5	57
0.48	46.5	52	54	57	60

Source: *Metals Handbook*, 1948 Edition

Figure 52. Hardness of martensite

Thus if, 50%<M%<100% Hardness=f(C%, Martensite%)

The equations of the form: H= a*x2* +b*x*+c, *x*--- C%

The equation at 50% Martensite

y = -19.0476 x^2 + 64x + 20.1448

The equation at 80% Martensite

y = 7.14286 x^2 + 50.6429x + 25.6529

The equation for 95% Martensite

y = -2.38095 x^2 + 61.2143x + 28.011

The equation for 99.9% Martensite

y = -9.52381 x^2 + 62x + 32.2438

If martensite%<50%,

H=Hp*fP+HB*fB+ HM*fM

where,

Hardness of pearlite HP=ax2+bx+c, x--C%

Hardness of bainite HB=ax2+bx+c, x--C%

Hardness of martensite HM=ax2+bx+c, x--C%

The figure below gives the sample regression page.

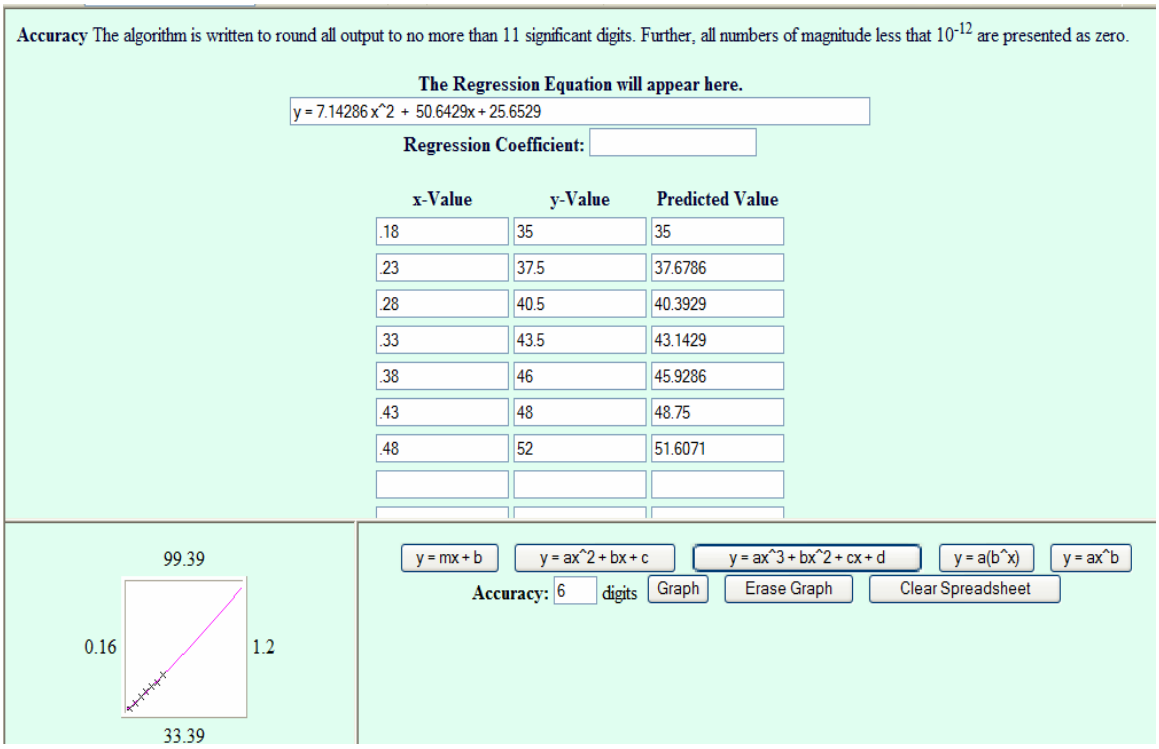

Figure 53. Regression analysis

4.1.4 Quench Factor Analysis:

Quench factor analysis is another method to predict the hardness after quenching. Presently in CHT-*q/t* we are not using this method. Quench factors are readily calculated from digital time-temperature (cooling curve) data and the C_T function describing the time-temperature-property (TTP) curve for the alloy of interest. Quench Factor analysis is mainly used for Aluminum due to non-availability of TTT diagram. Thus the only option to predict mechanical properties for Aluminum is time-temperature-property (TTP) curve. Although, TTP curves can be generated for steels as well, but this would be too cumbersome, as different grade of steel would require separate TTP curves. The easy availability of TTT diagrams makes it widely applicable for the determination of mechanical properties of steel after quenching.

The equation used to find C_T is as follows:

$$C_T = -K_1 \cdot K_2 \cdot \exp\left[\frac{K_3 \cdot K_4^{\,2}}{RT \cdot (K_4 - T)^2}\right] \cdot \exp\left[\frac{K_5}{RT}\right] \tag{53}$$

where,

C_T = critical time required to form a constant amount of new phase or reduce the hardness by a specified amount. (The locus of the critical time values as a function of temperature forms the TTP curve.)

K_1 = constant which equals the natural logarithm of the fraction untransformed during quenching, i.e, the fraction defined by the TTP curve

K_2 = constant related to the reciprocal of the number of nucleation sites.

K_3 = constant related to the energy required to form a nucleus.

K_4 = constant related to the solvus temperature.

K_5 = constant related to the activation energy for diffusion.

R = 8.3143 J/(^{0}K mole)

T = absolute temperature (^{0}K)

It should be noted that the TTP curves are not synonymous with the well known TTT (time-temperature-transformation) or CCT (continuous-cooling-transformation) curves. Although TTP curves are related to metallurgical transformation behavior, they are empirically derived and calibrated with respect to the property of interest for each alloy and chemistry.

The constants K_1, K_2, K_3, K_4, and K_5 shown in equation 51 define the shape of the TTP curve. The integration process is shown in Figure 53.

The incremental quench factor (q) for each time step in the cooling process is calculated according to equation (48).

$$q = \frac{\Delta t}{C_T} \tag{54}$$

where:

q = incremental quench factor

Δt = time step used in cooling curve data acquisition

C_T = is defined by equation (47)

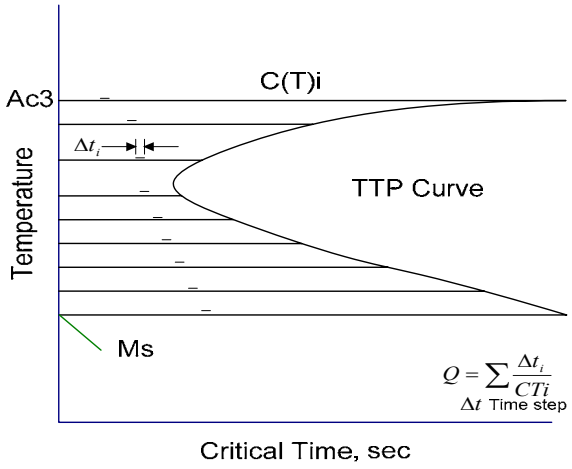

Figure 54. Quench factor analysis

The incremental quench factor (q) represents the ratio of the amount of the time an alloy was at a particular temperature divided by the time required for transformation to begin at that temperature.

The incremental quench factor is then summed over the entire transformation range to produce the cumulative quench factor (Q) as shown in equation 55.

$$Q = \sum q = \sum_{T_1 = Ar_3}^{T_2 = M_S} \frac{\Delta t}{C_T} \tag{55}$$

When calculating the quench factor (Q), the values of T_1 and T_2 are taken as the Ar_3 and M_s transformation temperatures respectively for the particular steel alloy. The cumulative quench factor (Q-Factor) is proportional to the heat removal characteristics of the quenchant as reflected by the cooling curve for the quenching process. Q-factors are single numbers that quantify quench severity which may be related to the metallurgical transformation behavior of steel.

The cumulative quench factor, Q, can be used to predict the as-quenched hardness in steel by:

$$P_p = P_{\min} + \left(P_{\max} - P_{\min}\right) \cdot \exp\left(K_1 Q\right) \tag{56}$$

where,

P_p = predicted property (e.g., hardness)
P_{min} = minimum property for the alloy,
P_{max} = maximum property for the alloy
exp = base of the natural logarithm
K_1 = ln(0.995) = -0.00501

4.3 Calculation of Ultimate Tensile Strength

Ultimate Tensile Strength is regarded as the function of hardness where the Brinell hardness (3000-kgf load) is used. The relationships used for calculation of UTS (Ultimate Tensile Strength) after quenching are mentioned below,

UTS=a*HB+b (57)

for some steels b might be zero.

UTS---unit psi,

The database of CHT-*q/t* contains the constants a and b for most of the steels. To enrich the database the variations of the constant values has been studied for all the grades of steels.

Variation in the constant for Carbon steels:

No specific trend has been observed for the alloy steels. The value of a is in the range 493 to 503.

Variation in the constant for Alloy steels:

No specific trend has been observed for the alloy steels. The value of a is in the range 494 to 504.

Variation in the constant for Stainless steels:

Table 5 Ultimate tensile strength - hardness relationship for stainless steels

Class	Designation and Grade	Hardness Range	Ultimate tensile strength
Austenitic	AISI Type 201	(250-400) HB	U.T.S = 606 HB - 31600
Austenitic	AISI 300-series	(140-180) HB	U.T.S = 457 HB + 16910
Austenitic	AISI 300-series	(190-370) HB	U.T.S = 534 HB - 16280
Ferritic	AISI 400-series	(140-190) HB	U.T.S = 430 HB + 6530
Martensitic	AISI 400-series	(156-595) HB	U.T.S = 508 HB - 3900
Precipitation-hardening	PH, AM, Custom series	(250-430) HB	U.T.S = 557 HB - 20710
Precipitation-hardening	PH, AM, Custom series	(25-46) HB	U.T.S = 4725 HRC - 2370

Variation in the constant for Tool steels:

Table. 6 Ultimate tensile strength - hardness relationship for stainless steels

Categories	Designation and Grade	Hardness Range	Ultimate tensile strength
Shock – resisting	AISI Type S1	(42-58) HRC	U.T.S = 7014 HRC – 94200
Shock – resisting	AISI Type S5	(37-59) HRC	U.T.S = 7829 HRC – 131700
Shock – resisting	AISI Type S7	(39-58) HRC	U.T.S = 6923 HRC – 92700
Oil - hardening	AISI Type O1	(31-50) HRC	U.T.S = 5899 HRC – 60120
Oil - hardening	AISI Type O7	(31-54) HRC	U.T.S = 6332 HRC – 78970
Air - hardening	AISI Type A2	(30-60) HRC	U.T.S = 5920 HRC – 53270
Chromium hot-work	AISI Types H11 & H13	(30-57) HRC	U.T.S = 6387 HRC – 62850
Special – purpose	AISI Type L2	(30-54) HRC	U.T.S = 6227 HRC – 59980
Special – purpose	AISI Type L6	(32-50) HRC	U.T.S = 6843 HRC – 83900
Mold	AISI Type P20	(26-54) HRC	U.T.S = 5535 HRC – 24880
Mold	AISI Type P20	(260-540) HB	U.T.S = 545 HB - 11770
Mold	AISI Type P20	(260-540) HRC	U.T.S = 520 HB

Ultimate Tensile strength after tempering

Ultimate Tensile Strength can be determined for as quenched and tempered steel based on a linear relationship with microhardness [35].

$$UTS = 3.412HV - 64.3 \tag{58}$$

The equation is valid for low-alloy case hardened and quenched and tempered steels with the following compositional range: 0.15 to 0.55%C, 0.17 to 0.4% Si, 0.5 to 1.3%Mn, 0.1 to 2%Cr, 0.02 to 0.3%Mo, 0.05 to 16%Ni, 0.01 to 0.3%V and 0.05 to 0.4%C.

4.4 Calculation of Yield Strength

Yeild strength can be calculated based on a linear relationship between yield strength σ_s and ultimate tensile strength σ_b

$$\sigma_s = k \cdot \sigma_b \tag{59}$$

The materials are classified into three categories, plain carbon, low alloy and alloy steel. For plain carbon steel *k* is between 0.6 to 0.65, for low alloy steel *k* is 0.65 to 0.75, and alloy steel *k* is 0.84 to 0.86.
The value of k has been further refined and added in the database for each grade of steel [25].
k = Yield strength / U.T.S

Yield strength after tempering:

Yield strength as quenched and tempered can also be calculated for all those steels having Ultimate Tensile Strength value. The equation used [25] is a function of UTS and volume fraction of martensite in %. The equation described below is used in CHT-*q/t* for the calculation of Yield strength after tempering.

$$YS = (117 - 0.007 f_m)UTS + 3.72 f_m - 484 \tag{60}$$

4.5 Calculation of Toughness

Toughness can be defined as the ability of a metal to rapidly distribute within itself both the stress and strain caused by a suddenly applied load, or more simply expressed, the ability of a material to withstand shock loading. It is the exact opposite of "brittleness" which carries the implication of sudden failure. A brittle material has little resistance to failure once the elastic limit has been reached.

The toughness value is measured by the charpy impact test. Charpy impact test can be defined as a pendulum-type single-blow impact test in which the specimen usually notched, is supported at both ends as a simple beam and broken by a falling pendulum. The energy absorbed, as determined by the subsequent rise of the pendulum, is a measure of impact strength or notch toughness.

Toughness is represented in KU for a U notch test piece. Toughness can be calculated for all those steels having Ultimate Tensile Strength value.
From literature, the relationship between toughness *KU* and ultimate tensile strength is a function of UTS and volume fraction of martensite in %.

$$KU = 296 - (0.285 - 0.00098 \cdot f_{\mathrm{m}})\sigma_b \tag{61}$$

where the unit of σ_b is MPa and *KU* is Joule and f_{m} is the volume fraction of martensite in %.

4.6 Calculation of Elongation

Elongation can be calculated for all those steels having Ultimate Tensile Strength value. The equation used is a function of UTS and volume fraction of martensite in %. The equation shown below is used in CHT-*q/t* for the calculation of elongation

$$A_{50} = 40 - (0.03 - 0.001 f_m)UTS \tag{62}$$

Elongation after Tempering

From literature, the elongation is calculated directly from the ultimate tensile strength. Therefore, if both elongation and σ_b can be found, then the relationship between them is formulated based on these data.

For example, the Ultimate Tensile Strength and Elongation of steel 4140 at different tempering temperature is listed below

Table 7 Properties of 4140 after tempering

Material	Tempering Temperature	Ultimate Tensile Strength	Elongation	Hardness
4140	400	257000	8	510
4140	600	225000	9	445
4140	800	181000	13	370
4140	1000	138000	18	285
4140	1200	110000	22	230

Therefore, the equations between elongation and σ_b can be obtained through numerical regression as,

$$EL = 4.3989e-10 \cdot \sigma_b^2 - 0.000258347 \cdot \sigma_b + 45.1839 \tag{63}$$

where EL is elongation. This relationship can be used to evaluate the elongation at other tempering temperatures.

CHAPTER 5. IMPLEMENTATION

The CHT-*q/t* system is validated with two case studies to check the accuracy of the various mathematical models, different interfaces and the parameters associated with the software. The case studies were conducted to validate the quenching model and the accuracy of the quenchant database. Gas quenchants were used for both of the case studies. One of them was conducted on a VFS Vacuum furnace, at American Heat Treating, Monroe, CT and another one on ABAR Vacuum furnace at Bodycote Worcester, MA. It has been observed that these case studies were insufficient to validate the whole model, especially the property prediction module, and more case studies are needed in future.

5.1 Case Study 1 at Bodycote, Worcester, MA

The main objective of the case study was to verify the user interfaces with the inputs from the industry and to make sure all the essential factors are taken into account for the calculation, and to validate the results obtained using the system. Especially the focus was to validate the new heat transfer module for quenching, and also the microstructure evolution and property prediction modules. This case study was performed on ABAR vacuum furnace at Bodycote Worcester, MA.

Furnace Information

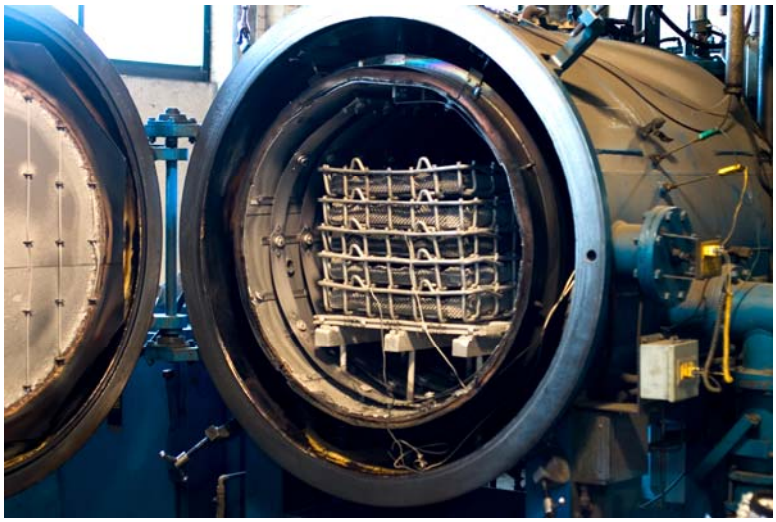

Figure 55. A picture of the furnace used for case study

Furnace – Abar Vacuum Furnace, Bodycote Thermal Processing, Worcester

Manufacturer – ABAR

Gas quench type – 2 bar

Workpiece Information

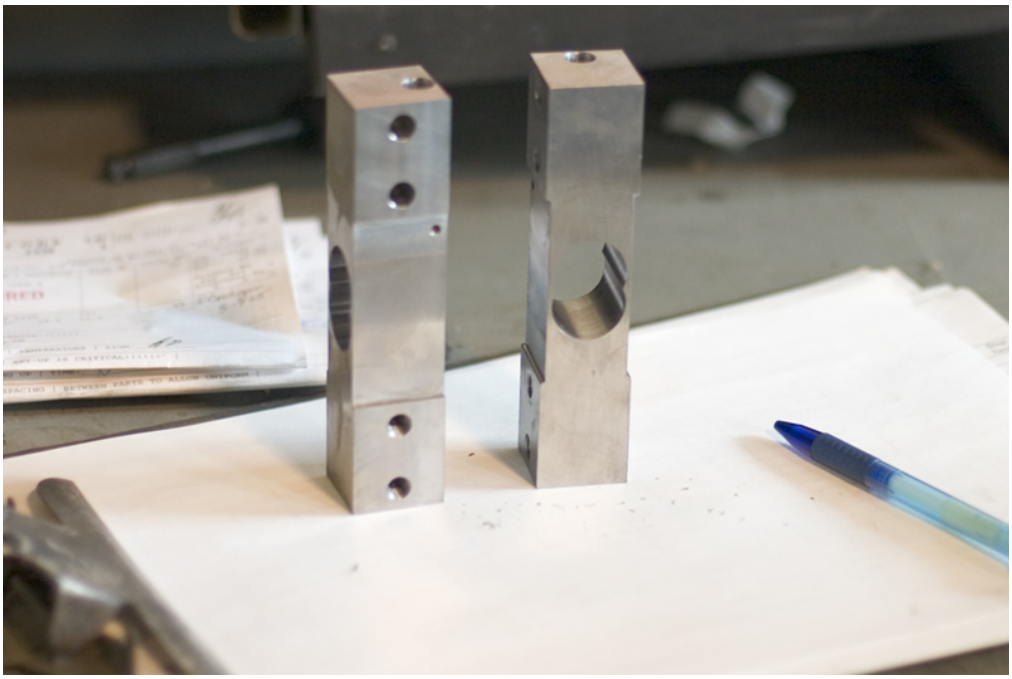

Figure 56. Picture of workpiece

Name – SS-bar

Weight – 3.8 lbs

Material – Stainless Steel 410

Process Information

The main cycle in the process is heating and quenching. The tests were ran our for the entire heat treatment cycle. The parameters are:

Quench Gas Atmosphere – Nitrogen

Quench Pressure – 2 bar

Blower HP – 200

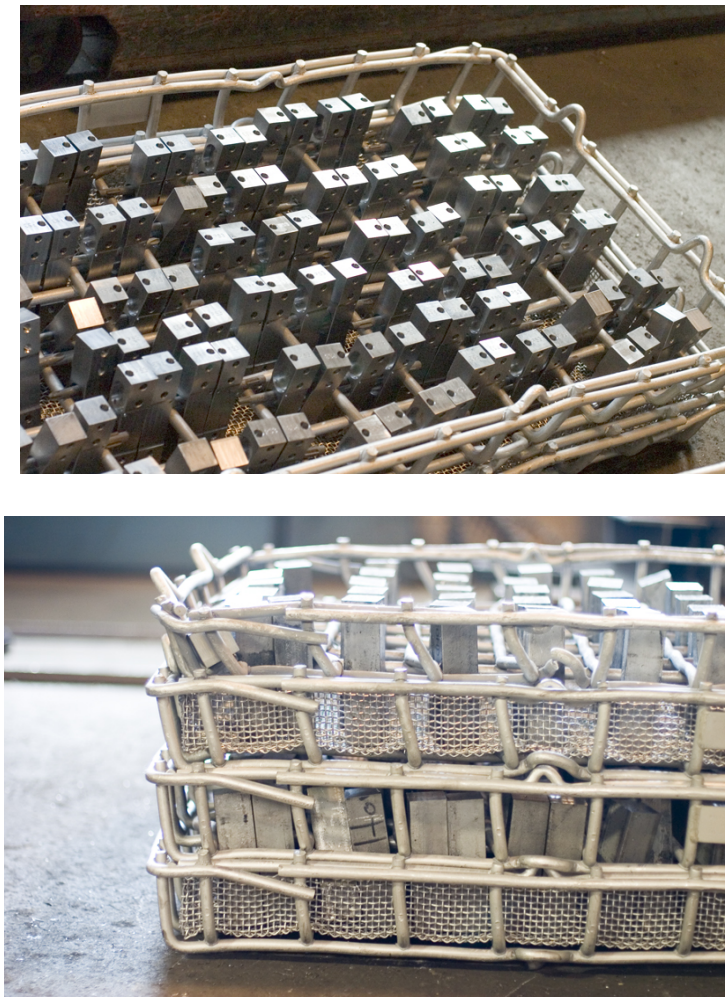

Figure 57. Arrangement of workpieces in the basket

The parts were arranged in 2 baskets with two layers one on top of another. Each basket containing parts arranged in 6 rows and 12 columns.

Table 8. Furnace temperature data (Case 1 – PEG)

Process	Atmosphere Content	Temperature (F)	Time (mins)
Heating	Vacuum	70-1900	from room temp.
Soaking	Vacuum	1900	200
Quenching	Nitrogen (2 bar)	200	200

Measured results

Two thermocouples were attached to the workpieces in the load and they were placed at the corner in the top basket and at the center in the bottom basket.

Calculation & observations

Based on the various input information the case was run using the CHT-*qt* system and the results obtained are shown in Figure 58.

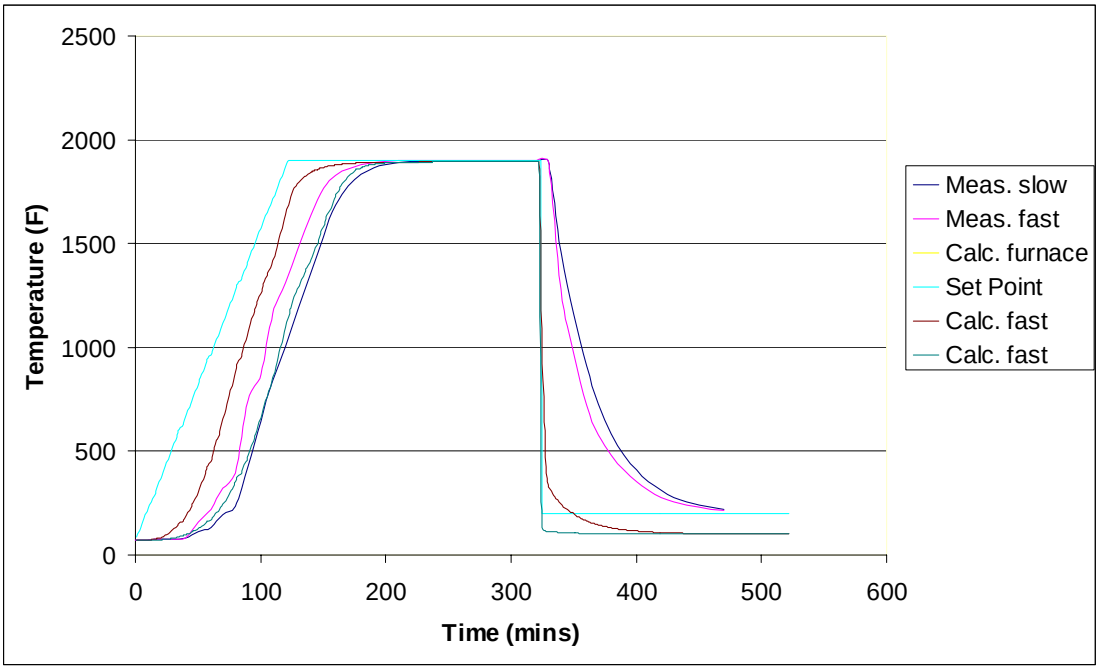

Figure 58. Comparison between the calculated & measured results – Case 1

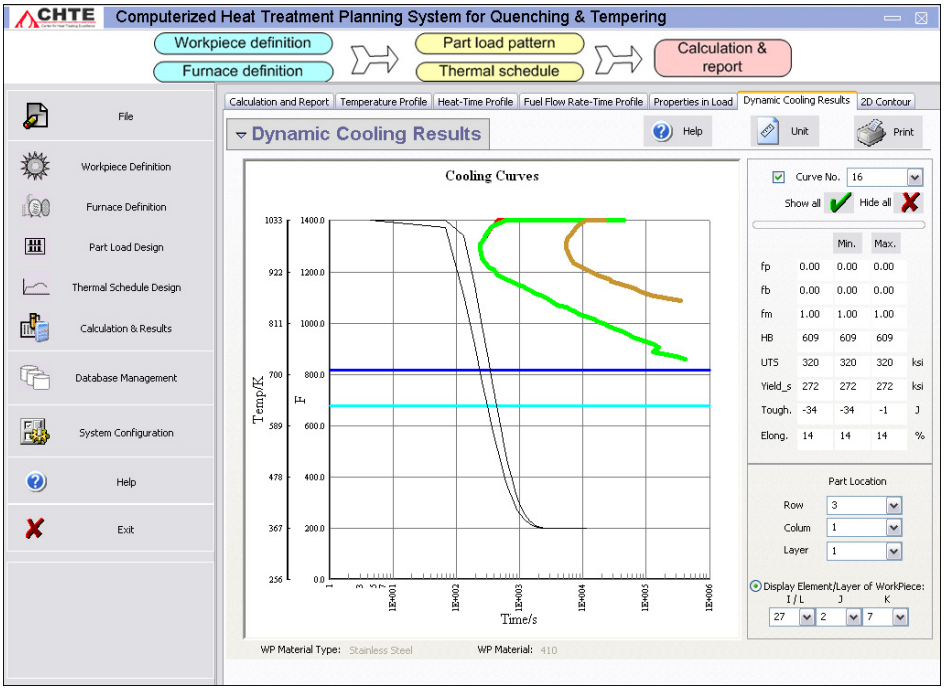

Figure 59. Cooling curves of workpieces in different places of the load plotted super imposed on a TTT curve of stainless steel 410

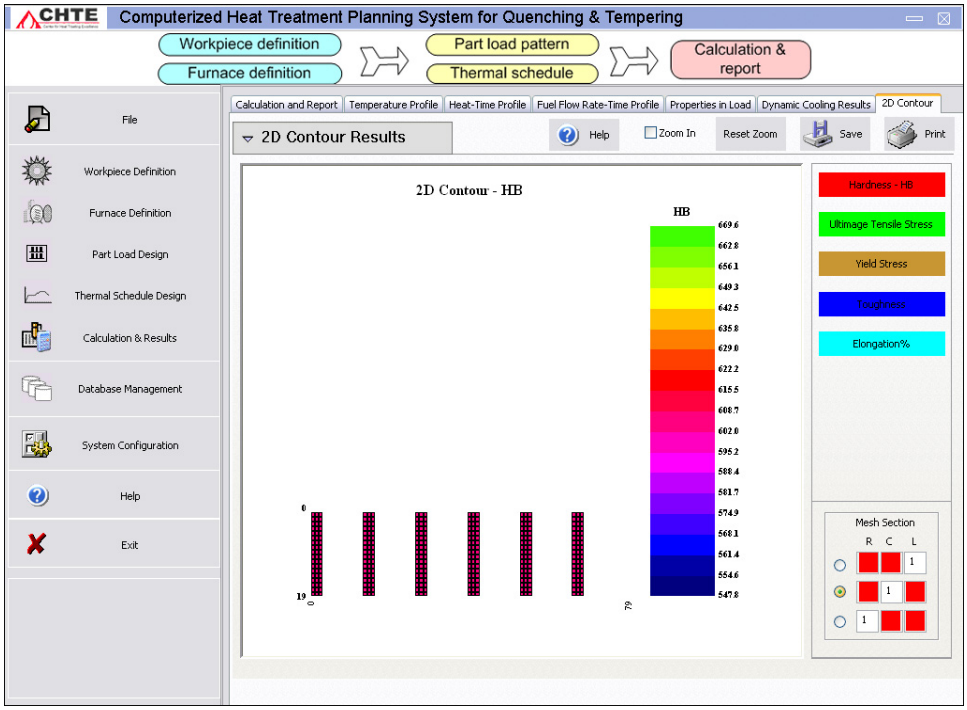

Figure 60. Property distribution of workpieces in the load shown in cross sections along the column

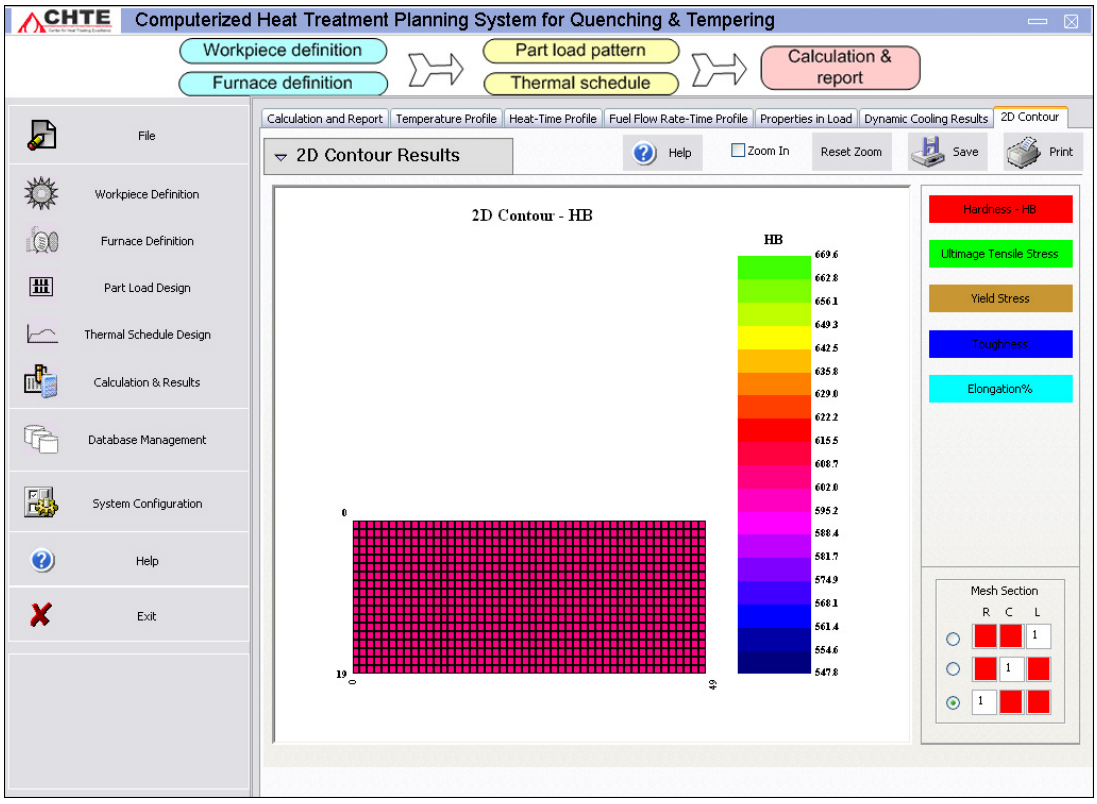

Figure 61. Property distribution of workpieces in the load shown in cross sections along the rows

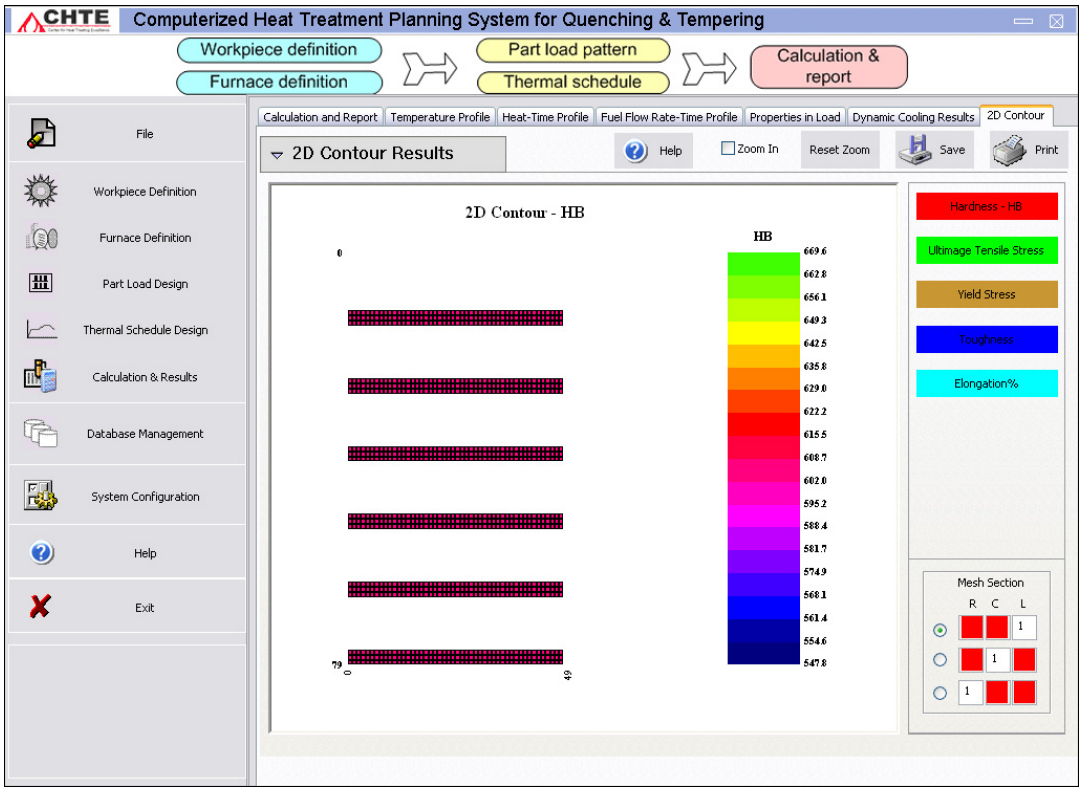

Figure 62. Property distribution of workpieces in the load shown in cross sections along the layers

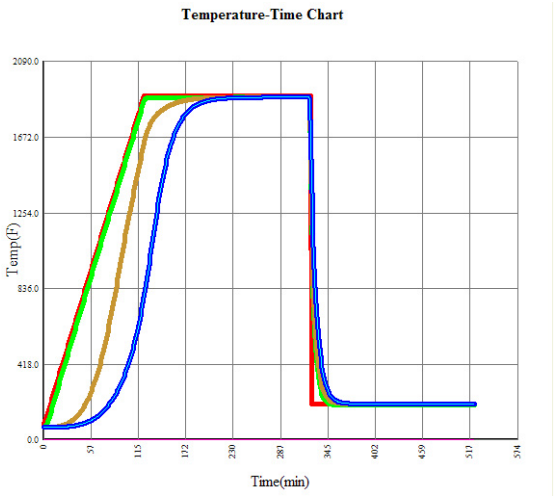

Figure 63. The cooling curve with modified ‘h’

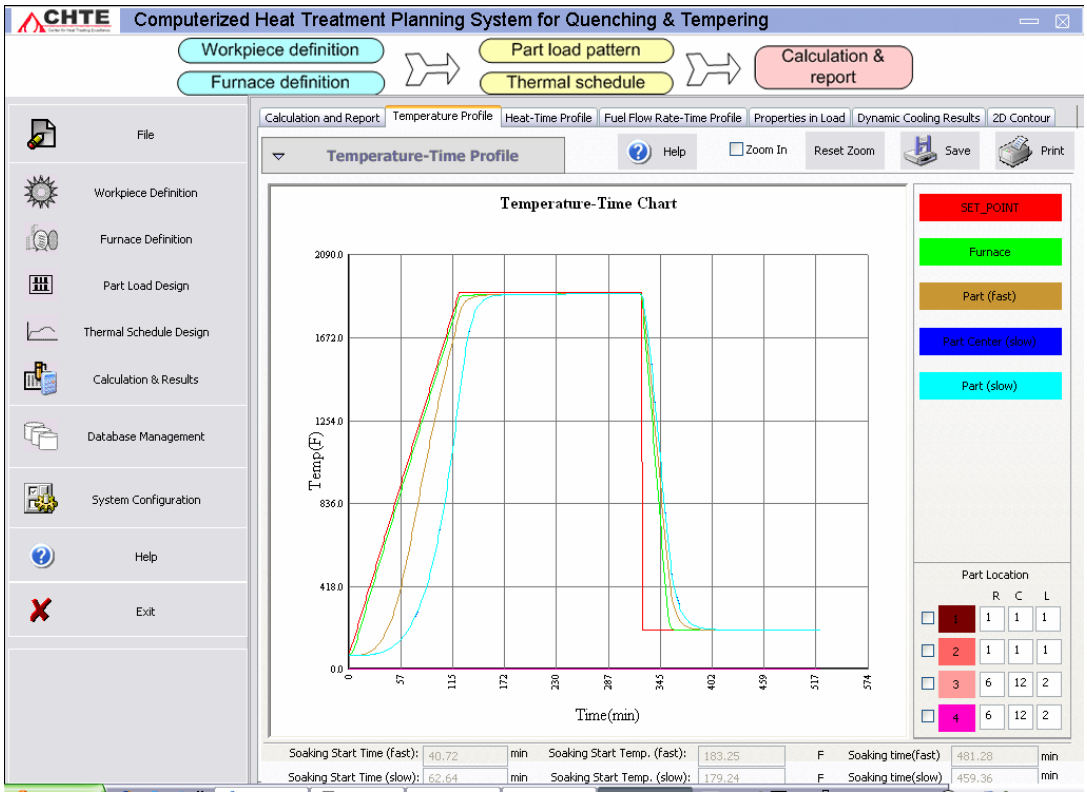

Figure 64. The result with different gas quenching temperature models

Results

Figure 63 shows the cooling curve after modifying the values of 'h' and gas temperature. The results are closer to the actual measured results when the value of 'h' is modified to suit the furnace conditions. The accuracy of the results is very sensitive to 'h'. Also another area of concern is the furnace model that has to include the change in HP of the blower motor during the quenching process, which at present, considered as a constant.

5.2 Case Study 2 at American Heat Treating, CT

This was one of the extensive case studies that I ran with 12 thermocouples at different locations to better understand the process and it was carried out to validate different modules of the software. A VFS vacuum furnace was used to conduct the case study.

Furnace Information

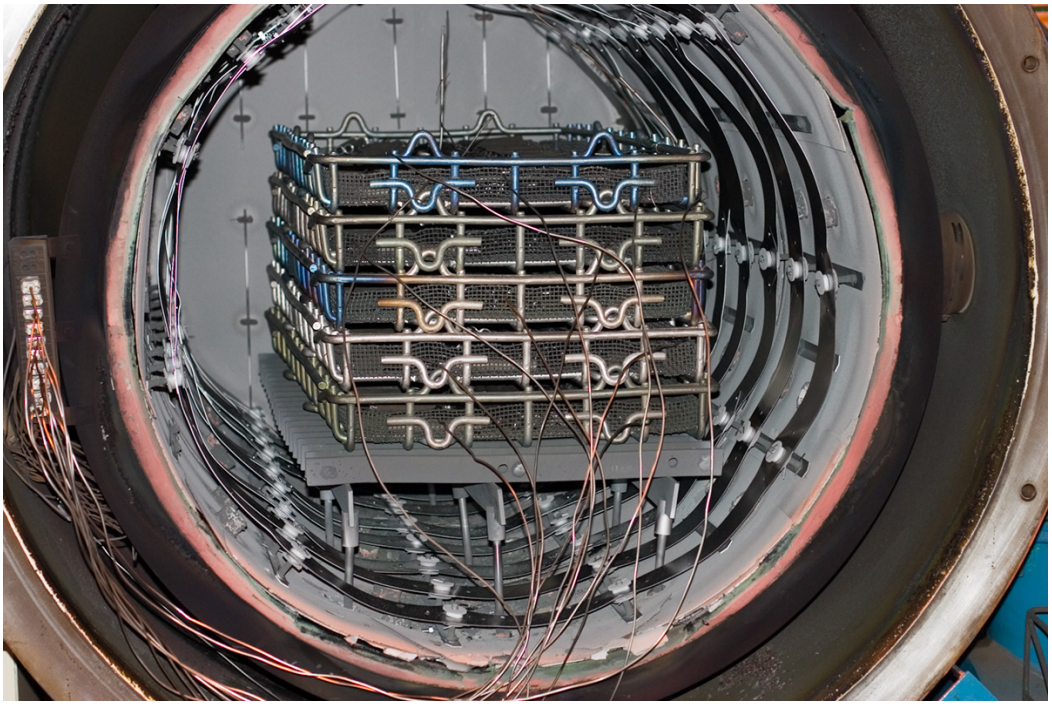

Figure 65. A picture of the furnace used for case study

Furnace –VFS Vacuum Furnace, American Heat Treating, Monroe, CT

Manufacturer – VFS

Gas quench type – 2 bar

Workpiece Information

Figure 66. Picture of workpiece

Name – Handle

Weight – 0.3 lbs

Material – Alloy Steel 4340

Process Information

The main cycle in the process brazing that also involves heating and quenching. The parameters are:

Quench Gas Atmosphere – Nitrogen

Quench Pressure – 2 bar

Blower HP – 160

Figure 67. Arrangement of workpieces in the basket and thermocouple placements

The parts were arranged in 5 baskets with one layer and baskets one on top of another. Each basket containing parts arranged in 2 rows and 62 columns.

Table 9 Furnace temperature data (Case 2 – Handle)

Process	Atmosphere Content	Temperature (F)	Time (mins)
Heating	Vacuum	70-1000	from room temp.
Soaking	Vacuum	1000	180
Soaking	Vacuum	1750	120
Soaking	Vacuum	1950	50
Quenching	Nitrogen (2 bar)	200	40

Measured results

Twelve thermocouples were attached to the workpieces in the load and furnace and they were placed at different locations.

Calculation & observations

Based on the various input information the case was run using the CHT-*qt* system and the results obtained are shown in Figure 68.

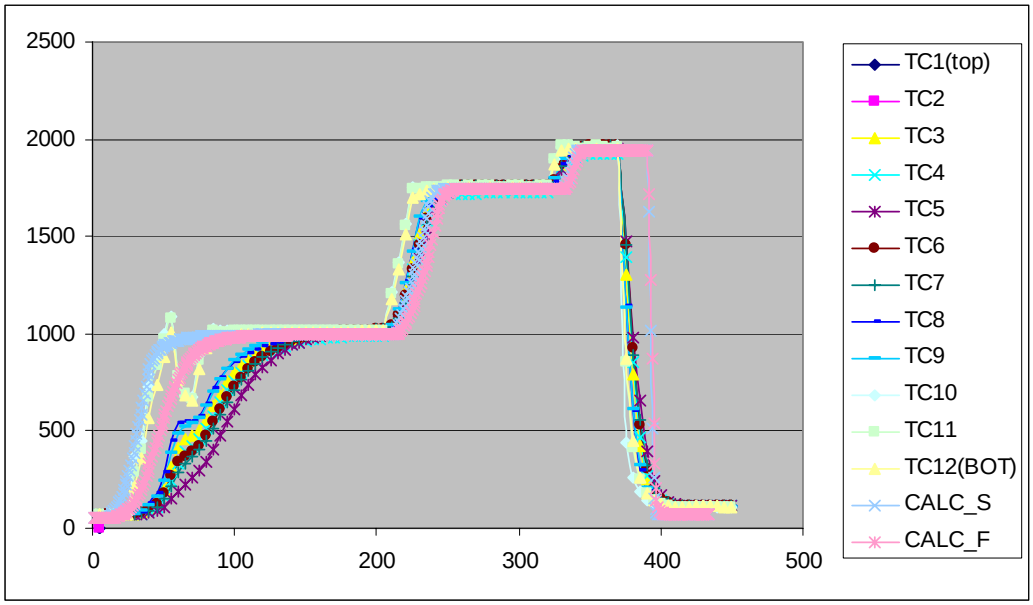

Figure 68. Comparison between the calculated & measured results – Case 2 (CALC_S & F are the calculated results)

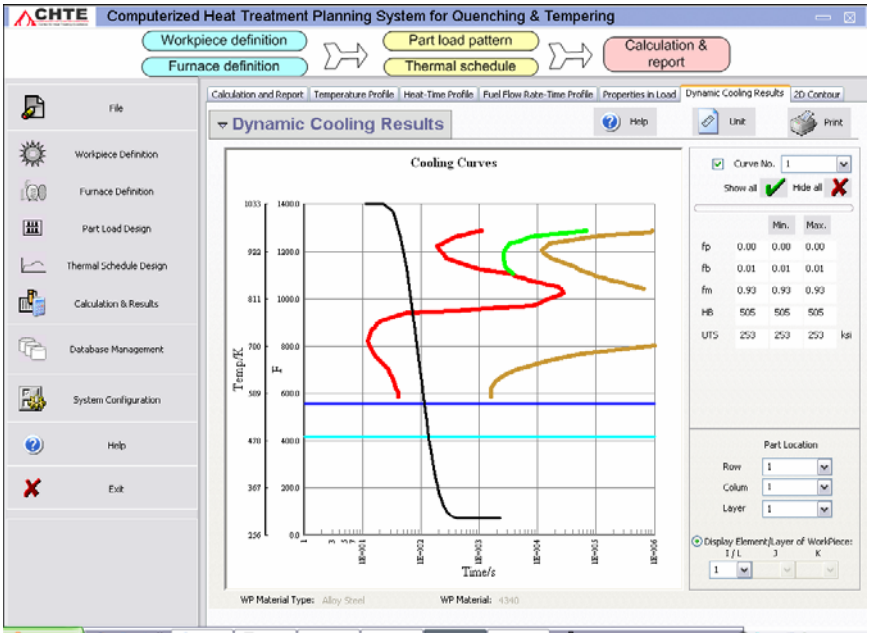

Figure 69. Cooling curves of workpieces in different places of the load plotted super imposed on a TTT curve of 4340 Steel

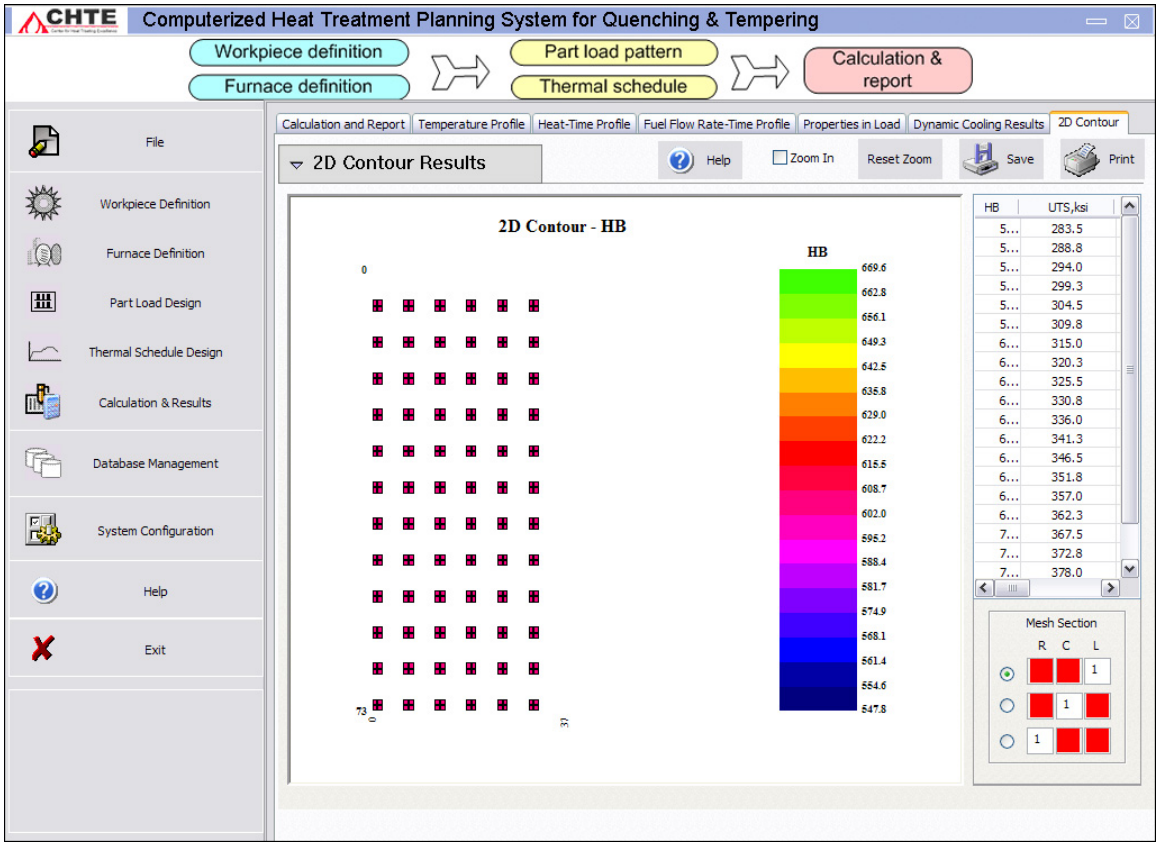

Figure 70. Property distribution of workpieces in the load shown in cross sections along rows, columns and layers

Results

As shown in Figure 68 slight variations are seen on the temperature profile as measured by thermocouple and the calculated value by CHT-*q/t.* The main reason for this is the convective heat transfer coefficient. The variation of blower horse power and the quench pressure affects the convective heat transfer coefficient, which should be taken into account. Figure 69 shows the cooling curve as superimposed to the TTT diagram. The user can get the idea of the mechanical properties by just viewing the picture. Figure 70 shows the variation of hardness at different nodes of the workpiece as well as in the entire

load. The user has the option to view the variation of hardness along rows, columns and layers. Finally, just two case studies are not enough for the validation of each modules of the software. The other mechanical properties i.e, ultimate tensile strength, toughness and percentage elongation were not calculated in the above case studies, and thus more case studies are required for complete validation of CHT-*q/t.*

CHAPTER 6. INDUSTRIAL APPLICATION OF CHT-*bf*

Bodycote Group is the world leading supplier of specialist metallurgical services e.g. heat treatment, hot isostatic pressing, metallurgical coatings and materials testing services. The Bodycote group has over 230 facilities in 22 countries.

CHT-*bf* was introduced at Bodycote Thermal Processing, Worcester. Pit and All case furnaces were chosen for the case study. The plant contains four all case furnaces, two of them have connected heat input of 60,000 Btu/hr and the other two with 100000 Btu/hr. Generally heavy parts are heat treated in the pit furnace which takes considerable time to reach the set point temperature. The detailed furnace description is given below in the case study.

6.1 Introduction to CHT-*bf*

Computerized Heat Treatment Planning System for Batch Furnace (CHT-*bf)* is a windows based stand alone software that can be used to simulate the heating of parts in a furnace. The graphical user interfaces are windows based and they were designed with much input from several commercial heat treaters and furnace manufacturers. CHT-*bf* contains a comprehensive database for materials of the part being heat treated, furnace elements, furnaces, furnace atmospheres and fuels. These data help the user to use the software without defining an exhaustive set of parameters.

The software mainly consists of five modules: workpiece definition, furnace definition, load pattern specification, thermal schedule specification, and calculation & report. There are other functions such as, file management, database & database management, serving as the foundation of the software.

The following output can be obtained by CHT-*bf*

1. Temperature vs time of all parts (optional)
2. Temperature curves of the fastest and slowest heated parts
3. Heat terms such as heat input, heat storage in load, heat storage in furnace, etc.
4. Fuel flow rate for gas-fired furnace

6.2 Objective

1. To study the effects of change in the load quantity and giving recommendations for the thermal schedule redesign.

2. To study the effect of change in load arrangement, determination of optimal load pattern from the calculated temperature values.

3. To determine the pre-heat required to reach the set point temperature and hence to determine cycle time.

4. Scheduling of jobs in furnace after determining exact cycle time.

5. To study the effect of part orientation on the quality and distortion and hence to determine best suited load orientation.

6.3 Case Study 1

This case study was carried out in the Pit furnace.

Workpiece data

The workpiece used for the study are shown in Figure 71 and Table 10

Figure 71. R. H. Handles workpiece

Table 10 Workpiece definition for case 1

Work piece Name	R. H. Handles
Work piece Material	1137
Work piece weight	2

Furnace Data:

The furnace is electric heated furnace, as seen in Figure 72. Its data is listed in Table 11 The furnace has three zones with the connected heat input of 120 Kw.

Figure 72. Pit furnace

Table 11. Furnace information

Furnace name	Pit furnace, 416
Body Shape (E.g. vertical, Horizontal)	Vertical
Heating type (E.g. direct/indirect fired, electric)	Electric
External size(Length×Width× Height) or (diameter × Height)	5 x 8
Work space (Length×Width× Height) or (diameter × Height)	45 x 60
Maximum Operating Temperature	2500 F
Minimum Operating Temperature	1000

Connected heat input	120 kw or 409416.58 BTU/hr	
Atmosphere content	Air	
Air preheated temperature	No preheat	
Excess of preheated air (%)	No	
Vacuum Furnace	[ ] Yes [x] No	
Opening area	0	
Recirculation Fan (one fan at top)	[x] Yes [ ] No	
	Material	303
	Horse power	2
	Diameter	14
	Height	4.5
	Speed	1140 R.P.M
	Weight	35
	Rate of cooling water	0
Furnace Accessories data (weight and material)	Heating elements	Graphite, 50lbs
	Cooling tubes	
	Grate	
	Supports	Alloy, 100lbs
	Roller rails	
	Others	Alloy, 1000lbs
Furnace wall data (thickness and material)	Top Layer 1	CF_Veneen_2, 10 inch
	Top Layer 2	
	Side Layer 1	CF_Veneen_2, 9 inch
	Side Layer 2	
	Bottom Layer 1	CF_Veneen_2, 9 inch
	Bottom Layer 2	

Load Pattern:

The workpiece considered to be arranged load pattern as shown in Figure 73. The furnace was loaded with one basket containing 181 workpieces. Two thermocouples were attached to the workpiece, one to the center part and the other to the workpiece located at the outer ring. Load pattern can be seen in Figure 73.

Figure 73. Load pattern for case 1

Table 12. Load pattern

Fixture type (basket/plate)	Basket
Fixture shape (rectangular/round)	Round
Side wall, bottom (solid/net like)	Solid
Fixture weight	300 lbs
Fixture size (diameter , height) inch	35, 25
Load pattern, Fixture configuration	Arraged
Total quantity of workpiece in fixture	181
Total weight of workpiece in fixture, lbs	362

Table 13. Arrangement of load pattern

Quantity in each ring			
Row	Quantity	Row	Quantity
Ring (Row)1	23	Ring 6	18
Ring 2	22	Ring 7	17
Ring 3	21	Ring 8	16
Ring 4	20	Ring 9	14
Ring 5	19	Ring 10	11

Result by CHT-*bf*

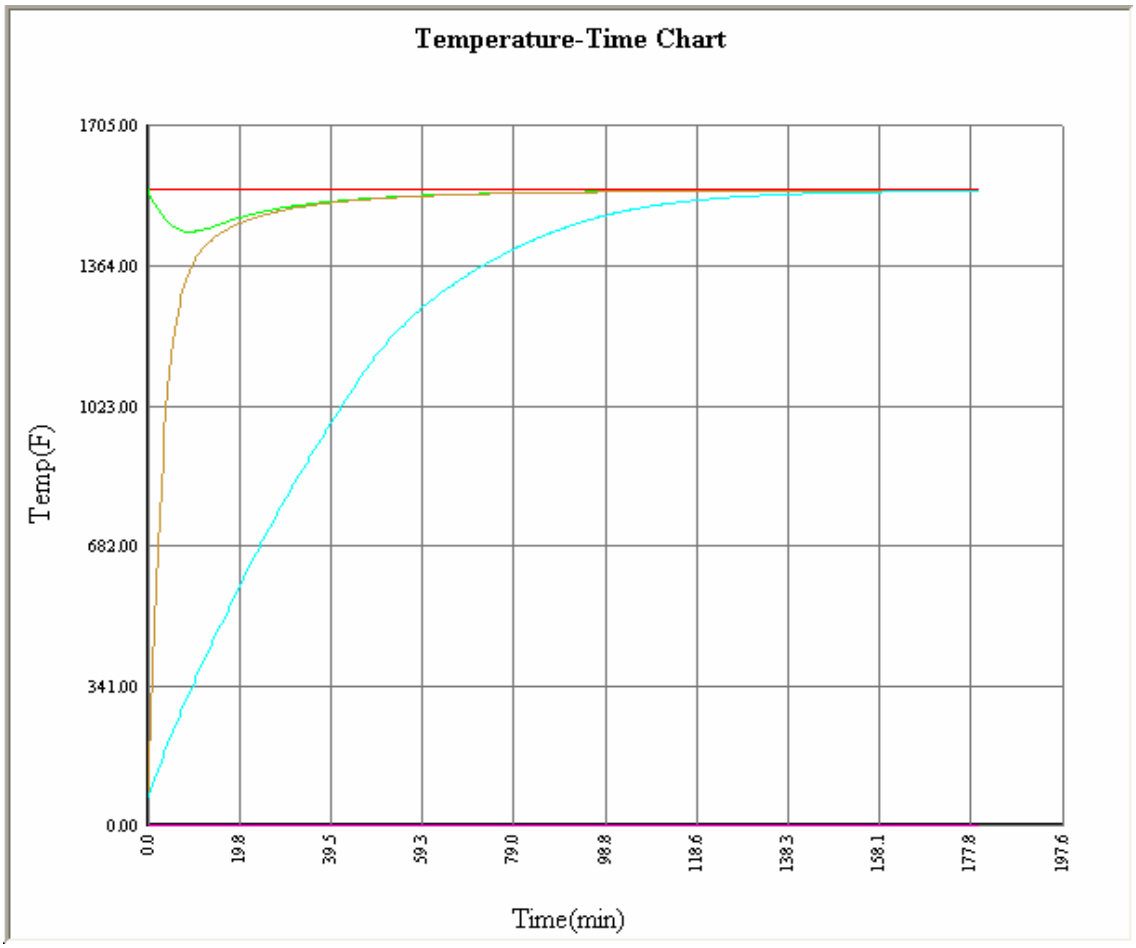

Figure 74. Time-temperature chart

Actual result of the case study as measured by thermocouple:

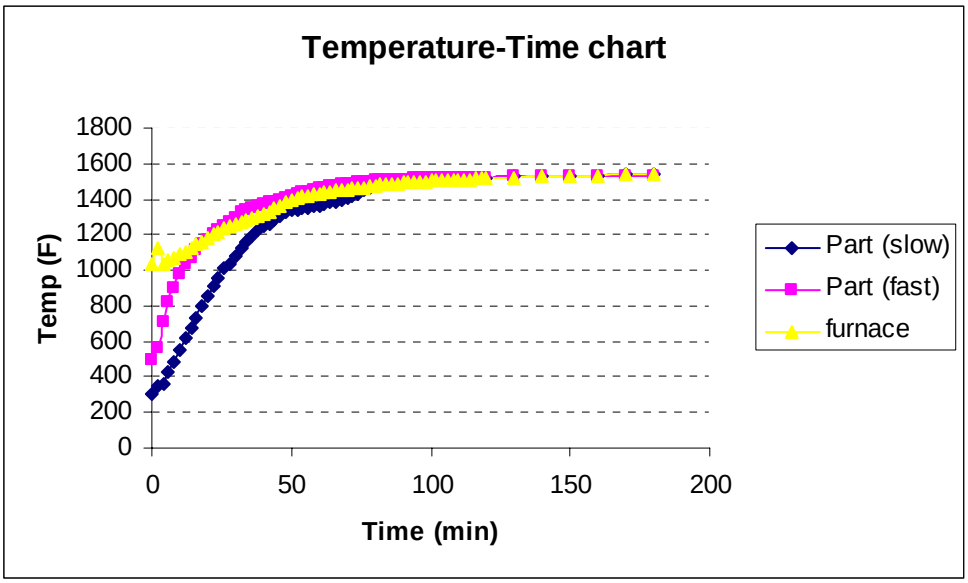

Figure 75. Thermocouple result

The actual temperature profile measured by thermocouple to that predicted by CHT-*bf* closely matches each other

The soaking time taken for the present case study is 305 minutes instead of 180 minutes.

Actual result of the case study as measured by thermocouple with soaking time as 305 minutes:

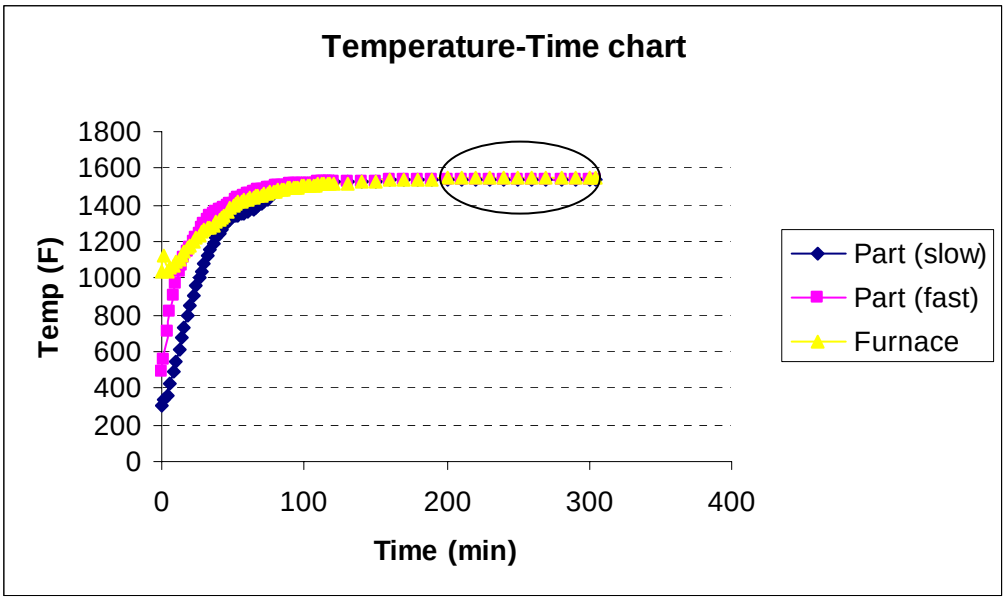

Figure 76. Thermocouple result with increased soaking time

Result from CHT-*bf*, with time as 305 minutes

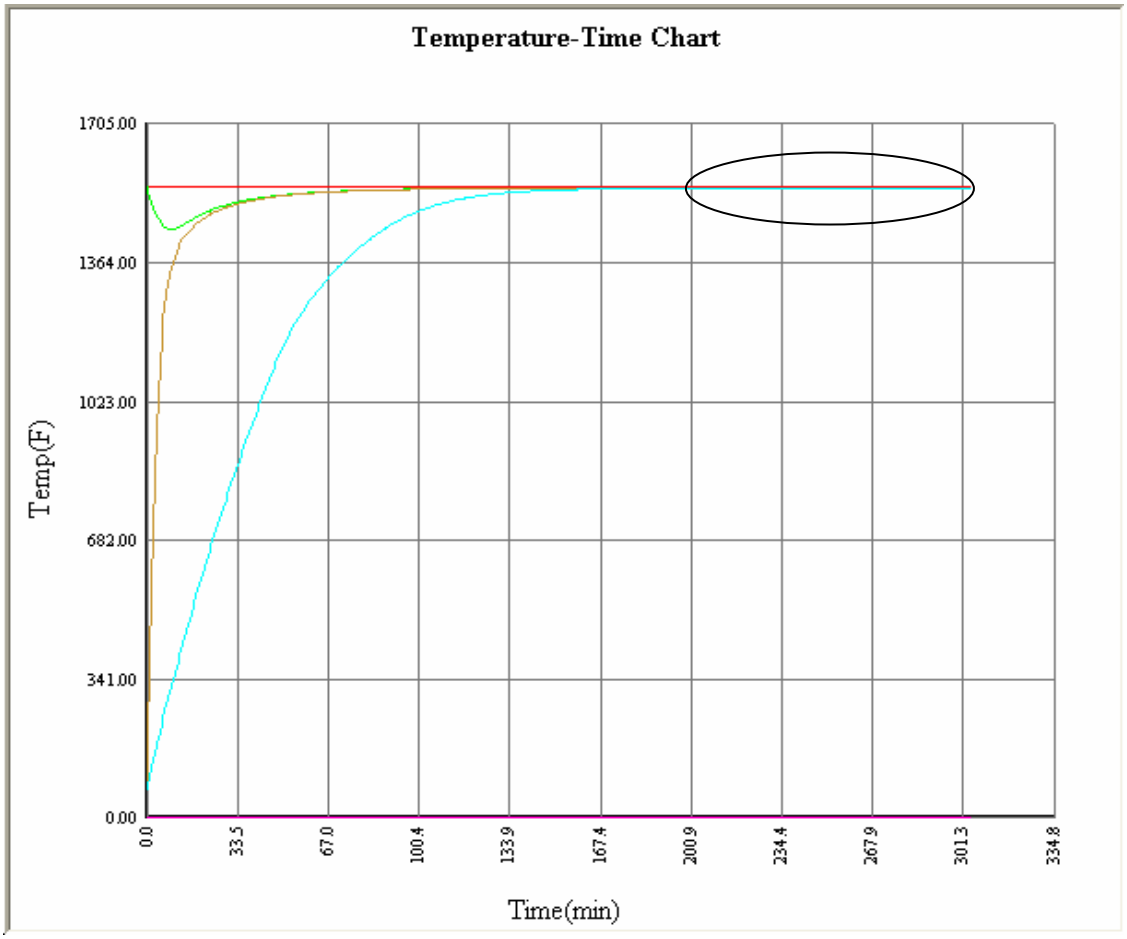

Figure 77. CHT-*bf* result with increased soaking time

Conclusion:

It can be concluded by the result, part temperature remains almost constant after 180 minutes. Thus we can determine the optimum cycle time prior to heat treating the load in furnace. If no specific heat treatment process i.e carburizing, nitriding is been performed, then we can easily reduce the cycle time by running the case in CHT-*bf* prior to actual process.

6.4 Case Study 2

Workpiece Information:

The workpiece of this case study is shown in Figure 78. and workpiece information in Table 14.

Table 14. Workpiece Information

Work piece Name	Numa part
Work piece Material	6418
Work piece weight	Different types of part in the load 1. Qty = 3, wt. = 1, Material: 6418 2. Qty = 10, wt. = 325, Material: 4340 3. Qty. = 9, wt. = 324, Material: 6418 3.1 Qty. = 10, wt. = 1300, Material: 6418 4. Qty. = 1, wt. = 38, Material: 6418 4.1 Qty. = 2, wt. = 62, Material: 6418 4.2 Qty. = 6, wt. = 192, Material: 6418 5. Qty. = 1, wt. 639 Total qty = 42, Total wt. = 4164 Thus average workpiece wt = 99.143

Workpiece picture

Figure 78. Workpiece

Furnace information:

The furnace used for the case study is the same as that used for case study 1.

Load pattern:

The workpiece considered to be arranged load pattern as shown in Figure 79. The furnace was loaded with two basket, each containing 21 workpieces of different shape and sizes. Average of all the dimensions and weight of workpiece was taken to simulate it in CHT-*bf*. Two thermocouples were attached to the workpiece, one to the center part and the other to the workpiece located at the outer ring.

Figure 79. Load pattern

Table 15. Load Pattern

Fixture type (basket/plate)	Basket
Fixture shape (rectangular/round)	Round
Side wall, bottom (solid/net like)	Solid
Fixture weight	300 lbs
Fixture size (diameter , height) inch	35, 25
Load pattern, Fixture configuration	Arraged
Total quantity of workpiece in fixture	21
Total weight of workpiece in fixture	2082

Table 16. Arrangement of load pattern

Ring (Row)	No. of workpiece in each row
1	7
2	5
3	4
4	3
5	2

Result given by CHT-*bf*

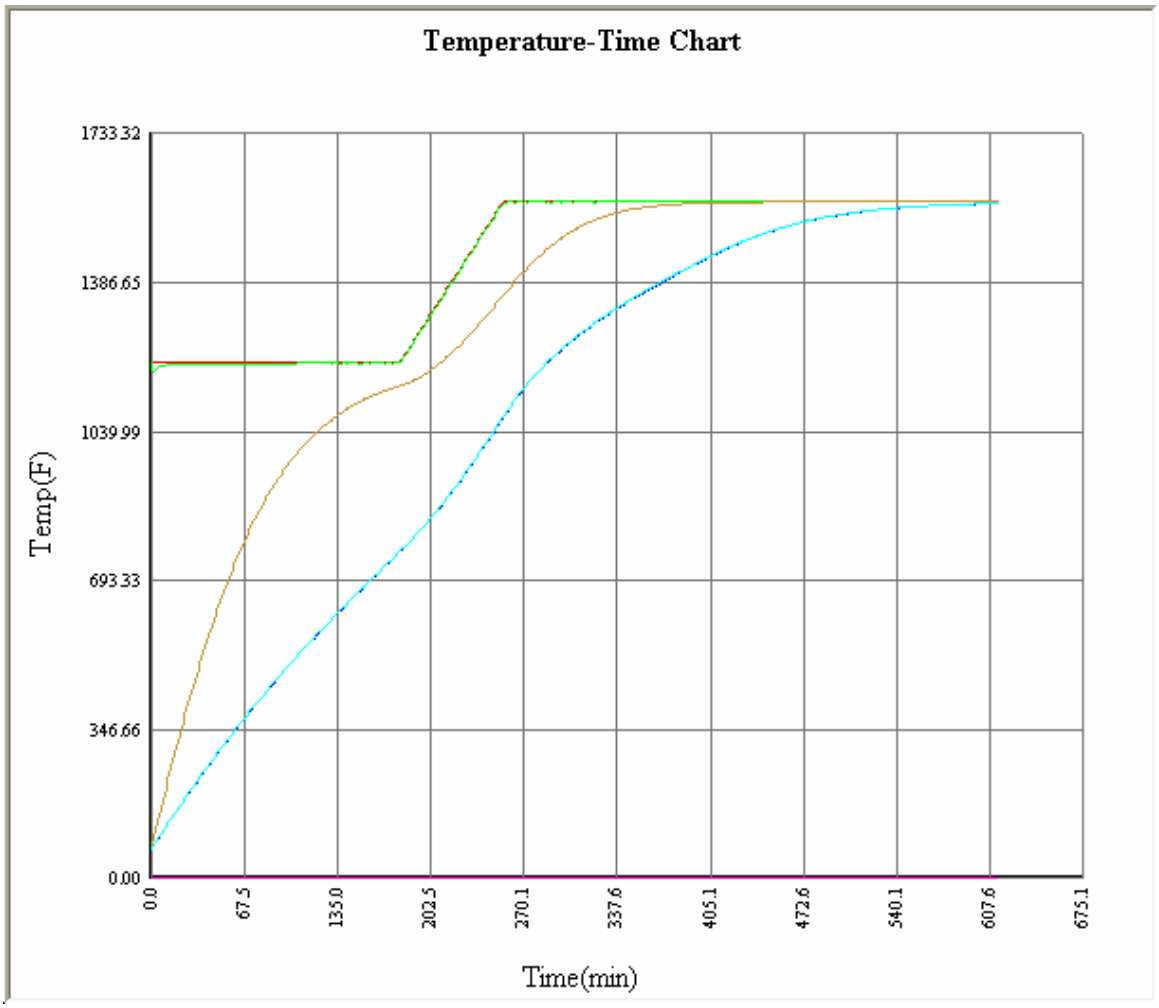

Figure 80. Result by CHT-*bf*

Interpretation of the result:

The profile of the part located at center never reaches the set-point temperature. This may be due to the amount of load, 4164 lbs of part were loaded in the furnace for heat treatment. Thus we can say that the soaking time is not sufficient.

Actual result measured by Thermocouple:

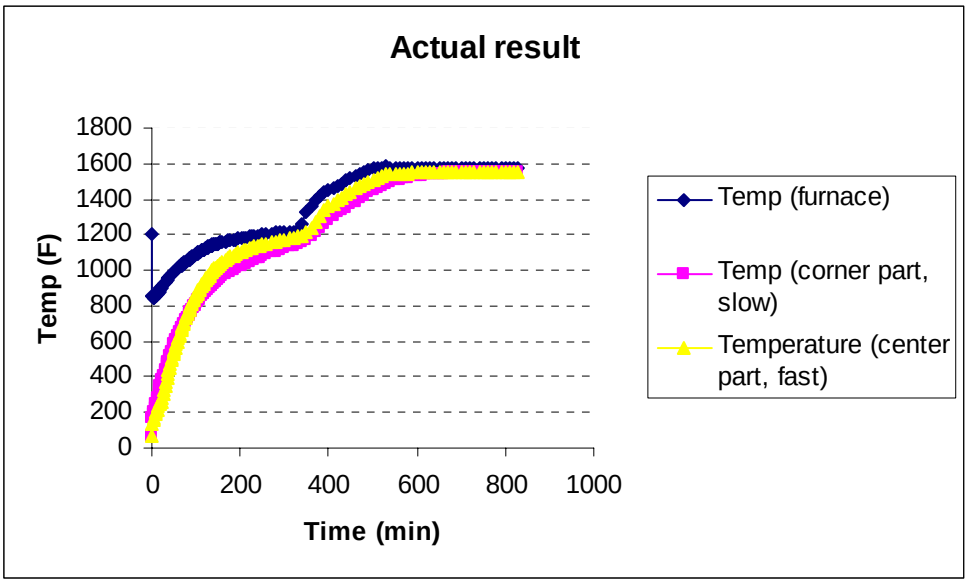

Figure 81. Thermocouple result

It can be observed from the result, the 540 minutes as previously mentioned in the information sheet is not sufficient for soaking the load and it needs some more time. Thus the load was kept for 826 minutes in the furnace.

Result by CHT-*bf* after increasing the soaking time:

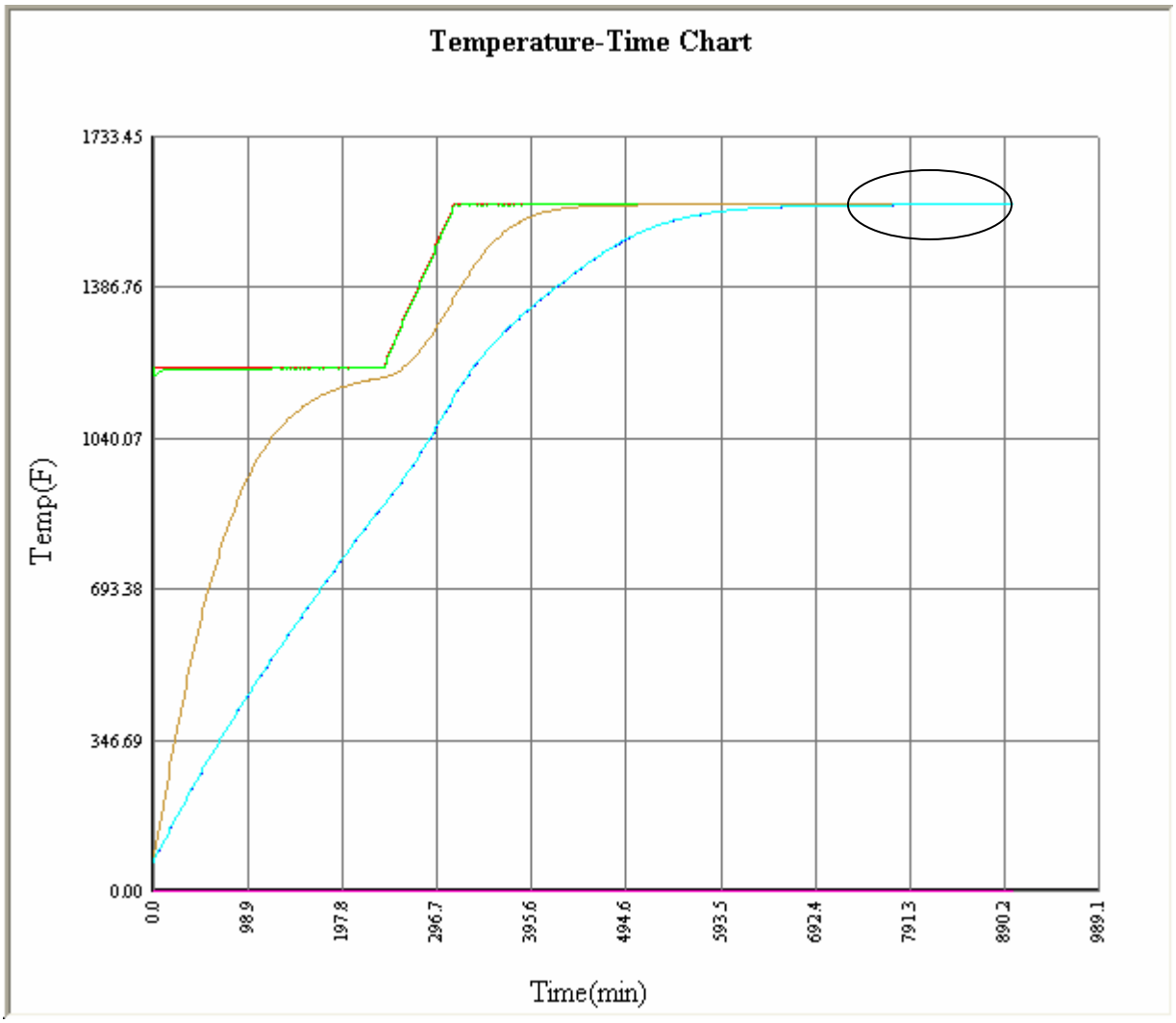

Figure 82. CHT-*bf* result with increased soaking time

Comparison of actual result and the result by CHT-*bf*:

The result by CHT-*bf* closely matches with the actual result. It can be concluded that even the part located at the center reaches the set point temperature after 700 minutes. The biggest advantage of using CHT-*bf* in the type of case study is to determine the cycle time prior to running the load. We can reduce the cycle time from 826 to 700 minutes, thus saving 126 minutes.

6.5 Case study 3

Workpiece information:

Table 17. Workpiece information

Work piece Name	Hitchiner part no. 87296 & 87292
Work piece Material	17-4 stainless steel
Work piece weight	Two types of part(same material) present in the load 1. Qty = 300 Wt. = 41 2. Qty = 903 Wt. = 45 Thus average workpiece wt = 0.0715

Workpiece picture

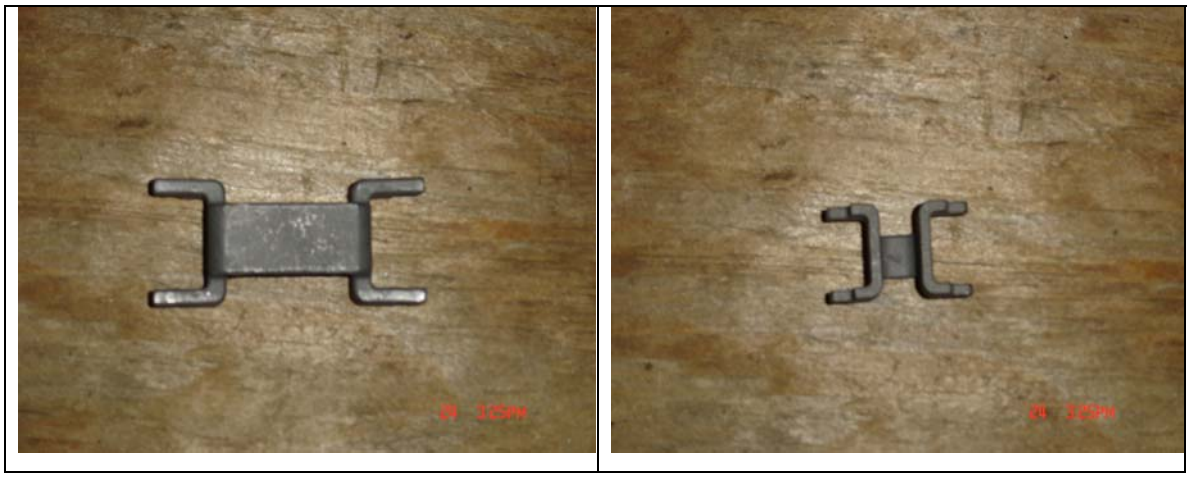

Figure 83. Workpiece

Furnace Information:

The furnace used for the case study is the same to that used for case study 1.

Load pattern

The parts are placed in the rectangular fixture, which is finally placed in a round fixture having solid walls. Two rectangular fixtures were placed in the round furnace. One of the rectangular fixture contained 300 parts and the total weight contained was 41 lbs and the second fixture contained 903 parts with the total wight of 45 lbs. Average of all the dimensions and weight of workpiece was taken to simulate it in CHT-*bf*. Two thermocouples were attached to the workpiece, one to the center part and the other to the workpiece located at the outer ring.

Figure 84. Load pattern

Table 18. Load pattern

Fixture type (basket/plate)	Basket
Fixture shape (rectangular/round)	Round
Side wall, bottom (solid/net like)	Solid
Fixture weight	300 lbs
Fixture size (diameter , height) inch	35, 25
Load pattern, Fixture configuration	Random
Total quantity of workpiece in fixture	(300 + 903)/2 = 601
Total weight of workpiece in fixture, lbs	(41 + 45)/2 = 43

Result by CHT-*bf*

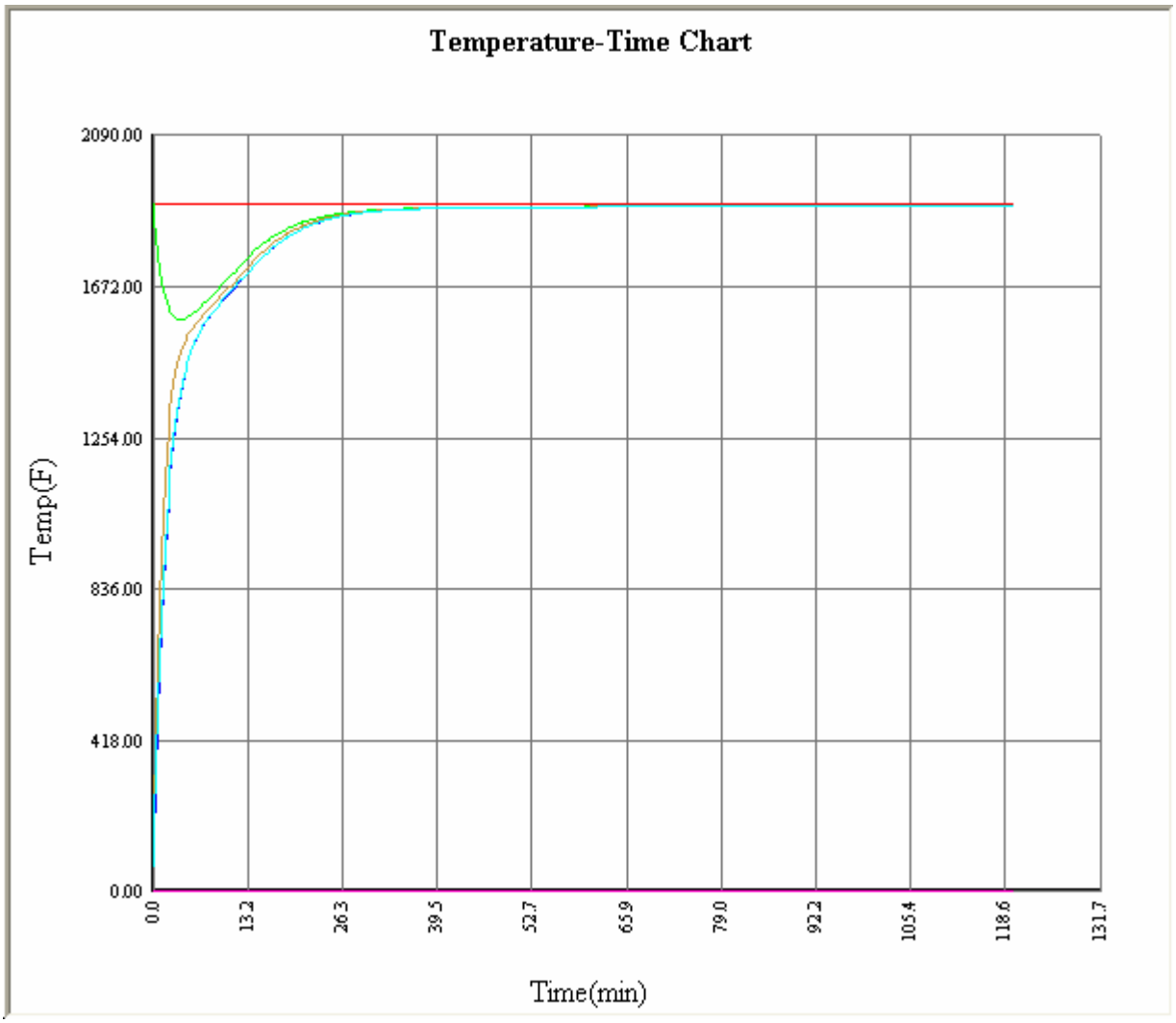

Figure 85. CHT-*bf* result

Interpretation of the result

The furnace takes around 60 minutes to reach the set point temperature. The thermal profile of the part (fast) and to that of the part (slow) is almost the same, which is due to small parts.

This is the first case study where "**Time Interval Constant**" has been used. The calculation was too slow and thus to speed it up I used the time interval constant as 100.

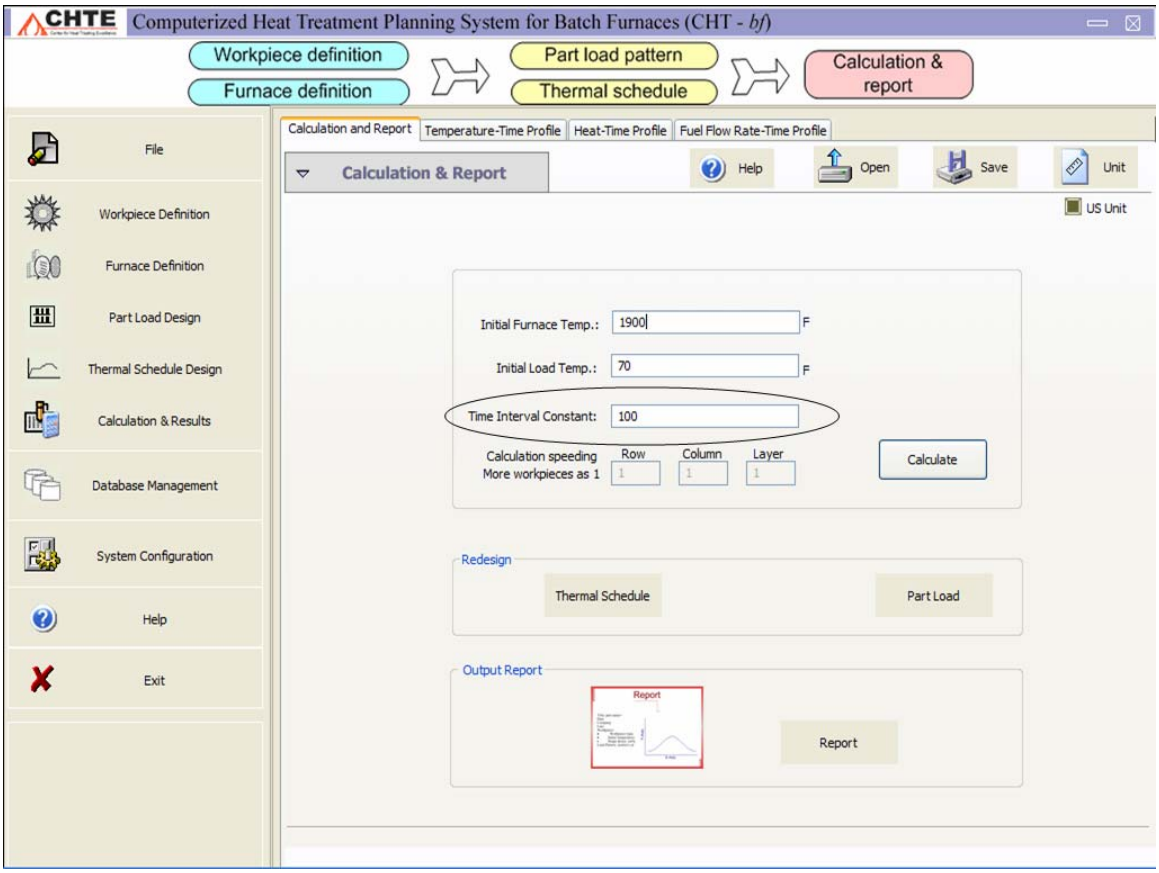

Figure. 86 Application of time-interval constant

Actual result:

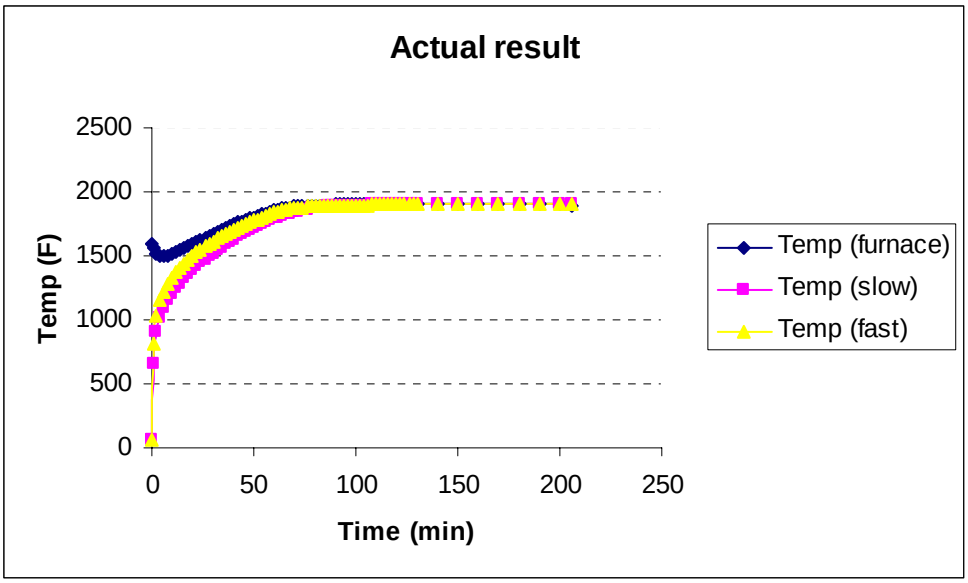

Figure 87. Actual result

The actual time taken by the load in the furnace is 206 min.

Result by CHT-*bf* with increased cycle time:

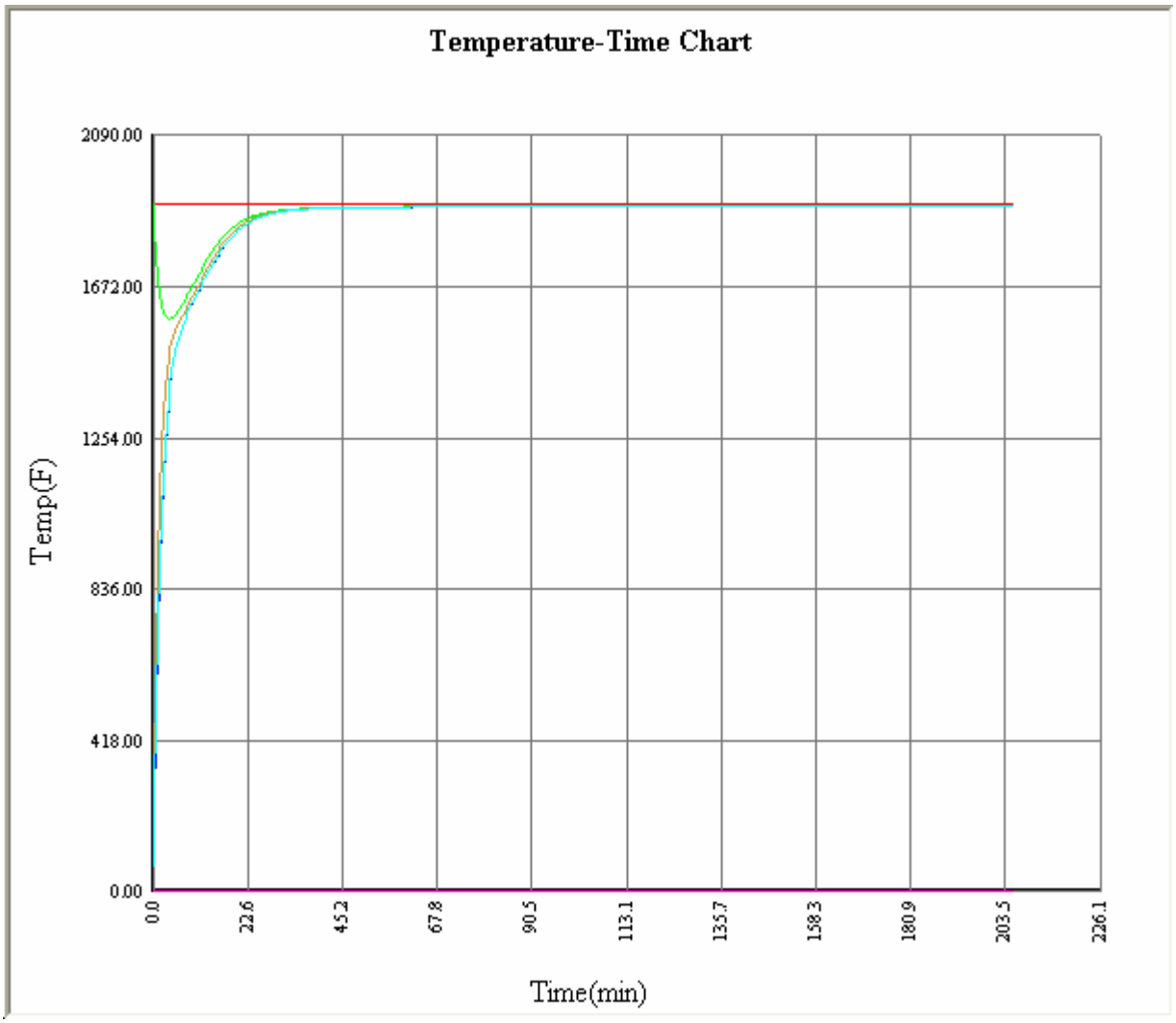

Figure 88. CHT-*bf* result with increased cycle time

Comparison between the actual result measured by thermocouple to that predicted by CHT-*bf*

The result predicted by CHT-*bf* closely matches with the actual result measured by thermocouple. Since the parts are too small and the total load was only 86 lbs, there is no significant difference between the thermal profiles of parts located at center to that located at corner. Here we have a great opportunity to reduce the cycle time. As predicted by CHT-*bf* the parts reached to the set point temperature in about 80 minutes. Thus the

cycle time of 120 minutes as mentioned in the order sheet is good enough for the heat treatment. We can save at least 86 minutes in the present case.

Case study on All case furnace

The following case studies were conducted on the All case furnace. The All case furnace is shown in Figure 90.

6.6 Case study 4

Workpiece:

The workpiece for this case study is shown in Figure 89 and the workpiece details are listed in Table 19.

Figure 89. Workpiece picture

Table 19. Worlpiece data

Work piece Name	Hitchiner part – 87191
Work piece Material	8620
Work piece weight	0.3188 lbs

Furnace specifications

The furnace shown in the figure is “All case” furnace. It is indirect gas fired furnace, and oil quenchant is used for the quenching purpose.

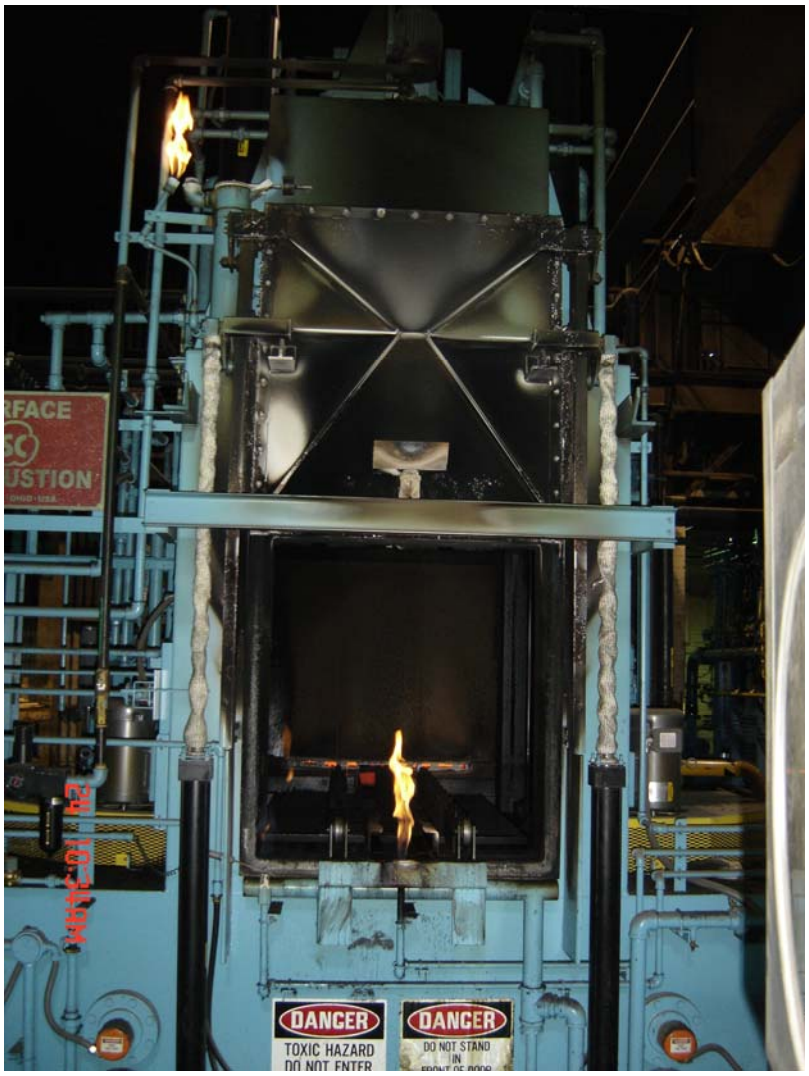

Figure 90. Allcase furnace

Table 20. Furnace data of Allcase furnace

Furnace name	All case, 405	
Body Shape (E.g. vertical, Horizontal)	Horizontal	
Heating type (E.g. direct/indirect fired, electric)	Indirect gas fired	
External size(Length×Width× Height) or (diameter × Height)	5.5 × 4.7 × 4.8 ft	
Work space (Width×Length ×Height) or (diameter × Height)	30-48-30	
Maximum Heating	1800	
Minimum Operating Temperature	1400	
Fuel (combustion air)	Natural gas	
Connected heat input	1000000 Btu/hr	
Atmosphere content	Endothermic (RX) with enriching gas, dilution air and ammonia additions	
Air preheated temperature (F)	850	
Excess of preheated air (%)	15	
Vacuum Furnace	[ ] Yes [x] No	
Opening area ($inch^2$)	900	
Recirculation Fan	[x] Yes [ ] No (one fan at top)	
	Material	330
	Horse power	5
	Diameter	10 inches
	Height	14.5 inches
	Speed	1800 R.P.M
	Weight	200
	Rate of cooling water	2 G.P.M

Furnace Accessories data (weight and material)	Heating elements	
	Cooling tubes	
	Grate	
	Supports	250 lbs
	Roller rails	50 lbs
	Others	450 lbs
Furnace wall data (thickness and material)	Top Layer 1	IFB_2300F, 3 inch
	Top Layer 2	Fiber Glass, 3 inch
	Top Layer 3	
	Side Layer 1	IFB_2300F, 3 inch
	Side Layer 2	Fiber Glass, 3 inch
	Side Layer 3	
	Bottom Layer 1	IFB_2300F, 3 inch
	Bottom Layer 2	Fiber Glass, 3 inch
	Bottom Layer 3	

Load Pattern:

Figure 91. Load pattern

Table 21. Load arrangement

Fixture type (basket/plate)	Basket
Fixture shape (rectangular/round)	Rectangular
Side wall, bottom (solid/net like)	Net like
Fixture weight	45 lbs
Fixture size (Length, width, height) inch	29, 23, 4
Load pattern, Fixture configuration	Random
Rows × Columns × Layers of fixtures in furnace	1 x 2 x 5
Total quantity of workpiece in fixture	199
Total weight of workpiece in fixture, lbs	63.5

Result by CHT-*bf*

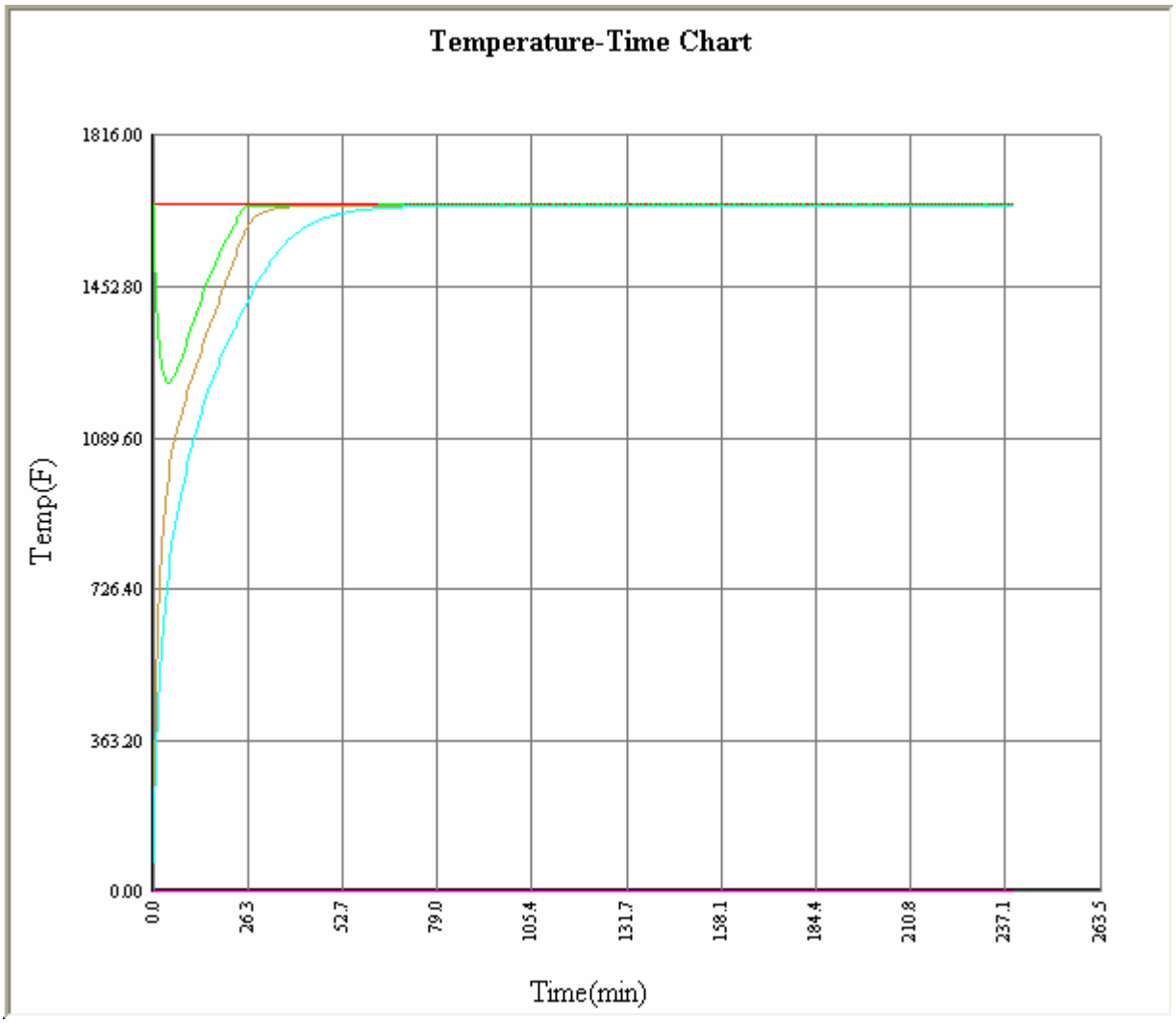

Figure 92. CHT-*bf* result

Interpretation of the result

It can be concluded from the result that, furnace takes around 30 minutes to reach the set point temperature. Time taken by the part located at center of the load to reach the set point temperature is 45 minutes and time taken by the part located at corner of the load to reach the set point temperature is 60 minutes. Thus it shows the actual cycle time for the heat treatment of the load, to be 225 minutes.

Advantages

We can determine the time required by the parts to reach the set point temperature and thus determine the actual cycle time. It will be a great advantage in scheduling, if we know the cycle time prior to running the load. We can also reduce the soaking time after determining an optimum cycle time by CHT-*bf* and thus saving time and money.

6.7 Case study 5

Workpiece

The workpiece for this case study is sown in Figure 93 and the workpiece data in Table 22.

Figure 93. Workpiece

Table 22. Workpiece information

Work piece Name	Hitchiner 243860
Work piece Material	8620
Work piece weight	0.2312 lbs

Furnace data:

Table 23. Furnace information

Furnace name	All case, 401	
Body Shape (E.g. vertical, Horizontal)	Horizontal	
Heating type (E.g. direct/indirect fired, electric)	Indirect gas fired	
External size(Length×Width× Height) or (diameter × Height)	5.5 × 4.7 × 4.8 ft	
Work space (Width×Length ×Height) or (diameter × Height)	30-48-30	
Maximum Heating	1800	
Minimum Operating Temperature	1400	
Fuel (combustion air)	Natural gas	
Connected heat input	600000 Btu/hr	
Atmosphere content	Endothermic (RX) with enriching gas, dilution air and ammonia additions	
Air preheated temperature	850	
Excess of preheated air (%)	15	
Vacuum Furnace	[ ] Yes [x] No	
Opening area ($inch^2$)	900	
Recirculation Fan	[x] Yes [ ] No (one fan at top)	
	Material	33TS42
	Horse power	5
	Diameter	24 inches
	Height	14.5 inches
	Speed	1220 R.P.M
	Weight	200

	Rate of cooling water	2 G.P.M
Furnace Accessories data (weight and material)	Heating elements	
	Cooling tubes	
	Grate	
	Supports	250 lbs, 330
	Roller rails	50 lbs, 330
	Others	450 lbs, 330
Furnace wall data (thickness and material)	Top Layer 1	k-23, 9 inch
	Top Layer 2	
	Top Layer 3	
	Side Layer 1	k-23, 4 inch
	Side Layer 2	k-25, 5 inch
	Side Layer 3	
	Bottom Layer 1	k-23, 4 inch
	Bottom Layer 2	k-25, 5 inch
	Bottom Layer 3	

Load pattern:

Figure 94. Load pattern

Load arrangement:

Table. 24 Load arrangement

Fixture type (basket/plate)	Basket
Fixture shape (rectangular/round)	Rectangular
Side wall, bottom (solid/net like)	Net like
Fixture weight	45 lbs
Fixture size (Length, width, height) inch	29, 23, 4
Load pattern, Fixture configuration	Random
Rows × Columns × Layers of fixtures in furnace	1 x 2 x 5
Total quantity of workpiece in fixture	607
Total weight of workpiece in fixture, lbs	140.4 lbs

Result by CHT-*bf*:

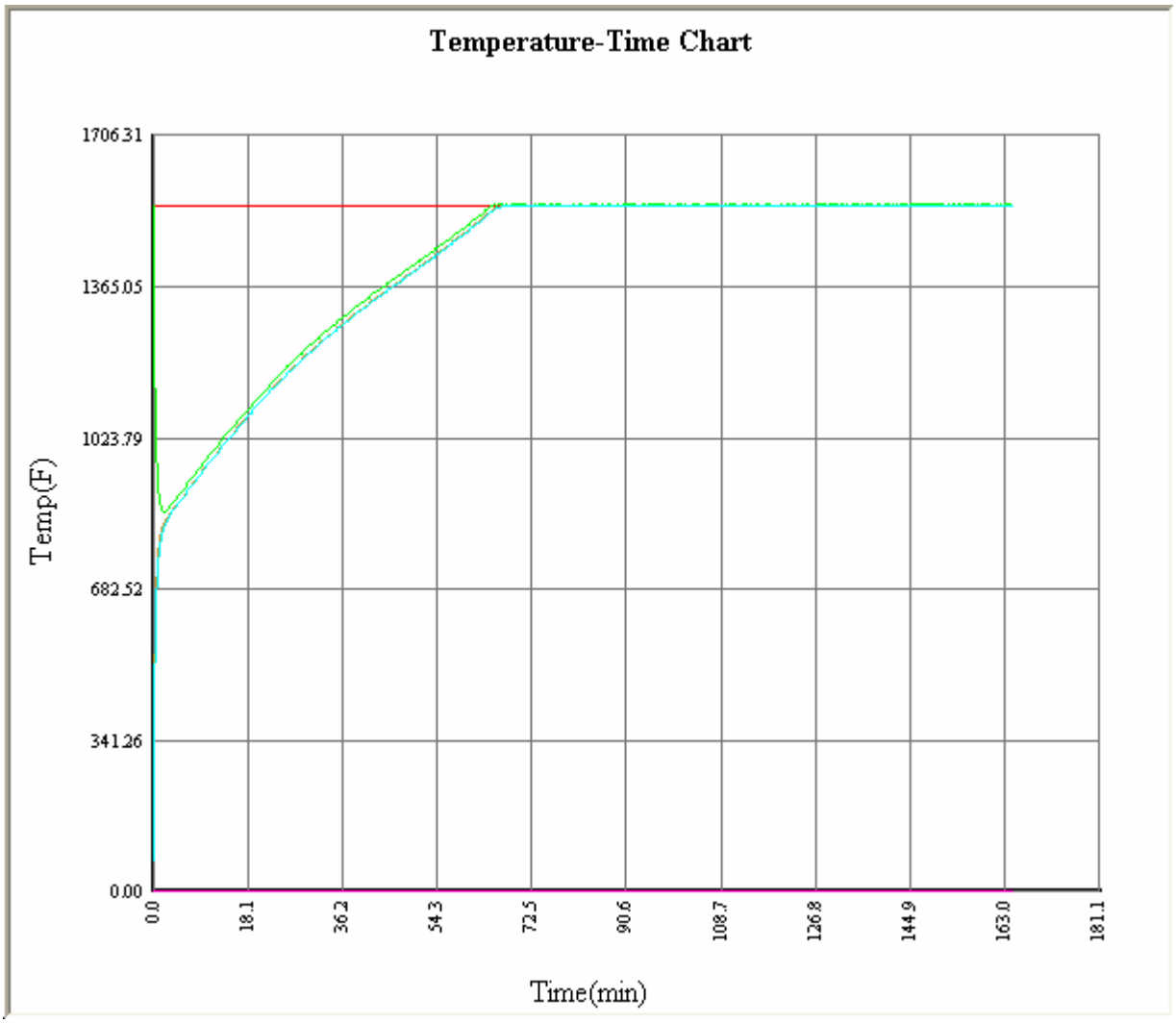

Figure 95. CHT-*bf* result

Interpretation of result

From the above profile it can be concluded that the load takes around 65 minutes to reach the set point temperature, although the time allotted to reach the set point temperature is 30 minutes. In all case furnace, 10 fixtures are used for the part load and generally the parts are randomly placed in the fixture, leaving no room to change the part load design.

Connected heat input of other all case furnaces in the plant (405 & 406) is 1 million Btu/hr. One way to reduce the cycle time is to increase the connected heat input.

Result by CHT-*bf* (same load in furnace 405 or 406 i.e increasing the connected heat input to 1 million Btu/hr)

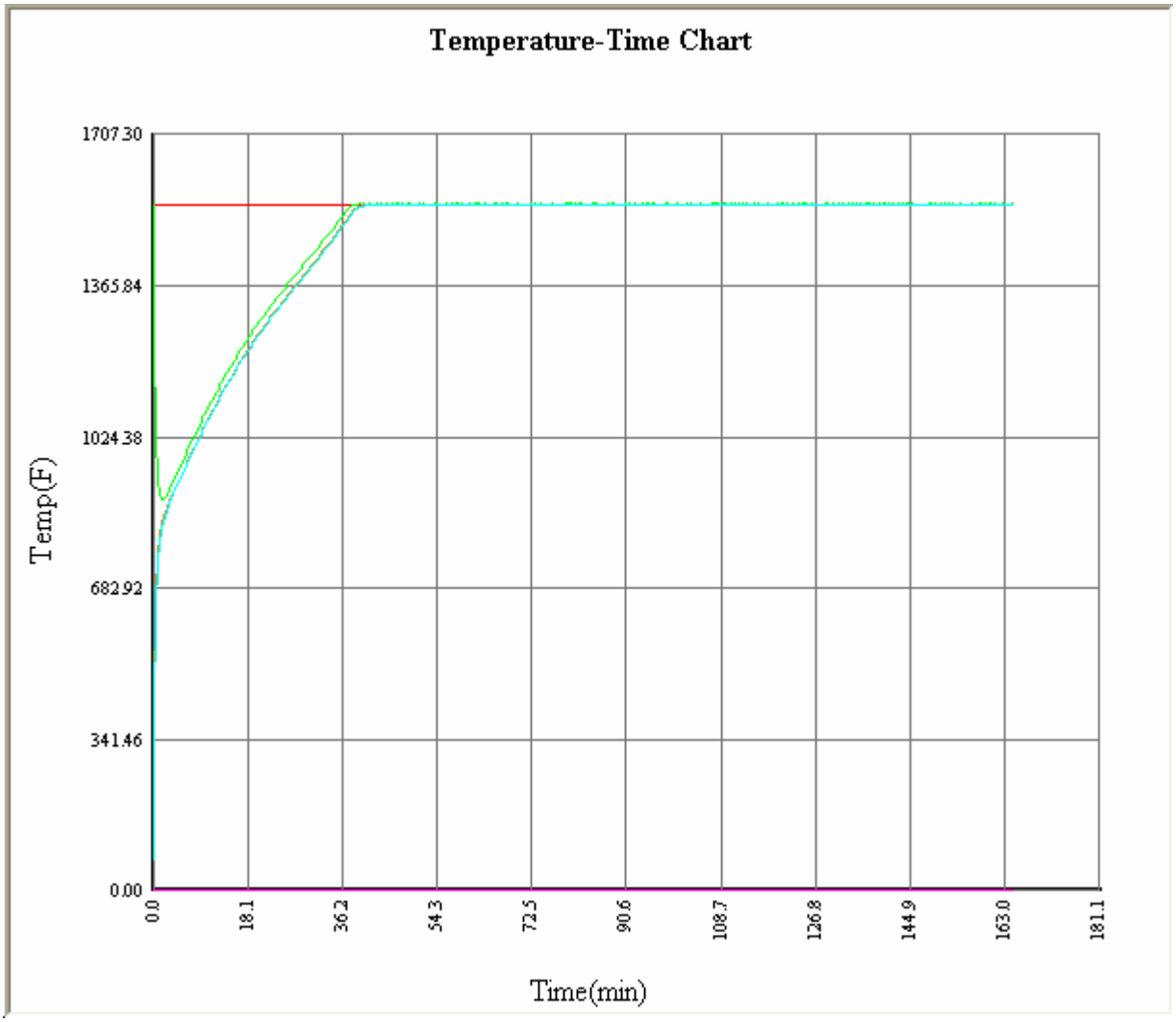

Figure 96. CHT-*bf* result with increased connected heat input

The time required by the load to reach set point temperature reduced from 65 to 40 minutes, as we increased the connected heat input from 600,000 Btu/hr to 1000000 Btu/hr. thus saving around 25 minutes. Thus the cycle time can be reduced if furnace 405 or 406 is used instead of 401.

Conclusion about All case Furnace

Connected heat input is the most important parameter for the All-case furnaces. We can determine suitable all case furnace for a specific load by applying CHT-*bf*

6.8 Application and Advantages of CHT-*bf* at Bodycote, Worcester

1. Application regarding the furnaces 405, 406 (connected heat input 60,000 Btu/hr): Generally the set point in the furnace is 1600^0 F. When the parts (which are at room temperature) are loaded in the heating zone of the furnace, the temperature of the furnace drops to around 1000^0 F and it takes about 40 mins to an hour to reach that temperature. This time adds to the cycle time. Thus CHT-*bf* will be very useful to determine the cycle time prior to the heat treatment of load, and a preheat can be added to reduce the total cycle time.

2. Allcase furnace: CHT-*bf* is helpful in deciding the appropriate furnace for a load (e.g. whether to use 405, 406 or 401, 402, since these furnaces have different connected heat input.)

3. CHT-*bf* can be used to determine the optimum part load design. Sometimes, furnace is not used up to the gross load capacity, the part load design can be altered to study its affect in the heating process to choose an optimum part load, prior to running the load in the furnace.

4. Application regarding the pit furnace, 426: The gross load capacity of pit furnace is 4500 lbs. Generally heavy parts go in the pit furnace and it takes longer time to reach the soaking temperature. CHT-*bf* is very helpful in determining the actual cycle time. We can determine it before running the load in furnace. For example, as shown in the case studies, we can reduce the total cycle time.

5. We can determine whether the heat input is sufficient for the part load, (and then can use the furnace effectively)

6. User friendly interface: The interface of CHT-*bf* is easy to understand

7. Very stable: I have never seen CHT-*bf* crashing in any of the case studies. It is highly stable.

6.9 Accuracy of the Temperature Profiles by CHT-*bf*

1. Initial furnace temperature: The initial furnace temperature is accurate, whereas it has been observed a difference of 10% by the error analysis as discussed in the next section, between the initial drop of the furnace temperature as predicted by CHT-*bf* to that of the actual drop. The drop temperature predicted by CHT-*bf* is 10% higher than the actual drop temperature.

2. Set Point temperature: The soaking temperature (in the thermal schedule design) is the setpoint temperature and it remains constant throughout the process.

3. Thermal profile of the part located at center ("fast", as denoted by CHT-*bf*) is accurately predicted by CHT-*bf*, it closely matches with the actual result.

4. Thermal profile of the part located at corner ("slow", as denoted by CHT-*bf*) is accurately predicted by CHT-*bf*, it closely matches with the actual result.

5. The thermal profile at the center of the part, located at center of the load and the thermal profile at the surface of the part, located at the center of the load are same for small parts, it may vary for very big parts.

6.10 Accuracy Analysis of the Case Studies

The above case studies discuss and compare the result predicted by CHT- *bf* to that measured by thermocouple. An error analysis is necessary to quantify the differences between the two results. This section shows the analysis for two case studies in pit furnace.

Analysis for case study 1:

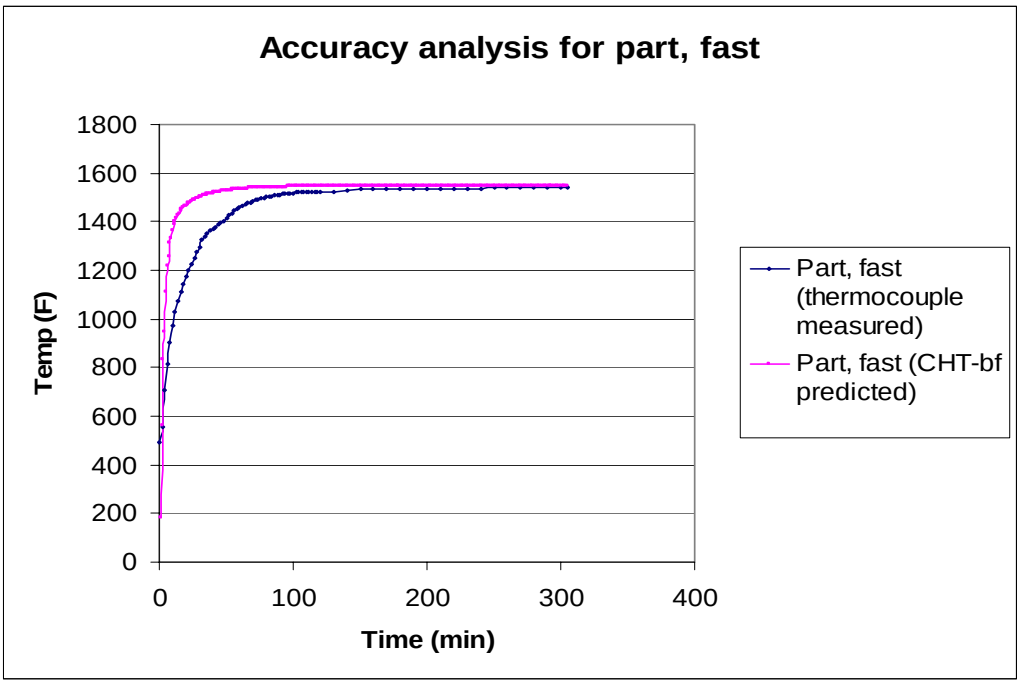

Figure 97. Accuracy analysis for the fastest heated part for case study 1

The notations of the curve are as follows:

Part, fast (thermocouple measured): Here the thermocouple is attached to the external surface of the part. Although, in this case we try to locate the part at the outer corner of the load for the fastest heated part, but it may not be the real case i.e thermocouple reading may not be of the fastest heated part.

Part, fast (CHT-*bf* predicted): This is the thermal profile of the fastest heated part predicted by CHT-*bf*. No part can have a higher heating rate than the profile shown by CHT- *bf*

Approximations involved in comparing the two curves: CHT-*bf* locates the fastest heated part and provides the thermal profile of the part surface. While comparing the above two curves we locate the thermocouple to the surface of the fastest heated part assumed. Sometimes the fastest heated may be other than the thermocouple attached and gives a room for approximation.

Figure 97 compares the thermal profile of fastest heated part. The accuracy analysis has been performed at different temperature values. The soaking time is the most important for the hardening process, thus we quantify the time taken to reach the setpoint time by the two curves. The accuracy analysis has been carried at 1500^0 F. The thermal profile predicted by CHT-*bf* takes 49 minutes to reach 1500^0 F, where as the thermocouple measured profile takes 60 minutes.

The accuracy can be measured as (49-60)/40 = -22.44%

This value represents the percentage by which the result given by CHT-*bf* is to be increased or decreased to reach the thermocouple measured data. As described earlier, this quantitative analysis depends on the accuracy of thermocouple location as well.

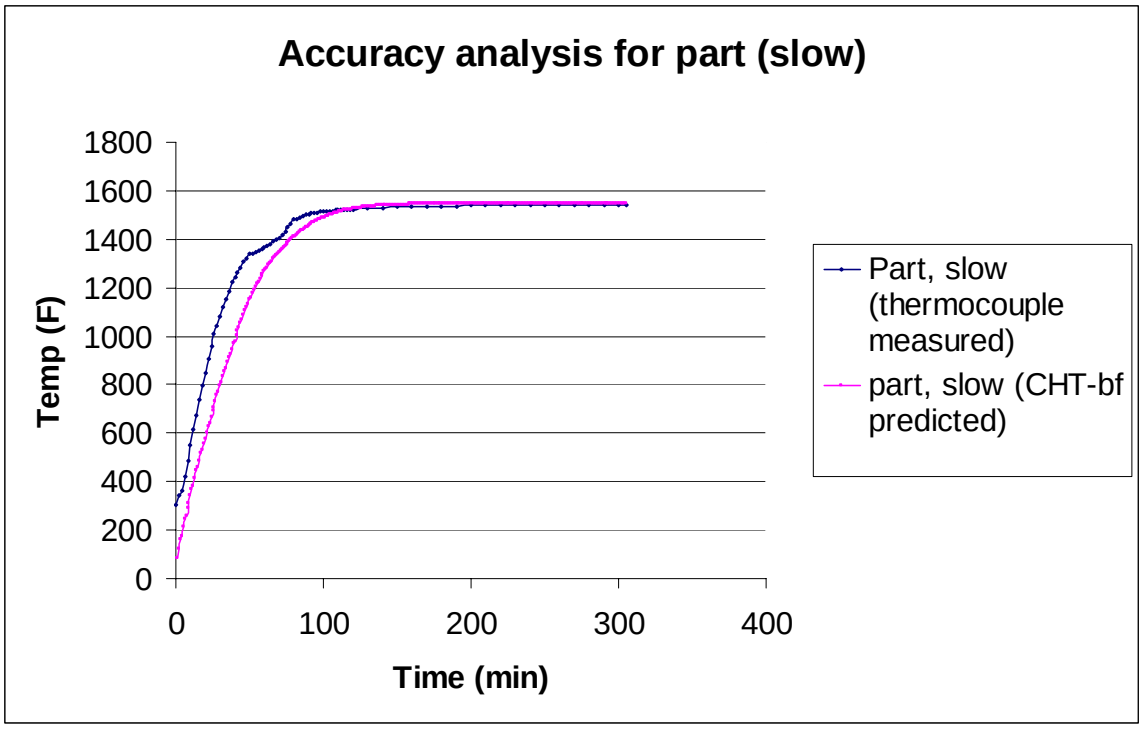

Figure 98. Accuracy analysis for the part (slow) for case study 1

The notations of the curve are as follows:

Part, slow (thermocouple measured): Here the thermocouple is attached to the external surface of the part located at the center of the load. Although, in this case we try to judge the center part, but it may not be the real case i.e thermocouple reading may not be the slow heated part temperature, but the reading of some nearby part.

Part, slow (CHT-*bf* predicted): This is the thermal profile of the surface of the slowest heated part in the load.

Approximations involved in comparing the two curves: CHT-*bf* locates the slowest heated part and gives the thermal profile of the surface temperature of the part. While comparing the above two curves we locate the thermocouple to the surface of the slowest heated part assumed. Sometimes the slowest heated may be other than the thermocouple attached and gives a room for approximation.

Figure 98 compares the thermal profile of the part (slow) as predicted by CHT- *bf* and measured by thermocouple. As it can be seen from the above chart, the two curves reaches the set point temperature in 90 minutes. The thermal profile predicted by CHT-*bf* takes 78 minutes to reach 1400^0 F, where as the thermocouple measured profile takes 70 minutes.
The accuracy can be measured as (78-70)/78 = 10.25%

The thermal profile predicted by CHT-*bf* takes 105 minutes to reach 1500^0 F, where as the thermocouple measured profile takes 90 minutes.
The accuracy can be measured as (101-94)/105 = 6.93%

While the negative value of error for the part (fast) shows, CHT- *bf* takes less time than the actual measured time by thermocouple and the positive value of error for the part (slow) shows more time take by CHT- *bf*

Analysis for case study 2

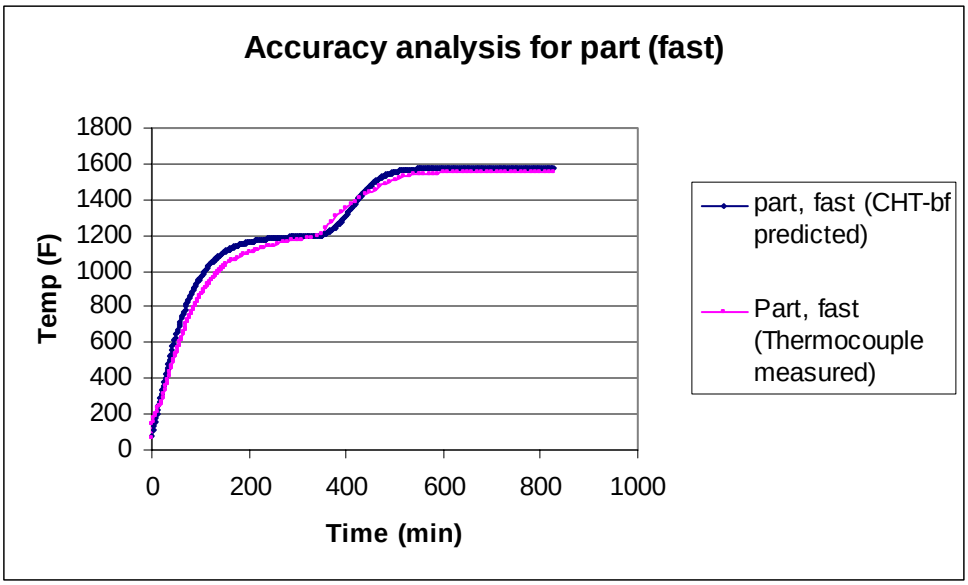

Figure 99. Accuracy analysis for the fastest heated part for case study 2

The notations and approximations remain same as described in the analysis of case study 1.

The above chart compares the thermal profile by CHT-*bf* and thermocouple measured, of fastest heated part. The result predicted by CHT-*bf* is very close to that the actual result, but we need an error analysis to quantify the difference. The accuracy analysis has been performed at different temperature values. The chart shows a small difference between the two curves at temperature values from 900 to 1150^0 F, and then both of the curve overlaps after 1200^0F.

The thermal profile predicted by CHT-*bf* takes 578 minutes to reach 1500^0 F, where as the thermocouple measured profile takes 550 minutes.

The accuracy can be measured as (578-550)/578 = 3.11%

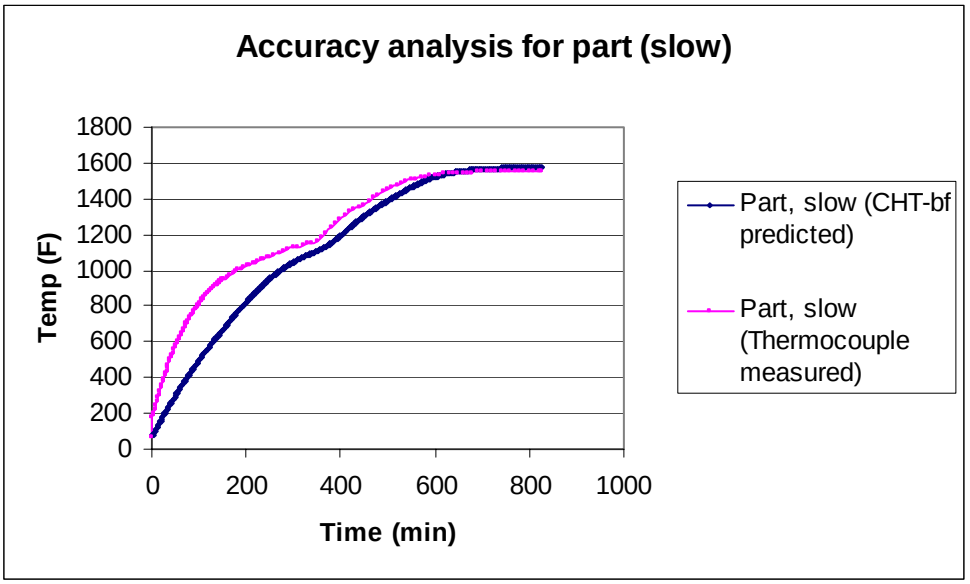

Figure 100. Accuracy analysis for the part (slow) for case study 2

The figure compares the thermal profile of the part (slow) as predicted by CHT- *bf* and measured by thermocouple. Difference can be seen between the two thermal profiles at the initial stage, but after 1400^0F the two profiles matches very well. The error analysis will provide a quantitative picture of the difference. The analysis is performed at 800, 1200 and 1500^0 F.

To reach 800^0 F, CHT-*bf* and thermocouple measured data takes 111 and 98 minutes respectively. Thus the error analysis gives 11.71% error. The CHT-*bf* overshoots by 11.71%.

At 1200^0 F, CHT-*bf* and thermocouple measured data takes 403 and 370 minutes respectively. Thus the error analysis gives 8.18% error. The CHT-*bf* overshoots by 8.18%.

Similarly, at 1500^0 F, CHT-*bf* and thermocouple measured data takes 578 and 550 minutes respectively. Thus the error analysis gives 4.84% error. The CHT-*bf* overshoots by 4.84%.

Conclusion:

The above analysis gave a quantitative picture of the error produced by CHT- *bf*. While, it has been observed that the error at the initial stage of heating is quite significant, it gradually decreases with time and CHT-*bf* is accurate in predicting the time taken to reach set point temperature. A table is shown below to summarize the error analysis.

Table. 25 Error analysis of the case studies

Case study 1	
Temperature	Percent error
1500 F, part (fast)	-22.44
1500 F, part (slow)	6.93

Case study 2	
Temperature	Percent error
1500 F, part (fast)	3.11
1500 F, part (slow)	4.84

6.11 Input Accuracy of CHT-*bf*:

The following section describes the process to isolate the source of a problem in CHT-*bf* and its recommended solution. An unpredicted result in CHT-*bf* arises due to some wrong input data, e.g. if the connected heat input is less than that required then the furnace will never reach the set point temperature. Information is a key for accurate prediction, and

sometimes CHT-*bf* needs approximation for the unavailable information. It may need several iterations to adjust the input values to match the simplified model condition to the real condition. The inverse approach can be used to get the solution of the most obvious problem in CHT-*bf*. The approach consists of working with the Heat-time chart. The heat time chart shows the heat input (gross heat input, fan heat input), heat storage (heat storage in load, heat storage in furnace) and heat losses (heat loss by shell cooling, heat loss by fan cooling, wall heat loss and opening heat loss). If there is any error in the data sheet, it will become obvious by observing the heat-time chart, e.g if the heat losses by any means are greater the heat input, then it clearly indicates an error in defining the furnace data input.

Following are some ways to check input accuracy of CHT-*bf*:

1) The calculation is too slow

    - Time step is too small. If the calculation is too slow such as several hours, we should increase the *time interval constant.* One example is shown in the case study (Hitchiner part for Pit furnace)
    - The total fixture weight is too big. It will decrease the time step very greatly. We have to check if the fixture weight is right.

2) The calculated temperature of workpiece is very low: If the calculated temperature of workpiece is very low, we have to check the heat-time profile. The problem could be caused by

    - Connected heat input is less: If the connected heat input is less than the required value, the furnace will keep on sucking heat and the furnace temperature will never reach to the set point temperature

- The heat loss by cooling water of shell or recirculation fan is too much: The possible reason is that the cooling water's temperature difference between inlet and outlet is too significant.

- The heat loss of wall could be very great: Because the size of furnace outside wall is wrong. In the furnace database and furnace input dialog box, the external size of the furnace is by foot not by inch. And the external size should be the effective size, usually it is not the same as the installation size because lots of accessories are attached to the furnace. And the thickness and material of the furnace wall are also very critical. Especially if there is material with large density, in this case we have to check its thickness and make sure it is right.

- The emissivity of the workpiece material is very small: So the heat is transferred into the load very slowly.

6.12 Limitation of CHT-*bf*

1. The effective use of CHT-*bf* requires knowledge of heat treatment and the functions and approximations of the system.

2. To schedule more than one type of parts of different geometry and material, we have to take average dimension and a closely resembling material. This may affect the result.

3. While providing the information about the load pattern, CHT- *bf* requires assumption in certain situations. For example, CHT-*bf* is not capable of specifying rectangular load in circular fixture, thus the load has to be approximated as circular load pattern having rings as the rows. One such approximation has been shown in case study 1. The other approximations can be

listed as its inability to specify distance between two parts in a row and between two rows in a circular load pattern.

4. The result given by CHT-*bf* is accurate for arranged load pattern, but CHT-*bf* needs improvement for the simulation of random load pattern.

5. Only applicable for heating process.

CHAPTER 7. INDUSTRIAL APPLICATION OF CHT-*cf*

CHT-*cf* was introduced at Bodycote Thermal Processing, Waterbury, CT. The furnace used was mesh belt furnace. The plant contains two mesh belt furnace having three and five zones. The detailed furnace description is given below in the case study.

7.1 Introduction to CHT-*cf*

Computerized Heat Treatment Planning System for Continuous Furnace (CHT-*cf*) is a windows based stand alone software that can be used to simulate the heating of parts in a continuous furnace. The graphical user interfaces are windows based and they were designed with much input from several commercial heat treaters and furnace manufacturers. CHT-*cf* contains a comprehensive database for materials of the part being heat treated, furnace elements, furnaces, furnace atmospheres and fuels. These data help the user to use the software without defining an exhaustive set of parameters.

The software mainly consists of five modules: workpiece definition, furnace definition, thermal schedule specification, load pattern specification, and calculation & report. There are other functions such as, file management, database & database management, serving as the foundation of the software.

The following output can be obtained by CHT-*cf*

5. Temperature vs time of all parts (optional)
6. Temperature curves of the fastest and slowest heated parts
7. Heat terms such as heat input, heat storage in load, heat storage in furnace, etc.

7.2 Objective

2. To study the effects of change in the load quantity and giving recommendations for the thermal schedule redesign.

2. To study the effect of change in load arrangement, determination of optimal load pattern from the calculated temperature values.

6. To study the effect of part orientation on the quality and distortion and hence to determine best suited load orientation.

7. To study the effect of belt speed and gross productivity on the thermal profile of parts and hence determine optimum belt speed and load capacity to maximize productivity.

8. To get an optimum cycle time for proper scheduling of furnaces.

7.3 Case Study 1

The workpiece for this case study is shown in Figure 101 and the workpiece details in Table 26.

Figure 101. Workpiece

Table 26. Workpiece data

Work piece Name	XHD005 screw
Work piece Material	1020 carbon steel
Work piece weight (lbs)	0.04

Furnace specification

The furnace seen in Figure 102 is a mesh belt furnace capable of performing the complete heat treatment cycle (i.e heating, quenching and tempering). It has 3 zones and 12 burners. The connected heat input of each burner is around 175000 Btu/hr. One of the burners was not in the working condition at the time of case study.

Figure 102. Mesh belt furnace

Furnace data

Table 27. Furnace information

Furnace name	A.F.C 1820
Body Shape	[ ]pipe [x]box
Heating type	[ ]Direct [x]indirect fired [ ]electric
External size(Width× Height) Or (diameter) (in)	90 x 96
Work space (Width× Height) Or (diameter) (in)	56 x 56
Moving belt/conveyor width (in)	54
Moving belt/conveyor unit weight (lbs/in2)	0.27
Belt or conveyor return	[x] internal [ ] external
Opening area of the entrance zone (in2)	324
Opening area of the end zone (in2)	0
Through air flow (cft)	N/A
Rate of shell cooling water (GPM)	N/A
Fuel	Natural gas
Air preheated temperature (F)	900
Excess of preheated air (%)	15
Vacuum Furnace	[ ] Yes [x] No
Furnace efficiency % (based on furnace age)	90

Zone	Connected heat input (Btu/hr)	Length (in)	Atmosphere content	Zone temperature (F)	Fan Horse power (HP)	Wall Insulation height (in)	Through metal area (in2)
1	300000	136	Air	500	0	0	0
2	875000	72	Air	1600	0	0	0
3	700000	72	Air	1600	1	0	0
4	525000	50	Air	1600	5	0	0

5							
6							
7							
8							
9							
10							
Furnace wall data (thickness and material)			Top Layer 1		12, Kaowool		
			Top Layer 2				
			Top Layer 3				
			Side Layer 1		4, IFB_2300F		
			Side Layer 2		4, IFB_2300F		
			Side Layer 3		4, IFB_2300F		
			Bottom Layer 1		4, IFB_2300F		
			Bottom Layer 2		4, IFB_2300F		
			Bottom Layer 3		4, IFB_2300F		

Load pattern arrangement

The load was randomly placed on the mesh belt. The table gives the random load data.

Figure 103. Load pattern arrangement

Table 28. Load arrangement

Gross productivity (lbs/hr)	600
Actual load width (in)	54
Height of layers (in)	0.35
Workpiece length	2.5
Workpiece width	2.5
Workpiece height	0.1875

As shown in the Figure 103 thermocouples were attached to the part. The first thermocouple was attached to the part located at extreme right of the mesh belt, the second one at the extreme left and the third one at the center of the belt.

Result by CHT-*cf*

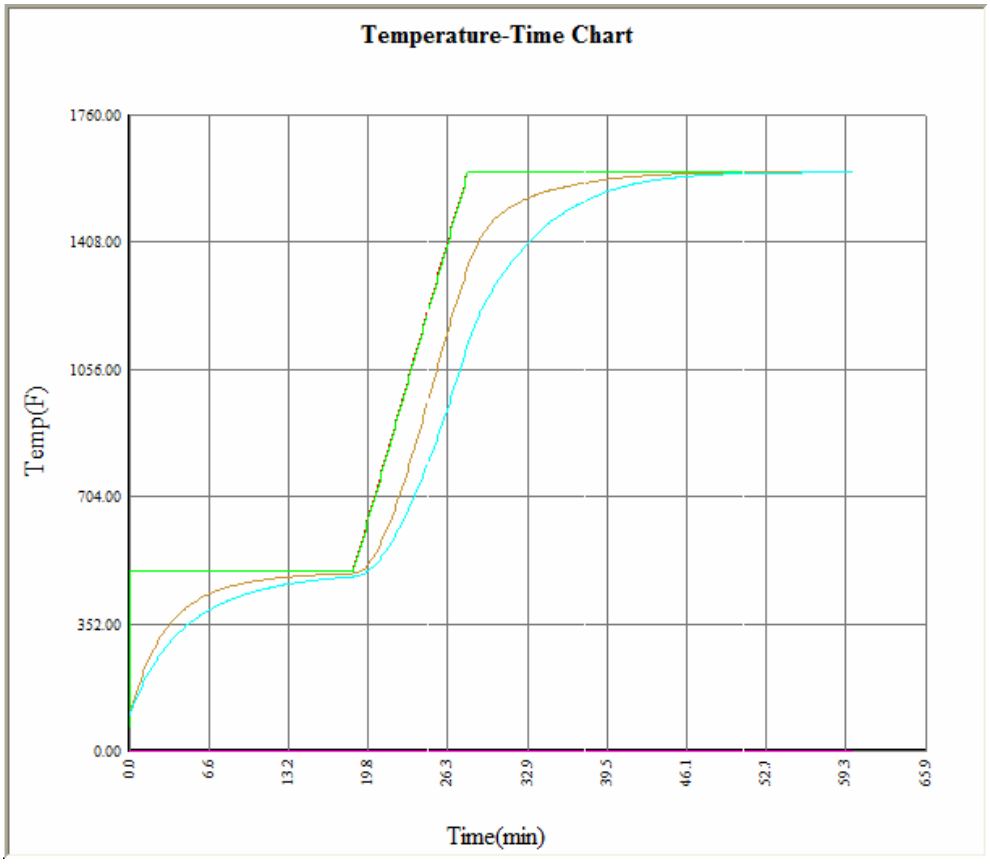

Figure 104. Time-temperature chart by CHT-*cf*

Measured result by thermocouple:

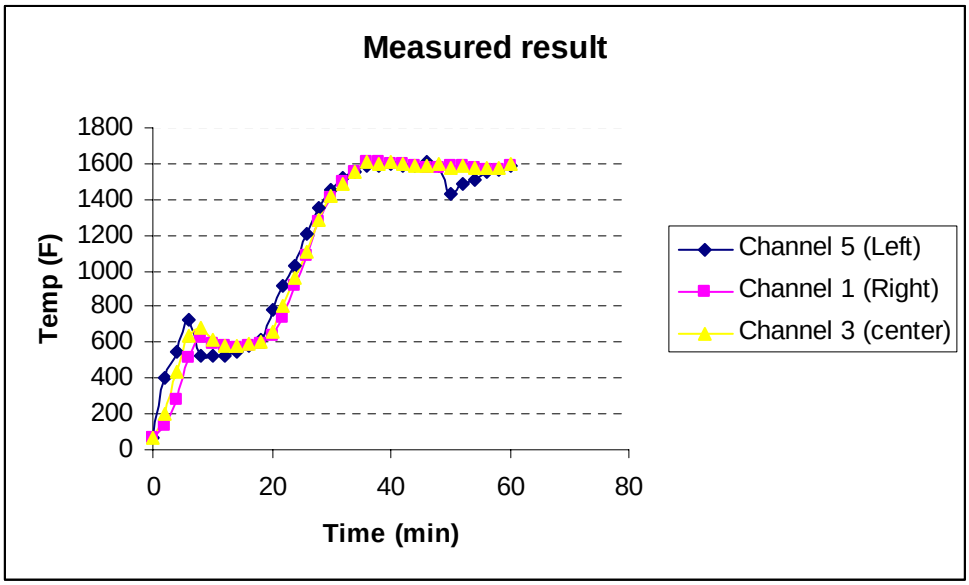

Figure 105. Thermocouple result

Comparison of the measured result and the result given by CHT-*cf*

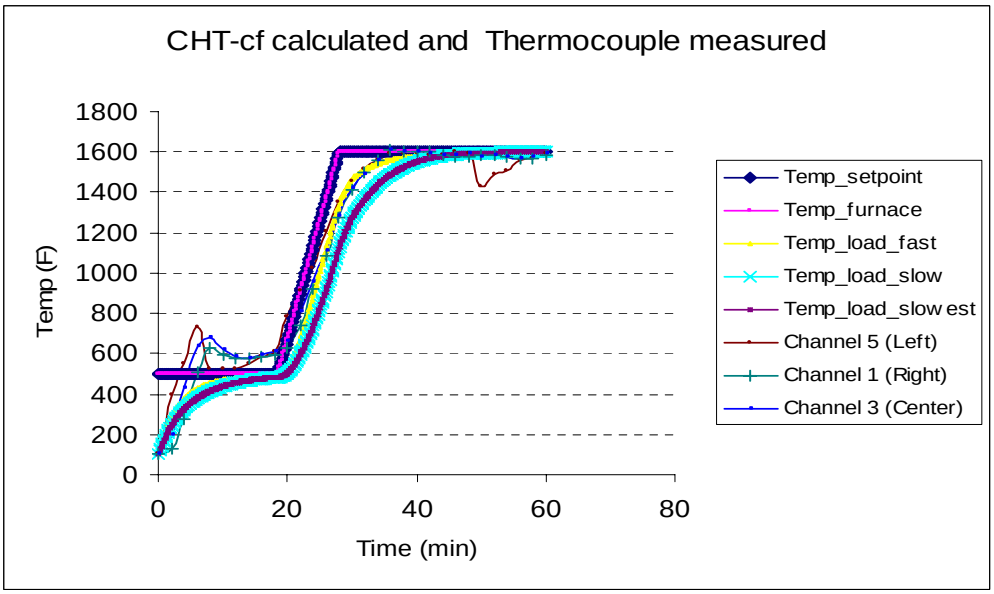

Figure 106. Comparison between thermocouple measured and CHT-*cf* calculated result

Interpretation of the result:

The result by CHT-*cf* closely matches with the measured result by thermocouple. The initial steep rise in the temperature of parts is due to the flame at the opening of the furnace. The flame at the left side of the opening is greater in magnitude as compared to the right side. Thus we observe a higher temperature increase in the left thermocouple. All the three thermocouple readings are almost the same. The thermal profile of the part remains almost same irrespective of its location

Application

1. Production rate

Application of CHT-*cf* has been studied by increasing the production rate. The production rate was increased from 600 lbs/hr to 800 lbs/hr. To accommodate the increased number of parts, the height of layers was increased from 0.25 to 0.3 inch.

Result by CHT-*cf*, with increased production rate:

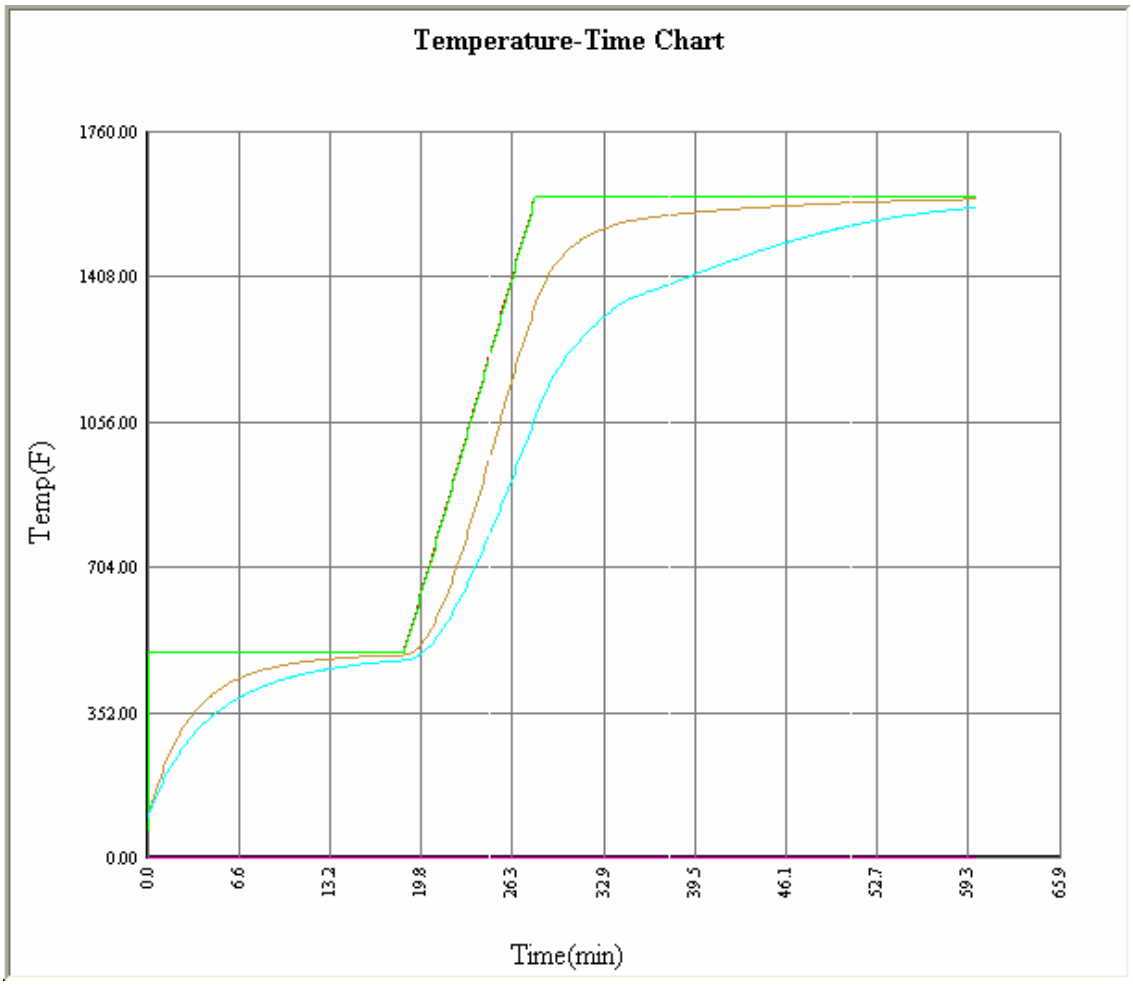

Figure 107.CHT-*cf* result with increased production rate

Discussion

The above chart shows, only the fastest heated part reaches the set point temperature. Thus increasing in production rate would not be a wise option to increase the productivity.

3. **Belt speed**

Application of CHT-*cf* has been studied by increasing the belt speed. The belt speed was increased from 5.5 inch/min to 8 inch/min.

Result by CHT-*cf* with increased belt speed

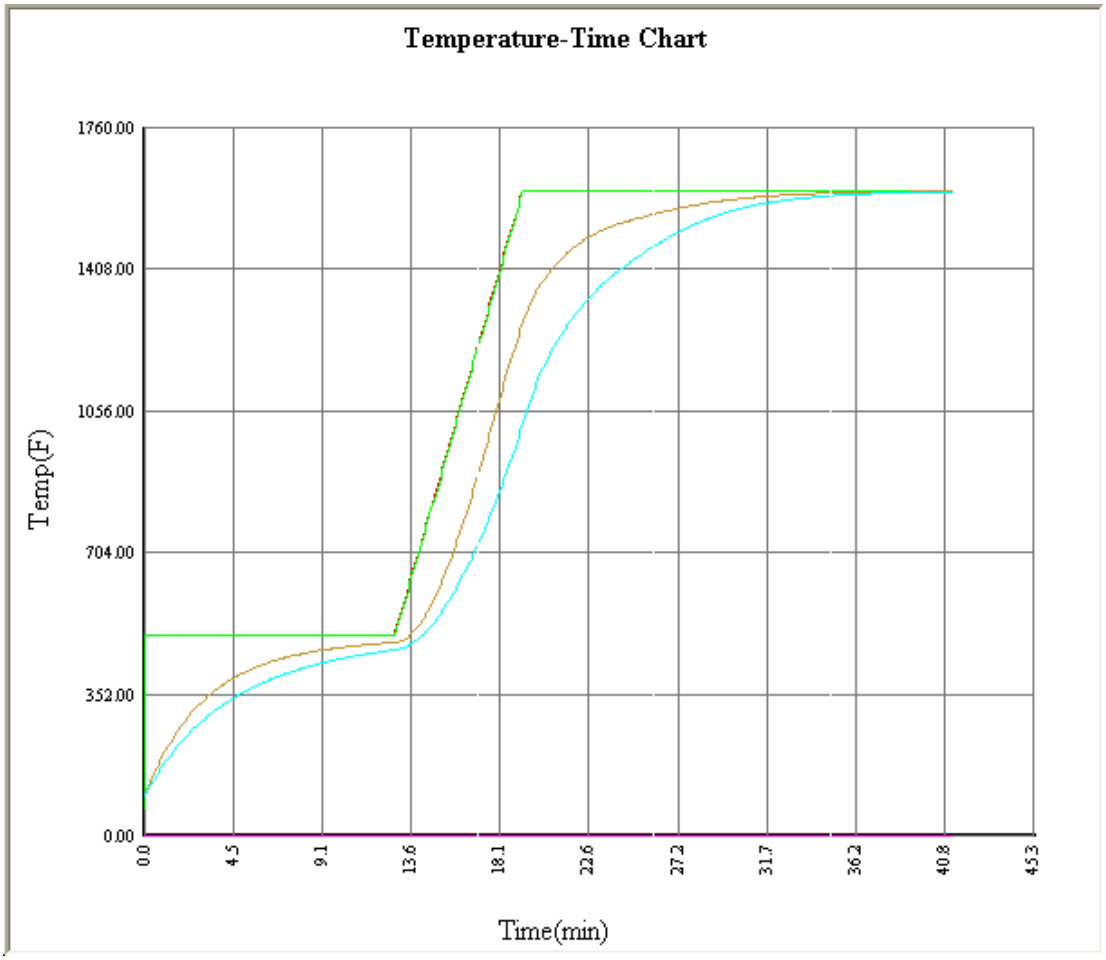

Figure 108. CHT-*cf* result with increased belt speed

Discussion

The above chart does not show any significant difference in the result, even though we increased belt speed by 2.5 inch\min. Still the fastest heated as well as slowest heated part reaches the set point temperature. Thus we have an option of increasing the belt speed to increase the productivity. We can make any decision only after closely studying the

quality requirements and the time required for carburization or other heat treatment process.

7.4 Case Study 2

This case study has been performed with different load patterns, demonstrating the load orientation.

Workpiece specification:

Figure 109.Workpiece picture

Workpiece data

Table 29. Workpiece information

Work piece Name	14004 standard screw
Work piece Material	1020 carbon steel
Work piece weight (lbs)	0.02

The furnace used for the case study is the same that used in case study 1.

Load pattern:

Figure 110. Load pattern

Table 30. Random load arrangement

Load pattern **Random load without Container**	Gross productivity (lbs/hr)	600
	Actual load width (in)	54
	Height of layers (in)	0.375
	Workpiece length	2
	Workpiece width	2
	Workpiece height	0.125

Initial workpiece temperature

Figure 111. Flame at the opening of furnace

As shown in the above picture, the initial temperature of the parts is considered as 250^0F instead of room temperature due to the flame at the opening.

Result by CHT-*cf*

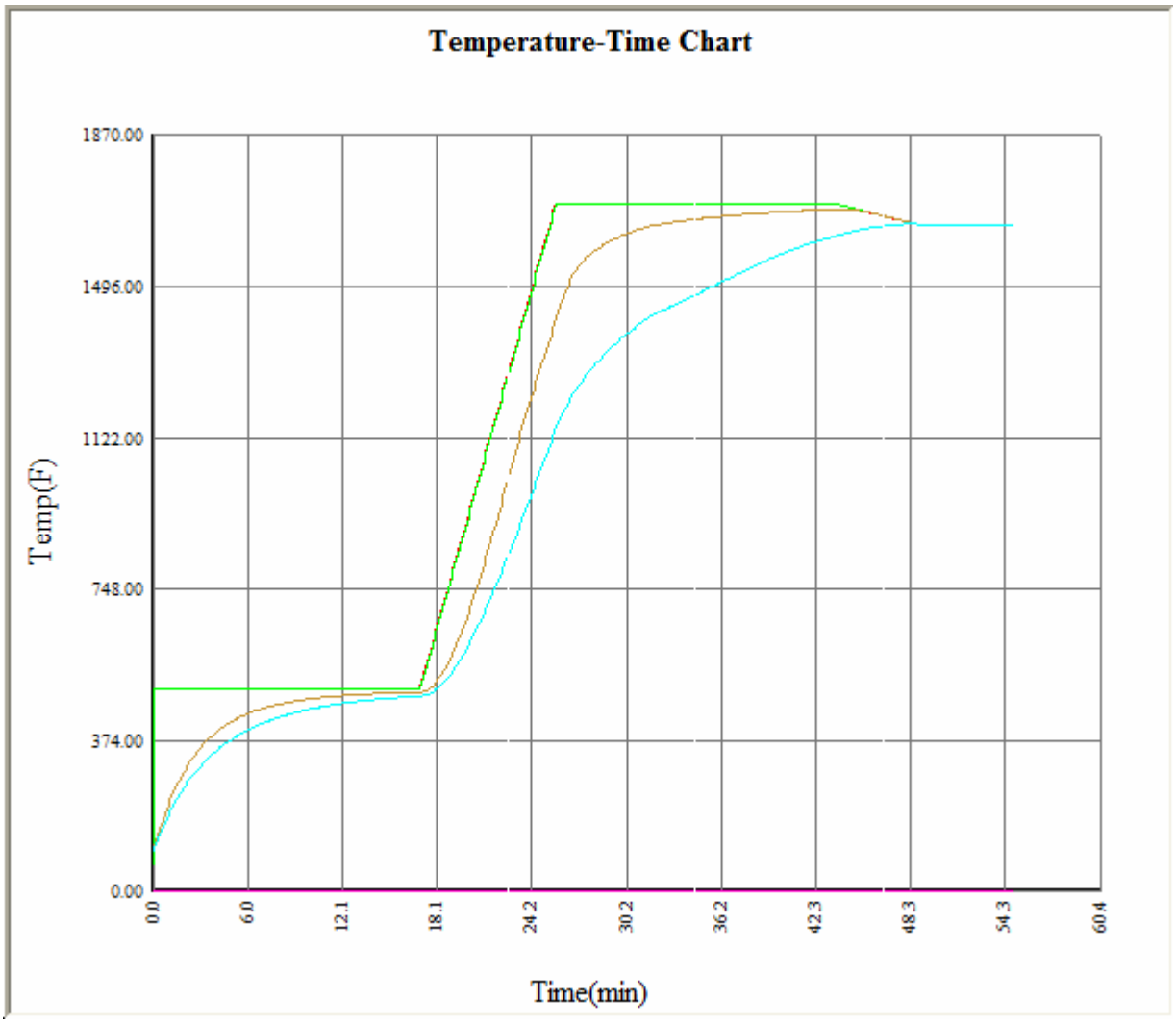

Figure 112. Result by CHT-*cf*

Interpretation of result:

The result shows a considerable difference between the thermal profile of fastest and slowest heated part.

Result by CHT-*cf* with arranged load pattern:

Part load design:

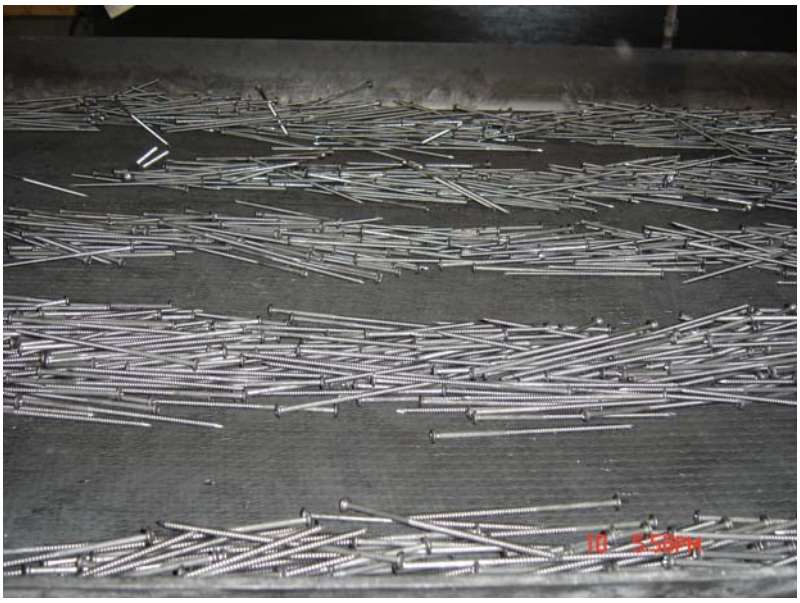

Figure 113. Arranged load pattern

Assumption for the arranged load pattern

As shown in the picture, load was arranged in five columns. For the application of arranged load pattern in CHT-*cf* a group of 10 parts are assumed as one, just to assign single part in each column in the width direction. The weight and surface area have been changed accordingly. The following table gives the revised load pattern

Table 31. Arranged load pattern

Load pattern:	Gross productivity (lbs/hr)	600
	Actual load width (in)	54
Arranged load	Height of layers (in)	0.375
without Container	Workpiece length	4
	Workpiece width	6
	Workpiece height	0.125
	Workpiece in width	5
	Workpiece in height	3

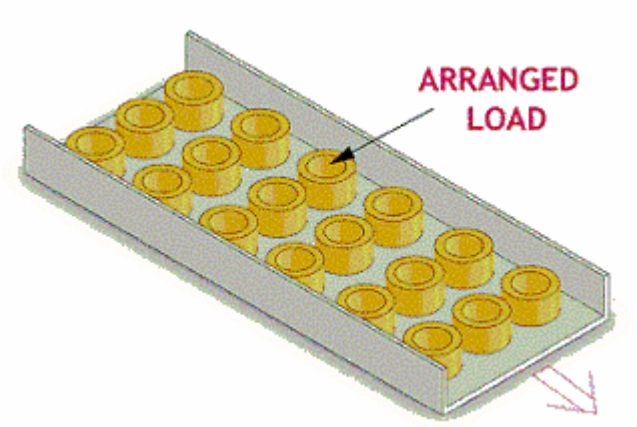

Figure 114. Arranged load pattern as depicted in CHT-*cf*

The above picture shows the structure of arranged load pattern in CHT-*cf*.

Result by CHT-*cf*:

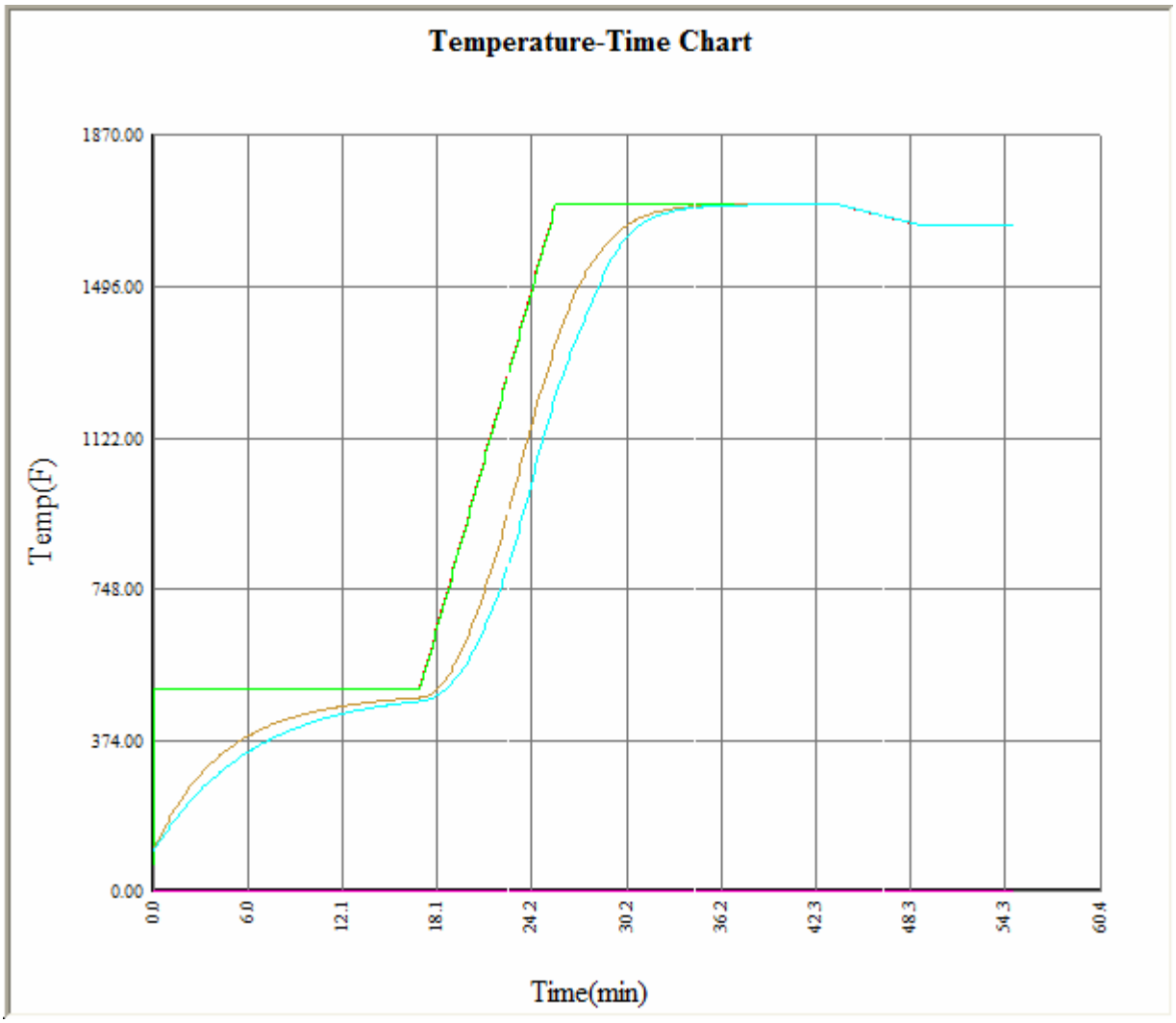

Figure 115. Result by CHT-*cf*

Result by CHT-*cf* with different orientation:

The part orientation is assumed in a manner that its length is perpendicular to the moving belt direction. In this orientation each part is considered as one entity without any grouping. The table below gives the load pattern.

Table 32. Load pattern with different orientation

Load pattern:	Gross productivity (lbs/hr)	600
	Actual load width (in)	54
Arranged load without Container	Height of layers (in)	0.375
	Workpiece length	0.125
	Workpiece width	4
	Workpiece height	0.125
	Workpiece in width	5
	Workpiece in height	3

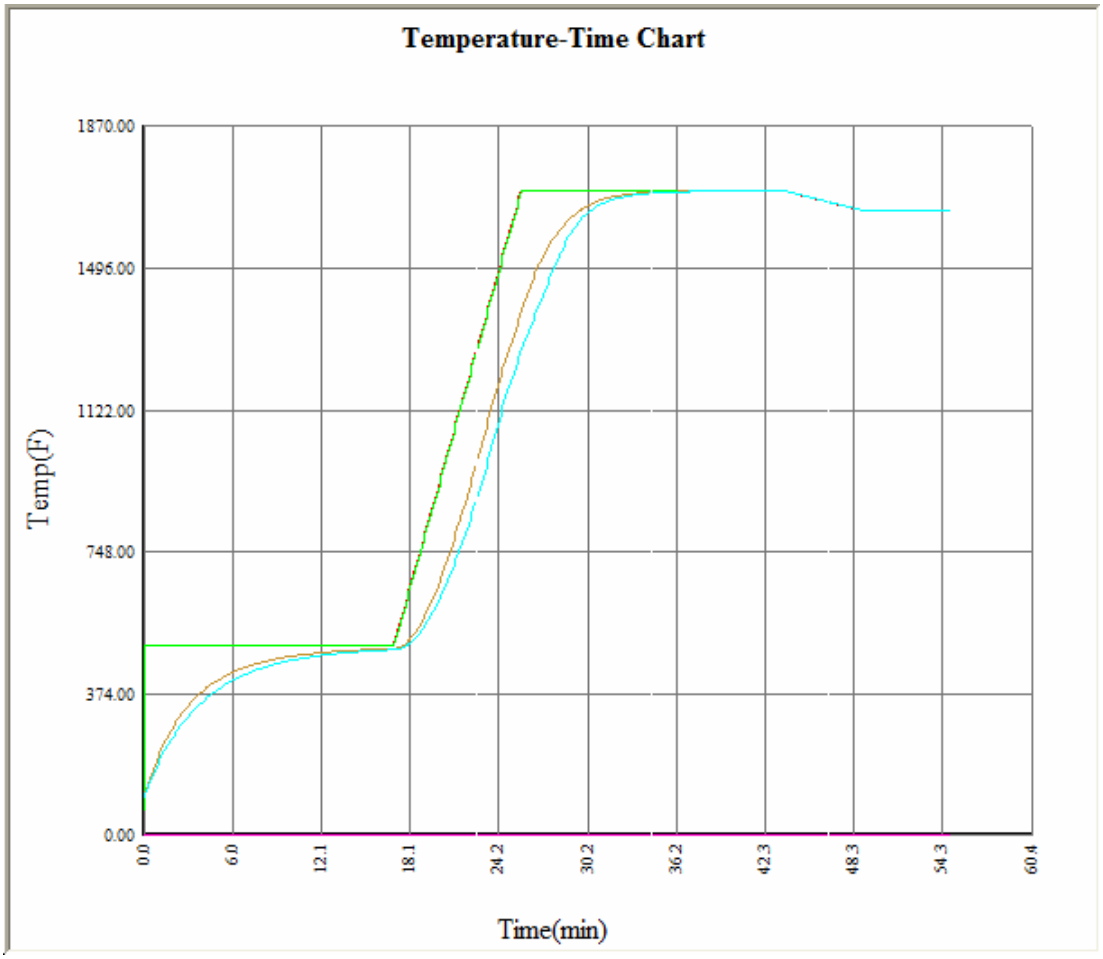

Figure 116. Result by CHT-*cf* after changing part load orientation

The result remained same even after we changed the orientation of parts.

7.5 Case Study 3

Workpiece:

The workpiece for this case study is shown in Figure 117 and the workpiece details in Table 33.

Figure 117. Workpiece

Table 33. Workpiece data

Work piece Name	XHD005 screw
Work piece Material	1020 carbon steel
Work piece weight (lbs)	0.040

Furnace specification:

The furnace seen in Figure 118 is a mesh belt furnace capable of performing the complete heat treatment cycle (i.e heating, quenching and tempering). It has five zones and 22 burners. 11 burners in each side, 6 at the top of the mesh belt carrying load and 5 below the belt. The connected heat input of each burner is around 175000 Btu/hr. Zones are divided based on the atmosphere content of the furnace. It has five inlets for the atmosphere. Kaowool is used as the refractory in the top wall and brick is used at the side and bottom walls.

Figure 118. Mesh belt furnace

Furnace data:

Table 34. Furnace information

Furnace name	CAN-ENG 1850
Body Shape	[ ]pipe [x]box
Heating type	[ ]Direct [x]indirect fired [ ]electric
External size(Width× Height) Or (diameter) (in)	77 x 64
Work space (Width× Height) Or (diameter) (in)	54 x 40
Moving belt/conveyor width (in)	44
Moving belt/conveyor unit weight (lbs/ft2)	0.27
Belt or conveyor return	[x] internal [ ] external
Opening area of the entrance zone (in2)	324
Opening area of the end zone (in2)	0
Through air flow (cft)	N/A

Rate of shell cooling water (GPM)	N/A
Fuel	Natural gas
Air preheated temperature (F)	900
Excess of preheated air (%)	15
Vacuum Furnace	[ ] Yes [x] No
Furnace efficiency % (based on furnace age)	90

Zone	Connected heat input (Btu/hr)	Length (in)	Atmosphere content	Zone temperature (F)	Fan Horse power (HP)	Wall Insulation height (in)	Through metal area (in2)
1	300000	70.5	Air	500	0	0	0
2	1050000	76.5	Ammonia	1600	0	0	84
3	700000	76.5	Air	1600	2	0	56
4	525000	76.5	Air	1550	2	0	42
5	875000	97	Air	1550	2	0	70
6	700000	59	Air	1550	0	0	56
7							
8							
9							
10							

Furnace wall data (thickness and material)	Top Layer 1	18, Kaowool
	Top Layer 2	
	Top Layer 3	
	Side Layer 1	4, IFB_2300F
	Side Layer 2	4, IFB_2300F
	Side Layer 3	4, IFB_2300F
	Bottom Layer 1	4, IFB_2300F
	Bottom Layer 2	8, IFB_2300F
	Bottom Layer 3	8, IFB_2300F

Load pattern:

Figure 119. Load pattern

Table 35. Random load arrangement

Load pattern **Random load without** **Container**	Gross productivity (lbs/hr)	1100
	Actual load width (in)	36
	Height of layers (in)	0.47
	Workpiece length	2.5
	Workpiece width	2.5
	Workpiece height	0.156

Result by CHT-*cf*

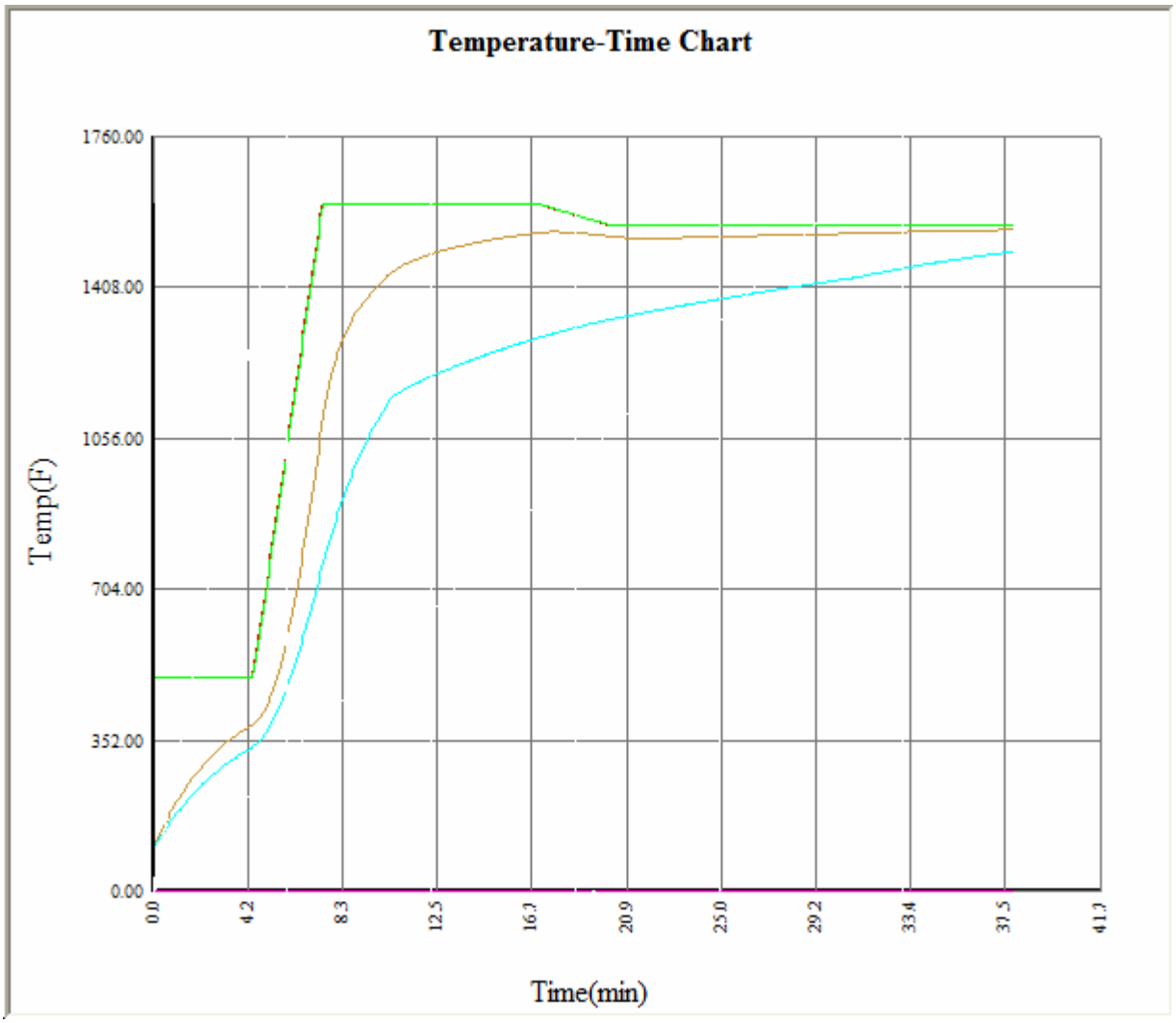

Figure 120. Result by CHT-*cf*

Measured result:

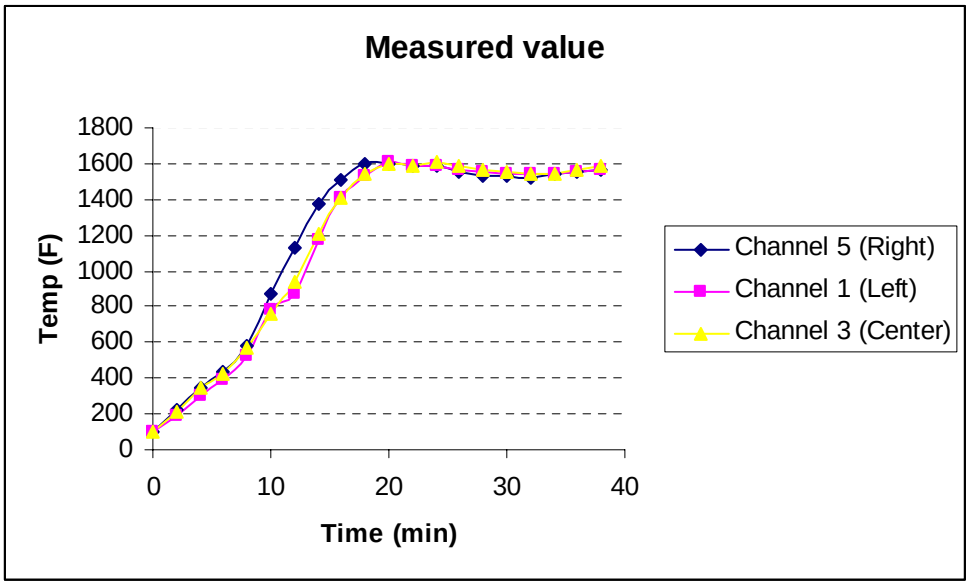

Figure 121. Thermocouple measured result

Comparison between the measured result and the result predicted by CHT-*cf*

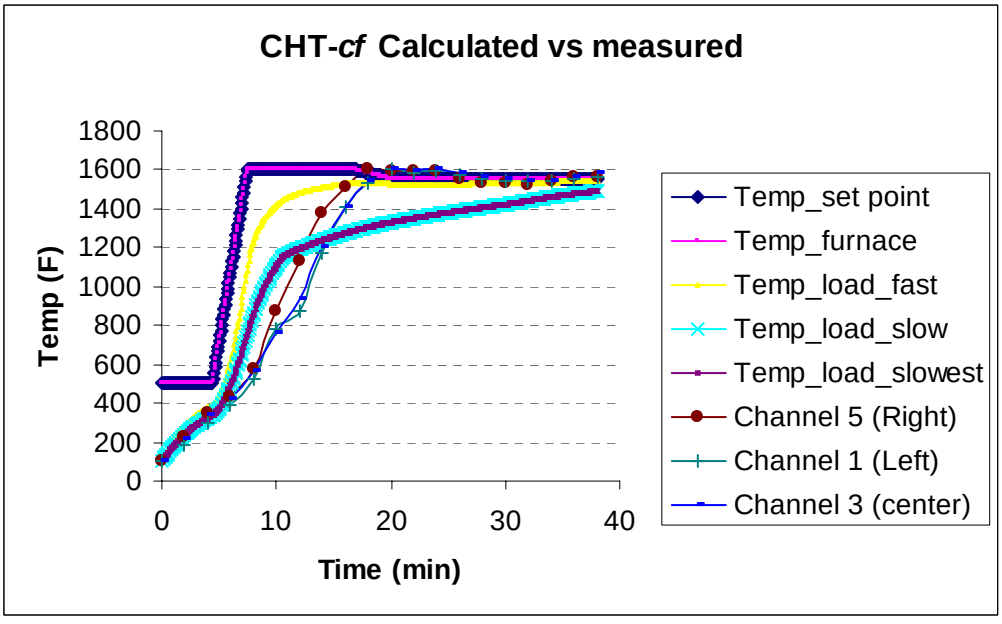

Figure 122. CHT-*cf* calculated vs measured result

In the measured result all the thermocouples readings are very close.

Result by CHT-*cf* assuming arranged load pattern:

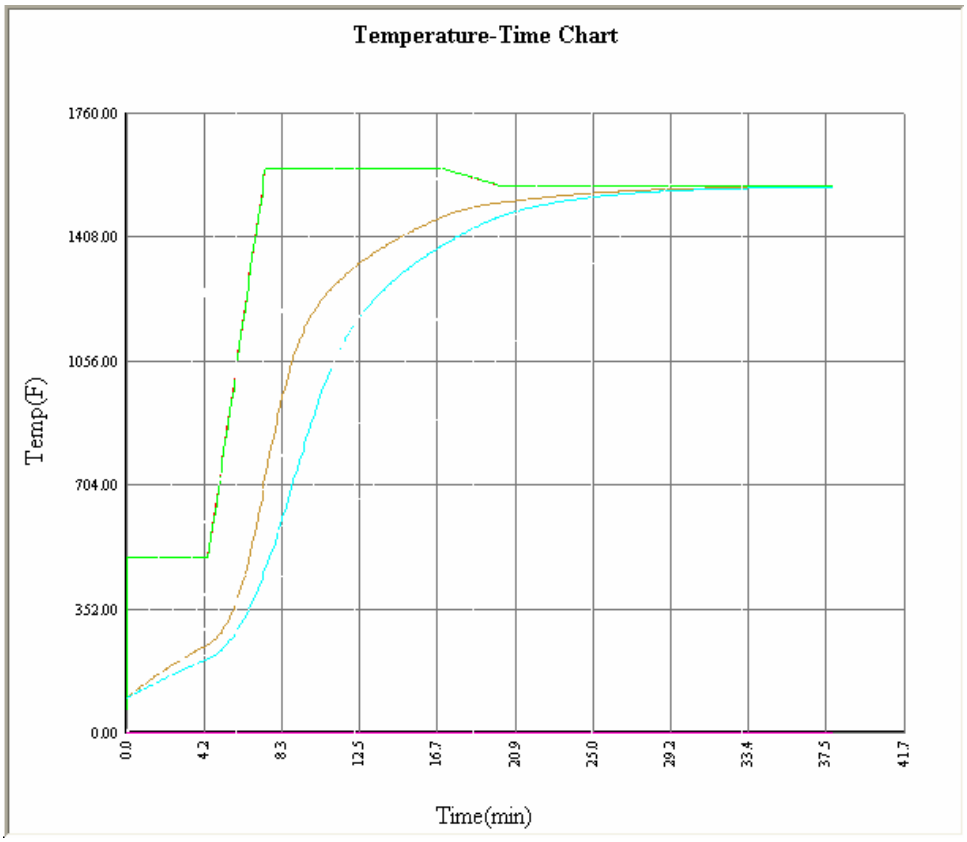

Figure 123. CHT-*cf* result assuming arranged load pattern

Conclusion:

Arranged load pattern was considered with the assumption of considering 10 workpiece as 1, and 5 rows of workpiece on the belt. The weight and surface area is modified accordingly. Uniformity in the thermal profile can be achieved by arranged load pattern.

7.6 Application and Advantages of CHT-*cf*:

1. Application with respect to 1820: CHT-*cf* is very useful in determining the part load arrangement. As shown in the case studies, uniformity of temperature can be achieved by choosing arranged load pattern.

2. Orientation of parts: We can decide about the part orientation that gives the uniformity in temperature

3. Optimum cycle time can be determined by using CHT-*cf*. Thus belt speed can be determined prior to running the load.

4. Furnace Planning: CHT-*cf* can help us determining the important parameters required for the furnace, e.g the connected heat input required for each zones, and thus we can decide about the number of burners required for each zones.

Figure 124. shows the "heat in each zone". The line in bold represents the "Gross heat input". From the chart it can be concluded that the first zone requires maximum amount of heat input. Thus it needs more burners than that required by other zones.

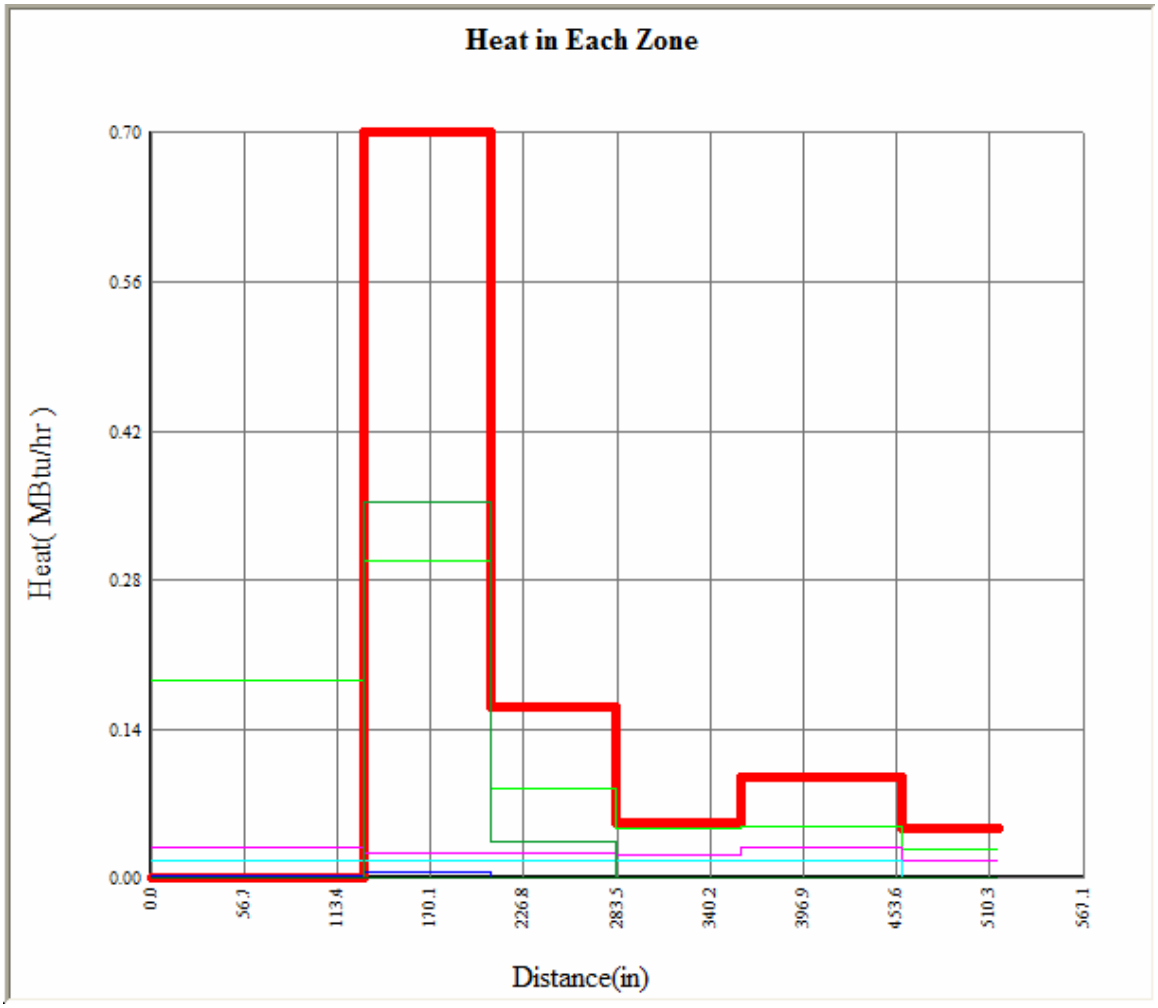

Figure 124. Heat in each zone

7.7 Limitations of CHT-*cf*:

1. In the "Atmosphere content', only atmosphere name can be mentioned. No option to quantify the atmosphere content.

2. While simulating the part load by CHT-*cf*, distortion of parts are not considered, while in actual industrial practice the cycle time, production rate and load pattern arrangement are mostly considered keeping in view the final quality and distortion.

CHAPTER 8. SUMMARY AND FUTURE WORK

The thesis presented a Computerized Heat Treating and Planning System for Quenching and Tempering (CHT-*q/t*) with its various function modules with database and results. CHT-*q/t* has been developed to assist the heat treating operation in industries. The basic objective of CHT-*q/t* is to complete the heat treating process by adding quenching and tempering. Apart from predicting the property after quenching it determines the temperature of various parts both in heating as well as cooling. Two case studies are presented for CHT-*q/t* with different analysis results and compared with actual results. The case studies help to determine the system application scope and accuracy of the system. The application scope for CHT-*q/t* is wide variety of workpieces of different shape and material, different kinds of furnaces and load arrangements. Apart from these the thesis presents the industrial application of CHT-*bf* and CHT-*cf* . Several case studies were performed at Bodycote Thermal Processing at their plants at Worcester, MA and Waterbury, CT. Extensive application of these softwares were found with respect to energy saving in heat treating industry.

Future Work

1. More case studies with different kinds of furnace and conditions are to be carried out.
2. The material database can be expanded with more number of TTT diagrams.
3. Furnace database can be enriched further by adding dual chamber furnaces and vacuum furnaces used for quenching, shaker furnaces for heating. In addition quench tanks can be added for liquid quenching.
4. An analytical approach for the calculation of convective heat transfer coefficient can be developed.
5. Enhance the database for gas as well as liquid quenchants.
6. More workpiece shapes (especially gear shaped) can be added in the database.
7. An analytical approach to calculate the volume fraction of various microstructures after tempering can be developed as well.

8. To increase the accuracy of the system, grain size, incubation time before microstructure evolution and stress can be considered while calculating the volume fraction of microstructure.
9. CHT-*q/t* can be further developed for aluminum using Time-Temperature-Property (TTP) diagrams for property prediction.

REFERENCES

[1] J. B. Austin, The flow of heat in metals, 1941.

[2] H. K. Nandi, M. C. Tomason and M. R. Delhunty, "Software Tool Optimizes Furnace Design and Operation," Industrial Heating Progress, Nov. 2002.

[3] ICON and DCON Manual, GRI and Purdue University, 1995

[4] SYSWELD System Documentation, SYSWELDv2003, ESI Group, The Virtual Try-Out Space Comany

[5] Adrian Bejan, *Heat Transfer*, John Wiley & Sons Inc. 1993

[6] Scattering of Heat Transfer Coefficient in High Pressure Gas Quenching. Th. Lubben, F. Hoffman, P. Mayr, IWT, C. Laumen, AGA AB

[7] Anthony F. Mills, Heat and Mass Transfer, Richard D Irvin 1995.

[8] Lindberg specification, *Lindberg Furnace Company (1994)*.

[9] Y. Rong, J. Kang, R. Vader and C. Bai, "Enhancement of Computer-Aided Heat Treating Planning System (CAHTPS)", Report 02-2 at CHTE Consortium Meeting, Nov. 13-14, 2002.

[10] Horizontal Internal Quench Vacuum Furnaces, Vacuum furnace systems, 1946 E. Cherry Lane, Souderton, PA. http://www.vfscorp.com/pdf/HIQ_Brochure.pdf

[11] http://www.ipsen-intl.com/vf_turbo.asp (2004)

[12] http://www.energysolutionscenter.org//HeatTreat/TechPro/SurfaceCombustion.htm (2002)

[13] Lohrmann, M., Hoffmann, F., and Mayr, P., Characterization of the Quenching Behavior of Gases, Conference Proceedings, Heat Treating Equipment and Processes, ASM International 1994, Schaumburg, IL.

[14] Herring, D. H., Applying Intelligent Sensor Technology to Problems Related to Distortion, SME Conference Proceedings, Quenching and Distortion Control, 1998.

[15] Liscic, B., Critical Heat-Flux Densities, Quenching Intensity and Heat Extraction Dynamics During Quenching in Vaporizable Liquids, Conference Proceedings, 2003 Heat Treat Conference & Exposition, ASM International, Indianapolis, IN.

[16] *L &L special furnace Co. Inc,* Aston PA, U.S.A

[17] AJAX Electric Company, P.A, U.S.A

[18] Jerome Ferrari, Noam Lior, Jan Slycke. An evaluation of gas quenching of steel rings by multiple jet impingement. *Journal of Materials Processing Technology* 136 (2003) 190-201

[19] Dong-Ying Ju, Chuncheng Liu and Tatsuo Inoue, Numerical modeling and simulation of carburized and nitrided quenching process, Journal of Materials Processing Technology 143-144 (2003) 880-885

[20] S. Das, G. Upadhya, and U. Chandra, Prediction of Macro and Micro-Residual Stress in Quenching Using Phase Transformation Kinetics

[21] C.C. Liu, K.F. Yoa, X.J.Xu, Z. Liu, A FEM modeling of quenching and tempering and its application in industrial engineering, Finite Elements in Analysis and Design. 39 (2003) 1053-1070.

[22] C.C. Liu, K.F, X.J.Xu, Z. Liu, Models for transformation plasticity in loaded steel subjected to bainitic and martensitic transformations, Mater. Sci. Technol. 17 (2001) 983-988.

[23] C.C. Liu, Experimental research and numerical solution on the quenching processes of large forgings, Ph.D. Thesis, Department of Mechanical Engineering, Tsinghua University of China, 1999.

[24] S. Claudinon, P. Lamesle, J. J. Orteu and R. Fortinuer, Continuous in situ measurement of quenching distortions using computer vision, Journal of Materials Processing Technology 122 (2002) 69-81

[25] M. A. H. Howes, Factors Affecting Distortion in Hardened Steel Components, INFAC/IIT Research Institute, Chicago, Illinois.

[26] Shackelford, J.F. Introduction to material science, SI Edition – Fourth edition. (Prentice Hall Europe, Upper Saddle River, 1998), ISBN 0-13-807125-X

[27] Callister, W.D. Materials science and engineering, An introduction Third Edition. (John Wiley & Sons, Inc, New York, 1994), ISBN 0-471-30568-5

[28] Tempering of steel, Revised by Michael Wisti and Mndar Hingwe, Atmosphere Annealing, Inc.

[29] Modern Steels and Their Properties, Handbook 2757, 7th ed., Bethlehem Steel Corporation, 1972

[30] http://nick-gd.chat.ru/index2.htm

[31] Y. Rong, J. Kang, L. Zhang, R. Purushothaman, and A. Singh, Development of Computer Aided Heat Treatment Planning System for Quenching and Tempering (CHT-*q/t*), Report 05-01 at CHTE consortium meeting, May 2005.

[32] V. C. Prantil, M. L. Callabresi and J. F. Lathrop, Simulating Distortion and Residual Stresses in Carburized Thin Strips, vol. 125, April 2003

[33] M. A. H. Howes, Factors Affecting Distortion in Hardened Steel Components, INFAC/IIT Research Institute, Chicago, Illinois

[34] http://www.efunda.com/materials/alloys/alloy_home/steels.cfm

[35] http://www.macaudata.com/macauweb/book138/html/12601.htm